CHEMICAL REVIEWS

pubs.acs.org/CR

Review

Recent Advances in the Total Synthesis of the Tetrahydroisoquinoline Alkaloids (2002–2020)

Alexia N. Kim, Aurapat Ngamnithiporn, Emily Du, and Brian M. Stoltz*

Cite This: *Chem. Rev.* 2023, 123, 9447–9496

Read Online

ACCESS | Metrics & More | Article Recommendations

ABSTRACT: The tetrahydroisoquinoline (THIQ) natural products constitute one of the largest families of alkaloids and exhibit a wide range of structural diversity and biological activity. Ranging from simple THIQ natural products to complex trisTHIQ alkaloids such as the ecteinascidins, the chemical syntheses of these alkaloids and their analogs have been thoroughly investigated due to their intricate structural features and functionalities, as well as their high therapeutic potential. This review describes the general structure and biosynthesis of each family of THIQ alkaloids as well as recent advancements of the total synthesis of these natural products from 2002 to 2020. Recent chemical syntheses that have emerged harnessing novel, creative synthetic design, and modern chemical methodology will be highlighted. This review will hopefully serve as a guide for the unique strategies and tools used in the total synthesis of THIQ alkaloids, as well as address the longstanding challenges in their chemical and biosynthesis.

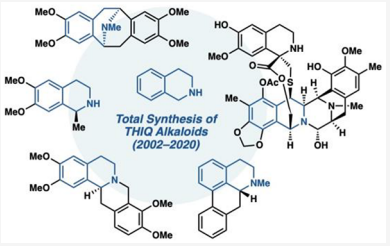

CONTENTS

Received: January 28, 2023
Published: July 10, 2023

ACS Publications

© 2023 The Authors. Published by American Chemical Society

https://doi.org/10.1021/acs.chemrev.3c00054
Chem. Rev. 2023, 123, 9447–9496

1. INTRODUCTION

The tetrahydroisoquinoline (THIQ) alkaloids make up one of the largest groups of natural products with a wide range of structural diversity and biological activity.[1] From simple tetrahydroisoquinolines such as salsolidine **1**, to complex tris-tetrahydroisoquinoline systems such as Ecteinsacidin 743 **2**, there is a wide variety in structure and activity between the families of isoquinoline alkaloids that possess the 1,2,3,4-tetrahydroisoquinoline ring system (Figure 1). Thus, the chemical syntheses of these alkaloids have been extensively investigated toward the development of efficient total syntheses and understanding of their biological activity.[2]

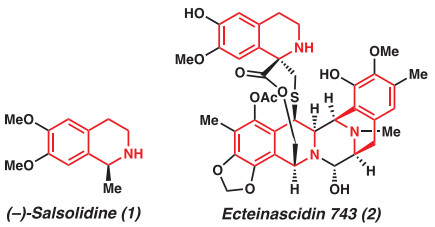

Figure 1. Tetrahydroisoquinoline alkaloids (−)-salsolidine **1** and Ecteinascidin 743 **2**.

While several review articles on the total synthesis of isoquinoline alkaloids have been published, including Williams' seminal review on the THIQ antitumor antibiotics,[3] there has been no comprehensive review of the chemical syntheses of tetrahydroisoquinoline alkaloids over the past several decades. Moreover, recent total syntheses have emerged by harnessing modern chemical methods and novel technology. As these synthetic strategies diverge from biomimetic approaches, they often provide a highly efficient route toward complex THIQ alkaloids compared to previous syntheses. This review will cover literature from 2002 to 2020, highlighting the chemical syntheses of a range of THIQ alkaloids that especially feature creative, novel synthetic approaches (Chart 1).

2. TETRAHYDROISOQUINOLINE (THIQ) ALKALOIDS

2.1. General Structure and Biosynthesis

Most simple THIQ alkaloids come from the Cactaceae, Chenopodiaceae, and Fabaceae cacti families.[1] These cactus species contain β-phenylethylamine alkaloids as well as simple tetrahydroisoquinolines that bear a stereogenic center at the C1 carbon with various oxidation patterns on the arene ring (Figure 2).

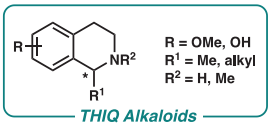

Figure 2. General structure of simple THIQ alkaloids.

Chart 1. General Structures of THIQ Alkaloid Families

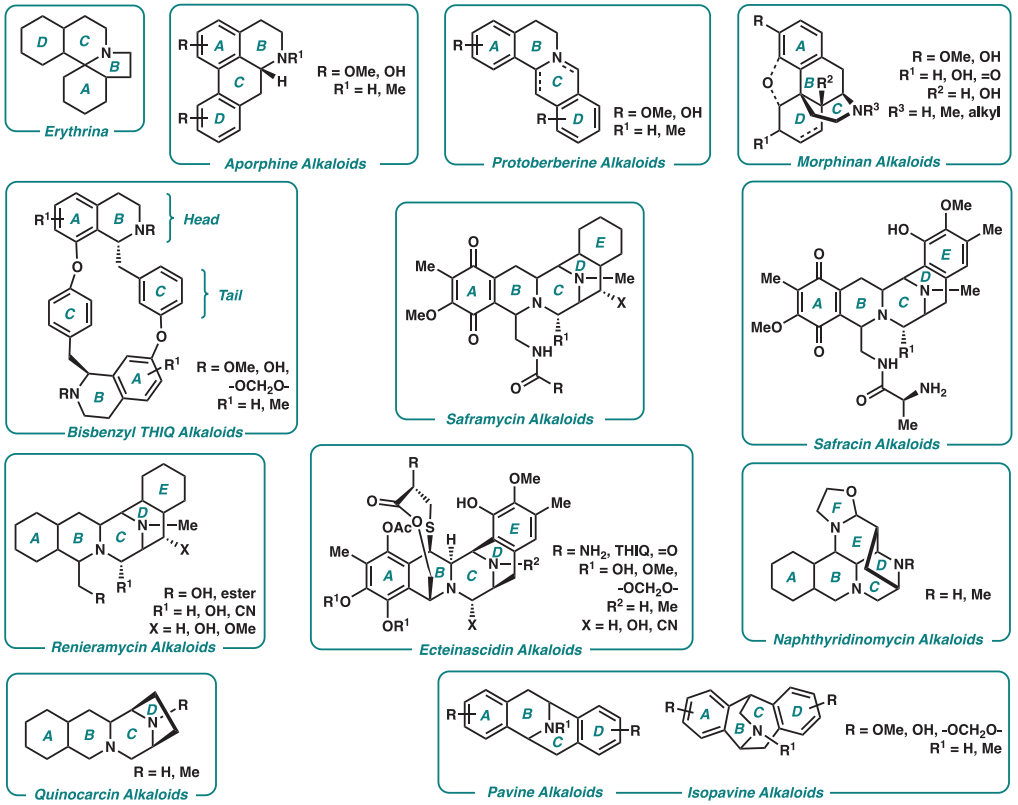

https://doi.org/10.1021/acs.chemrev.3c00054
Chem. Rev. 2023, 123, 9447−9496

The biosynthesis of these simple THIQs is generally achieved from the condensation of the corresponding β-phenylethylamine with a formaldehyde or acetaldehyde equivalent, accessing the tetrahydroisoquinoline motif as a single enantiomer.[4] These naturally require electron-rich functional groups on the arene ring to undergo an electrophilic aromatic substitution chemistry. Throughout this review, this key heterocyclic motif serves as a fundamental scaffold in all THIQ natural products that requires unique and creative synthetic approaches to install.

3. SPIROCYCLIC TETRAHYDROISOQUINOLINE ALKALOIDS

3.1. General Structure and Biosynthesis

From the Fabaceae family, the *Erythrina* genus consists of about 143 alkaloids that are characterized by the spirocyclic motif embedded in the tetracyclic scaffold (Figure 3).[1] There

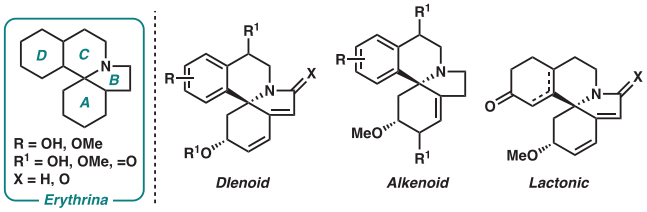

Figure 3. General structure of the *Erythrina* alkaloids.

are three main classes of *Erythrina* alkaloids referred to as the dienoid, alkenoid, and lactonic alkaloids.[5] The dienoid alkaloids feature a conjugated diene system, whereas the alkenoids have a 1,6-double bond in the A-ring and the lactonic alkaloids possess a lactone ring in ring D. These alkaloids have been discovered to possess an array of biological activity, including antiepileptic, anticonvulsant, and CNS depressing properties.

The biosynthesis of the *Erythrina* alkaloids is proposed to stem from norreticuline **3** as a key precursor (Figure 4).[1,6,7] Oxidative phenol coupling occurs to generate intermediate **4**, followed by rearrangement and ring opening of the

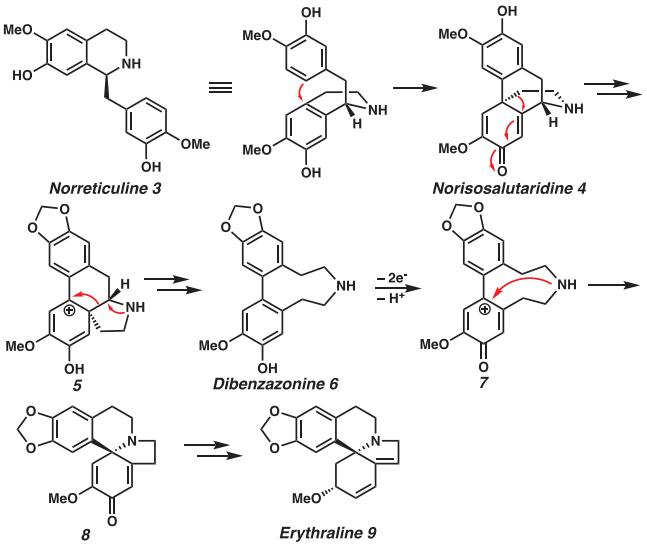

Figure 4. Proposed biosynthesis of *Erythrina* alkaloids.

tetrahydroisoquinoline ring to form dibenzazonine **6**. Zenk and co-workers utilized ^{13}C-labeling studies to suggest an allylic cation intermediate **7** that undergoes subsequent ring closure to access the natural product skeleton **8**. However, the specific enzymes that catalyze these transformations have not yet been fully elucidated.

3.2. Total Synthesis of Erythrina Alkaloids

Approaches to the synthesis of the core spirocyclic system of the *Erythrina* alkaloids are diverse, accessing several natural product members of this family in both racemic and enantioselective fashions. Three general strategies toward the construction of the THIQ core have been described, either through the disconnection of the C_1-C_{8a},[8−12] C_1-N,[13−15] and/or the $N-C_3$ bond (Figure 5). While electrophilic

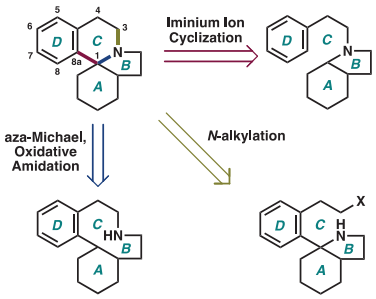

Figure 5. Synthetic approaches to *Erythrina* alkaloids.

aromatic substitution chemistry through iminium ion cyclization is most common to assemble the scaffold, other novel disconnections have also been explored to build the A-, B-, and C-rings.

In 2004, Matsumoto sought to construct the *Erythrinan* scaffold utilizing substitution chemistry for the key spirocyclization of *ortho*-quinone monoacetal **15** to establish the C-ring.[13] Toward the synthesis of *O*-methylerysodienone **17**, Matsumoto and co-workers initially access the biphenyl precursor **12** from a Suzuki−Miyaura coupling of arylboronic acid **10** and aryl bromide **11** (Scheme 1A). Further oxidative manipulations and substitution chemistry result in the installation of the nucleophilic nitrogen functional group in intermediate **14**. The C-ring was then established through the key spirocyclization step from *ortho*-quinone acetal **15**, using $BF_3{\cdot}OEt_2$ as the optimal Lewis acid compared with other metal triflates. Finally, *N*-alkylation to furnish the B-ring in **16** occurred smoothly under a methanol and phosphate buffer. Matsumoto and co-workers also demonstrated the enantioselective synthesis of *O*-methylerysodienone **17** by installing an additional *ortho* substituent on the A-ring, transmitting axial chirality of the biphenyl intermediate from its hindered rotation to the spirocyclic center of the natural product (Scheme 1B). Adding a trimethylsilyl group *ortho* to the biphenyl bond that was easily cleaved with Bu_4NF allowed the separation of both enantiomers and enabled the enantioselective synthesis of (+)-*O*-methylerysodienone.

Alternatively, Padwa and co-workers sought to construct the A-ring of the *Erythrina* alkaloids through an intramolecular Diels−Alder reaction that could yield intermediate **19**. The oxabicyclic adduct could then undergo regioselective ring-opening reactions with rhodium or tin to access building blocks **20** and **21** (Scheme 2).[16] A Rh(I)-catalyzed ring-opening cascade as demonstrated in Pathway A delivered intermediate **21** that underwent *N*-alkylation with alkyl

https://doi.org/10.1021/acs.chemrev.3c00054
Chem. Rev. 2023, 123, 9447−9496

Scheme 1. Matsumoto's Total Synthesis of *O*-Methylerysodienone

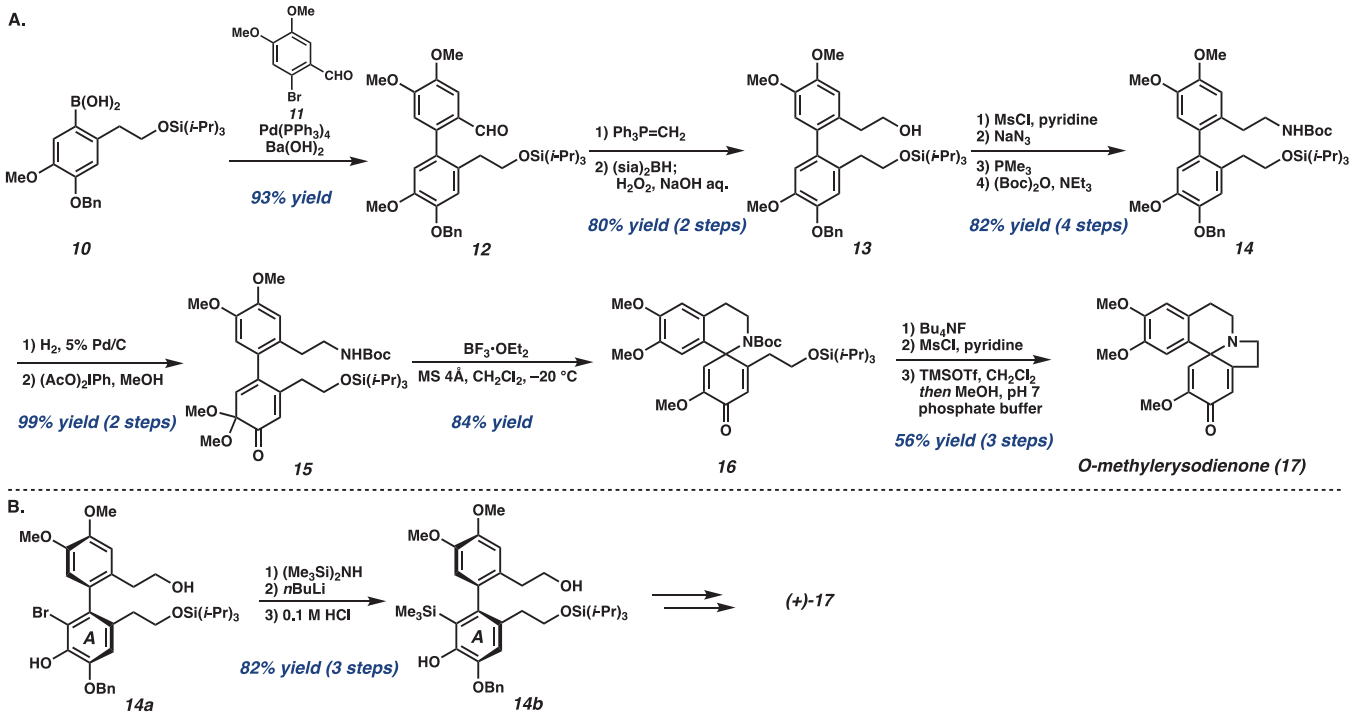

Scheme 2. Padwa's Synthetic Strategy toward the Erythrinan Alkaloids

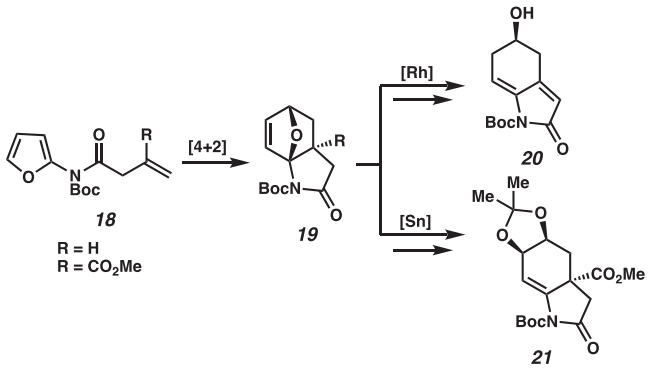

bromide to yield **22** (Scheme 3A). The bicyclic lactam then underwent smooth cyclization to generate spirocyclic tetrahydroisoquinoline **23** with NBS in CH_3CN. Reduction of the bromide and elimination of the alcohol then produce **24**, which underwent stereoselective allylic oxidation, subsequent reduction, and *O*-methylation to synthesize erysotramidine **27**.

Pathway B commenced with ring-opening by $SnCl_2$ followed by the addition of acetone to access acetonide **20** (Scheme 3B). *N*-Alkylation and treatment of acetonide with trifluoroacetic acid led to tetrahydroindolinone **29**. A Pictet–Spengler reaction with PPA then established the *Erythrinan* scaffold **30**, which was then subjected to hydrolysis, Barton decarboxylation, and reduction to access demethoxyerythratidinone **33**. This novel strategy toward the tetrahydroindolinone core allows access to several natural products of the *Erythrina* alkaloids based on an intramolecular Diels–Alder reaction of 2-imido-substituted furans.

Enantioselective approaches to the synthesis of demethoxyerythratidinone **33** have been explored over the past two decades.[17,18] Simpkins and co-workers demonstrated an asymmetric total synthesis of **33** through a key *N*-acyliminium ion cyclization using (*S*)-malic acid-derived lactams (Scheme 4).[19] Initially, the addition of butenyl magnesium bromide to imide **34** resulted in hydroxylactam **35** with excellent regiocontrol. Protection of the secondary alcohol followed by exposure to $BF_3{\cdot}OEt_2$ formed an acyliminium intermediate that allowed for cyclization to occur with diastereocontrol. Wacker oxidation of **36** and subsequent reduction removed the amide carbonyl, and aldol cyclization of the two oxidized ketones yielded (+)-demethoxyerythratidinone **33** in 50% yield, allowing access to both enantiomers of the natural product in simply eight steps.

Distinct from classic electrophilic aromatic substitution strategies to forge the THIQ core, Reisman and co-workers utilized their developed method of installing enantioenriched 4-aminocyclohexadienones to access **33**.[20] Having optimized a method for the diastereoselective 1,2-addition of organometallic reagents to benzoquinone monoketal-derived sulfinimines, they established spirocyclic THIQ **41** through the addition of aryllithium **40** to bromosulfinimine **39** to provide a single diastereomer in 74% yield (Scheme 5). Stille coupling then furnished the corresponding enol ether, with sulfinamide deprotection and *in situ* condensation accessing natural product scaffold **43**. Selective hydrogenation of triene **43** then completed the elegant and rapid total synthesis of (−)-demethoxyerythratidinone in only six steps with 26% overall yield.

Toward the total syntheses of (+)-demethoxyerythratidinone **33** and (+)-erysotramidine **27**, Ciufolini and co-workers employed an oxidative cyclization of a phenolic oxazoline, establishing the stereogenic center of the spirocycle.[21] Starting from oxazoline **44** prepared in five steps, oxidative amidation occurred smoothly to access **45** in 62% yield (Scheme 6). Upon treatment with TsOH, oxa-Michael addition then proceeds to furnish enone **46** as a single diastereomer. After several steps to remove the bridging serine moiety and further

https://doi.org/10.1021/acs.chemrev.3c00054
Chem. Rev. 2023, 123, 9447–9496

Scheme 3. Padwa's Total Synthesis of Erysotramidine and Demethoxyerythratidinone

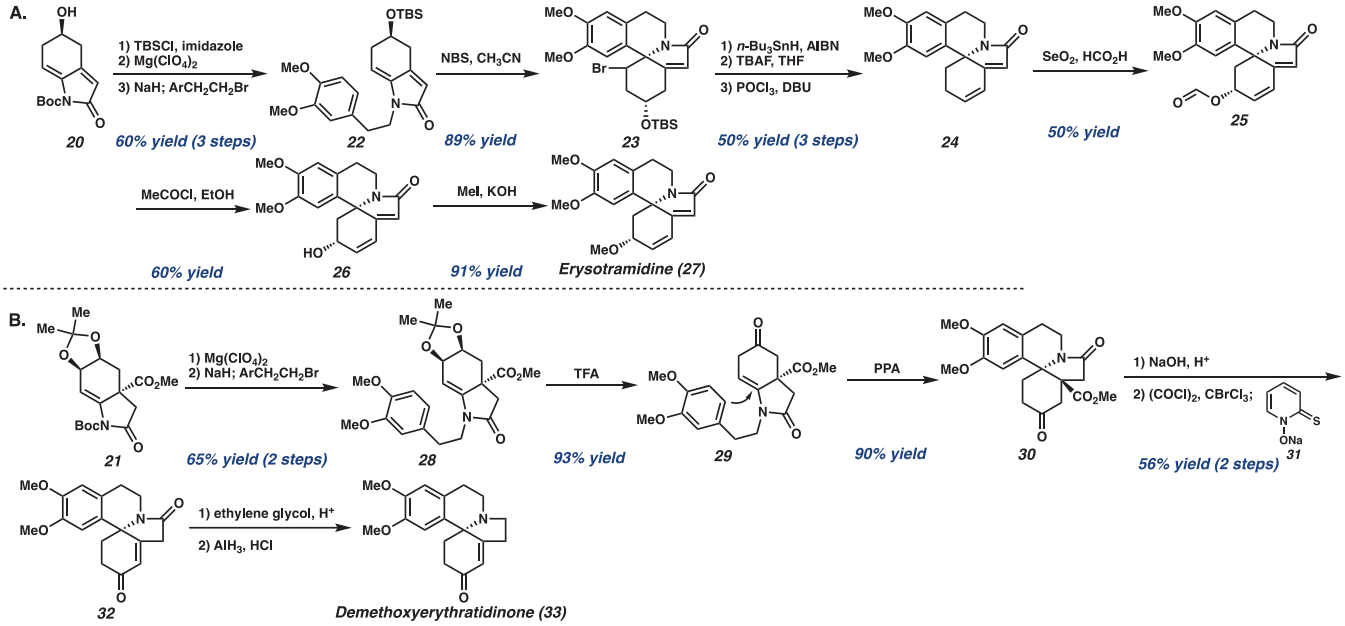

Scheme 4. Simpkins' Enantioselective Synthesis of (+)-Demethoxyerythratidinone

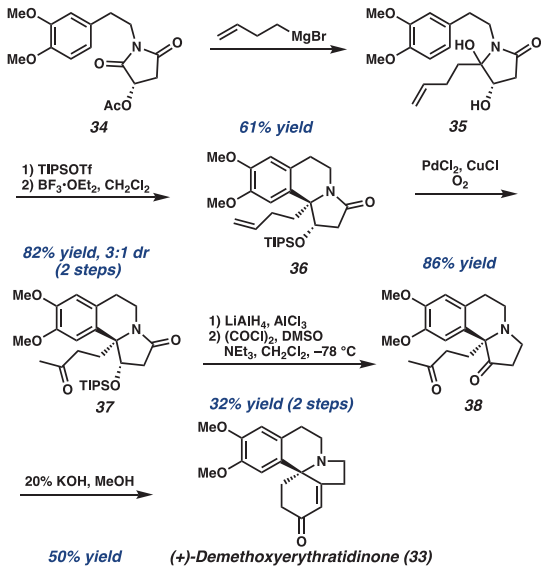

Scheme 5. Reisman's Enantioselective Synthesis of (−)-Demethoxyerythratidinone

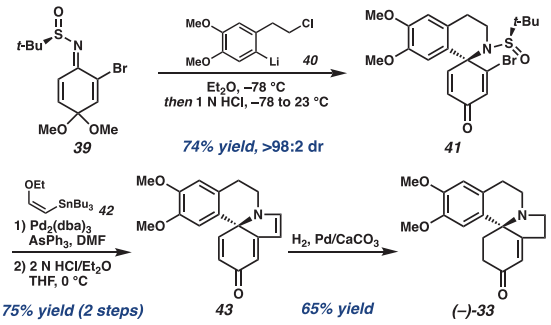

oxidative manipulations, late-stage intermediate **47** served as a universal precursor to access both natural products. First, *N*-acylation of **47** with $(EtO)_2P(O)CH_2COCl$ and subsequent treatment with aqueous KOH established a mixture of lactams **49** and **50**. Reduction of the mixture of products and acidic hydrolysis then resulted in the total synthesis of (+)-**33**.

Alternatively, silica gel chromatography of **47** and subsequent protection provided conversion to **51**, which underwent conjugate reduction with Li/NH_3 and elimination with *t*-BuOK to deliver **52** in a 64% overall yield. *N*-Acylation and cyclization then established the natural product scaffold, which was advanced to (+)-erysotramidine **27** in two subsequent steps. Overall, a unified approach to the *Erythrina* alkaloids was demonstrated through a key oxidative amidation and cyclization strategy.

Kaluza's synthetic strategy toward the asymmetric synthesis of (−)-erysotramidine **27** utilized a late-stage Heck cyclization to assemble the A-ring of the natural product scaffold.[22] Starting from imide **53** prepared in two steps from L-tartaric acid, addition of Grignard reagent **54**, and Lewis acid-mediated cyclization provided an epimeric mixture of diacetate **55** (Scheme 7). Silver-catalyzed cyclization then furnished dihydrofuranyl derivative **56**, with further reduction accessing the key intermediate **57**. Preparation of the (*Z*)-vinyl iodide for the late-stage Heck cyclization was achieved through Swern oxidation, then Wittig olefination of the crude aldehyde, and protection of the hydroxyl group to provide **59**. A Heck cyclization then established the A-ring of the natural product scaffold, providing **60** in a 62% yield as the sole product. A final methylation step of the alcohol furnished the unnatural enantiomer (−)-erysotramidine **27** in a good yield.

4. BENZYLTETRAHYDROISOQUINOLINE ALKALOIDS

Benzyltetrahydroisoquinoline alkaloids specifically feature a benzyl group at the C1 position of the isoquinoline ring and comprise one of the largest and most diverse groups of alkaloids. Despite the considerable variation in structure of benzyl THIQ alkaloids, the biosynthesis of these natural products is proposed to share early precursors.[1] Isoquinoline biosynthesis stems from dopamine **61** and *p*-hydroxyphenyla-

https://doi.org/10.1021/acs.chemrev.3c00054
Chem. Rev. 2023, 123, 9447−9496

Scheme 6. Ciufolini's Enantioselective Synthesis of (+)-Demethoxyerythratidinone and (+)-Erysotramidine

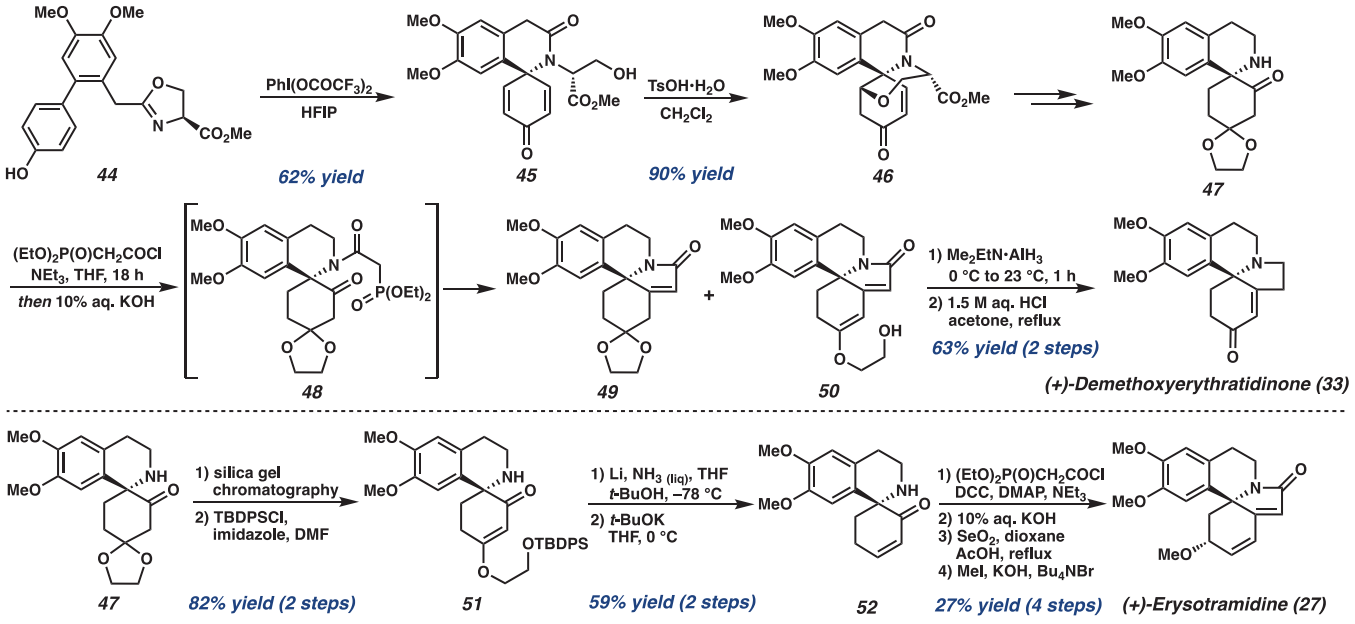

Scheme 7. Kaluza's Enantioselective Synthesis of (−)-Erysotramidine

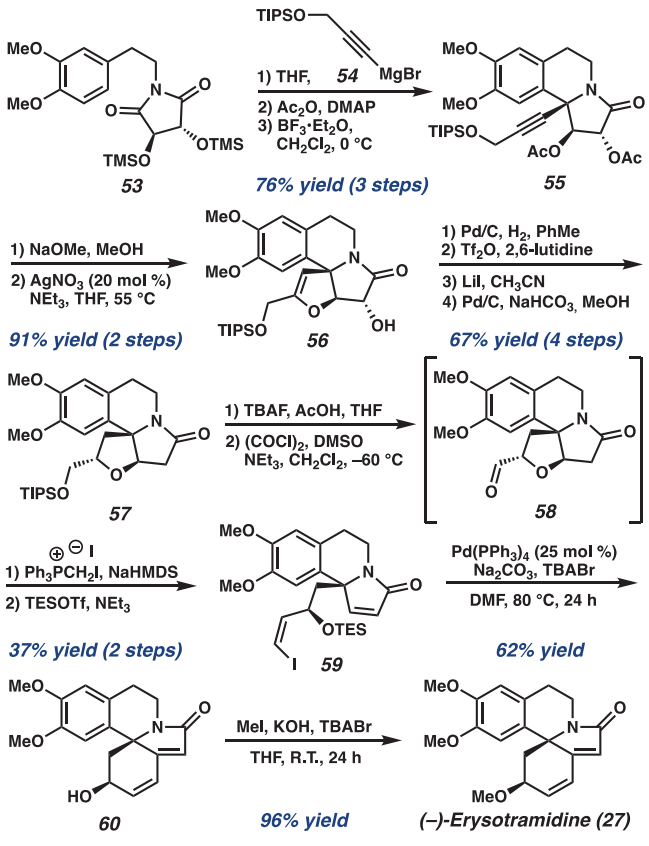

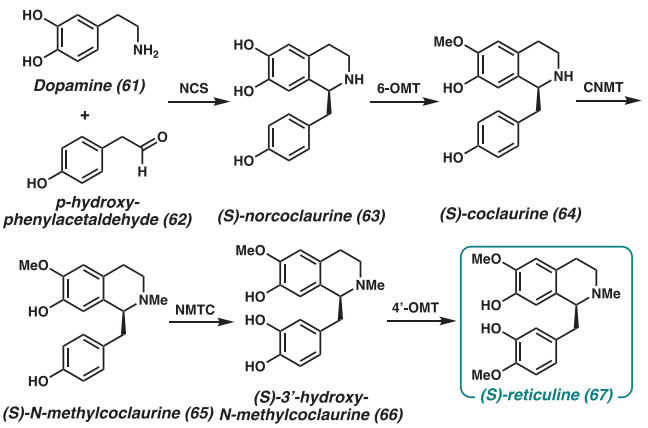

Figure 6. Early biosynthetic pathway to yield the central biosynthetic intermediate (*S*)-reticuline **67**.

cetaldehyde **62** to yield the central biosynthetic intermediate (*S*)-reticuline **67** (Figure 6).[23]

Condensation of **61** and **62** is catalyzed by the enzyme norcoclaurine synthase (NCS) to form (*S*)-norcoclaurine **63**. Methylation then occurs by a *S*-adenosyl methionine-(SAM)-dependent *O*-methyl transferase to access (*S*)-coclaurine **64**. After *N*-methylation to yield intermediate **65**, hydroxylation by *N*-methylcoclaurine 3′-hydroxylase (NMTC) followed by *O*-methylation produces the key precursor (*S*)-reticuline **67**. From this key intermediate, the biosynthetic pathways branch to form a variety of different structural classes of THIQ alkaloids (Figure 7).

4.1. Aporphine Alkaloids

4.1.1. General Structure and Biosynthesis. The aporphine alkaloids are based on the 4H-dibenzo[*de*,*g*]-quinoline structure or its *N*-methyl derivative, with a tetracyclic core as distinguished in Figure 8.[24] They contain a biphenyl ring system and highly oxidized substitution patterns with hydroxyl, methoxy, and methylenedioxy moieties situated over all four rings.

The aporphine alkaloids have been isolated from a variety of plants, including the genera *Glaucium flavum*, *Beilschmiedia elliptica*, and *Nandina domestica*. They are known to be promising agents in the prevention and treatment of metabolic syndrome due to their broad biological activity, including antihypertension, antidiabetes, antiobesity, antioxidation, and anti-inflammation.[25] In particular, many of the aporphines show various levels of preventing insulin resistance and

https://doi.org/10.1021/acs.chemrev.3c00054
Chem. Rev. 2023, 123, 9447−9496

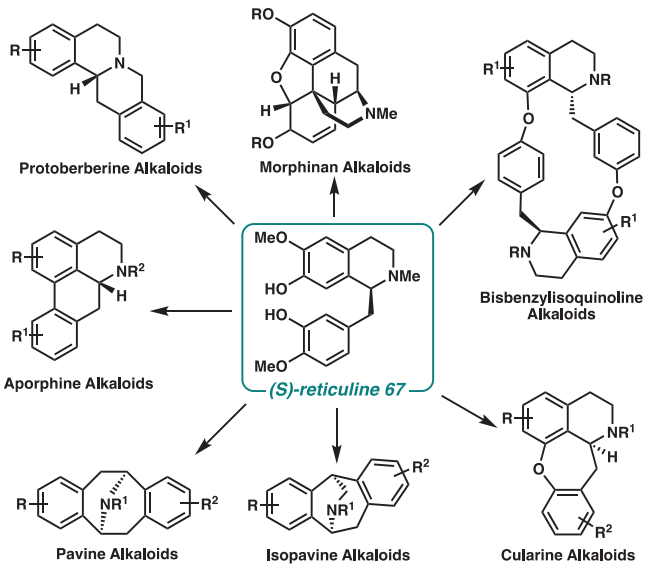

Figure 7. Diverging biosynthetic pathways from (*S*)-reticuline **67** that access a wide variety of structural classes of THIQ alkaloids.

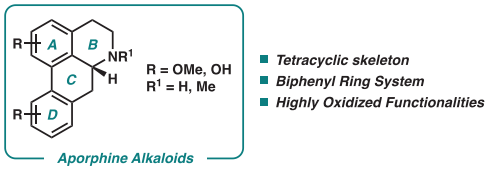

Figure 8. General structure of the aporphine alkaloids.

regulation of glucose homeostasis. The methoxy and hydroxyl substituents may be important for these biological activities.[25]

The aporphine alkaloids are presumably derived from reticuline **67**, which undergoes an intramolecular bis-phenol coupling to construct the core.[26] The CYP80G subfamily of cytochrome P450 monooxygenases has been correlated with aporphine biosynthesis in which CYP80G2 (corytuberine synthase) catalyzes conversion of (*S*)-reticuline **67** to (*S*)-corytuberine **68** via intramolecular C−C coupling (Figure 9).

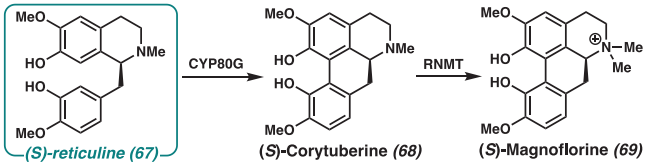

Figure 9. Proposed biosynthesis of aporphine alkaloid (*S*)-magnoflorine **69**.

N-Methylation of corytuberine **68** by the reticuline *N*-methyl transferase (RNMT) enzyme then delivers one of the aporphine natural products, magnoflorine **69**. Other related aporphine members of the family are proposed to arise from a similar route, delivering either the *N*−*H* or *N*-methyl aporphine or the quaternary aporphine salt.

4.1.2. Total Synthesis of Aporphine Alkaloids. Approaches toward the syntheses of the aporphine alkaloids commonly feature EAS chemistry to establish the THIQ core, followed by an intramolecular phenol arylation to achieve the natural product scaffold. In 2004, Cuny described the synthesis of aporphine **75** utilizing this synthetic strategy starting from *N*-tosyl tyramine **70** (Scheme 8).[27] A Pictet−Spengler cyclization with 2-bromophenylacetaldehyde **71** was effected

Scheme 8. Cuny's Synthesis of Aporphine

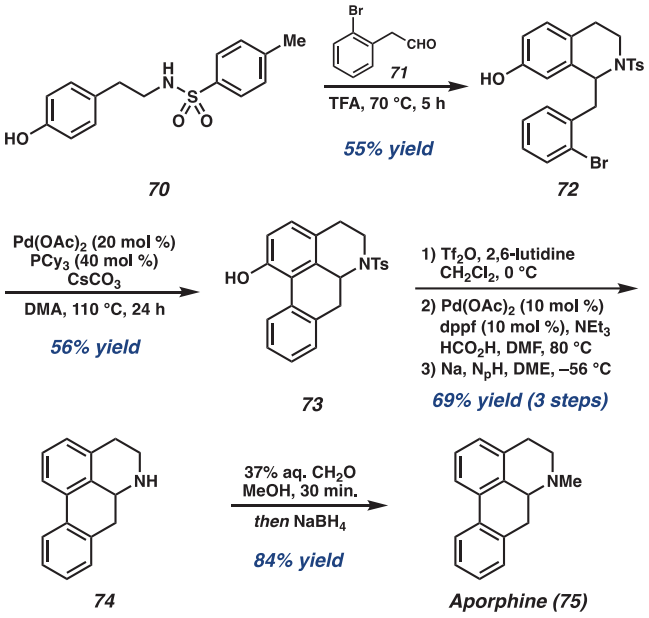

to afford THIQ **72** in 55% yield. A Pd-catalyzed intramolecular phenol *ortho*-arylation then delivered the key aporphine scaffold **73** in moderate yield. Finally, removal of the hydroxyl group and the sulfonamide, followed by reductive amination with 37% aqueous formaldehyde in the presence of $NaBH_4$ afforded aporphine **75**. Similar synthetic strategies have also been utilized in subsequent reports to access different aporphine natural products.[28−31]

Circumventing the need for prefunctionalization of the arene before direct arylation, Vicario and co-workers reported the total synthesis of (+)-glaucine using an oxidative biaryl coupling to establish the aporphine scaffold (Scheme 9).[32] From imine **76**, addition of Grignard benzylic reagents followed by hydrogenation to remove the chiral appendage

Scheme 9. Vicario's Synthesis of (+)-Glaucine

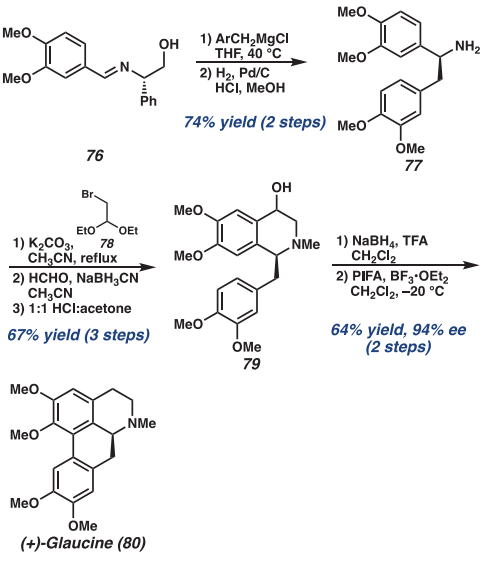

https://doi.org/10.1021/acs.chemrev.3c00054
Chem. Rev. 2023, 123, 9447−9496

delivered amine **77**. *N*-Alkylation with bromoacetaldehyde diethylacetal (BADA) allowed a Pomeranz−Fritsch cyclization to construct THIQ **79**. After reduction of the hydroxyl group, the final C−C biaryl oxidative coupling was accomplished using hypervalent iodine(III) reagent (bis(trifluoroacetoxy)-iodo)benzene (PIFA) that allowed the synthesis of (+)-glaucine **80** cleanly with no racemization observed.

Alternatively, Fürstner and co-workers constructed the aporphine scaffold through a key In-mediated cycloisomerization reaction from biphenyl derivatives.[33] From enamide **81**, a Suzuki coupling with 2-formylbenzeneboronic acid yielded functionalized biphenyl derivative **82**, constructing the C−C biphenyl bond early in the synthesis (Scheme 10). Conversion

Scheme 10. Fürstner's Synthesis of *O*-Methyl-dehydroisopiline

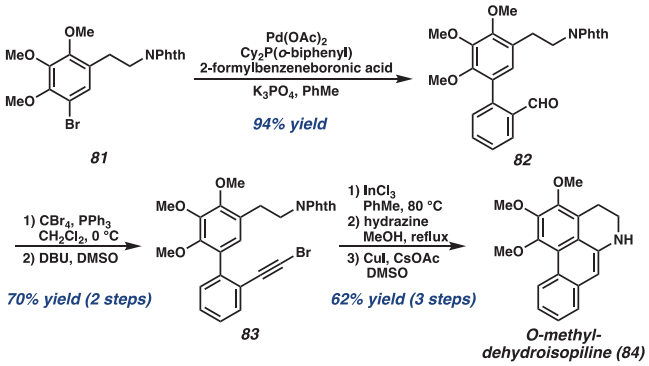

of the aldehyde to alkyne **83** then set the stage for the key carbocyclization, which was effected by using $InCl_3$ in toluene. After removal of the phthalimide protecting group, intramolecular amination forged the THIQ ring and completed the total synthesis of *O*-methyl-dehydroisopiline **84**.

An unusual approach toward the synthesis of the aporphine scaffold employs benzyne chemistry to construct two of the four rings in a single transformation. Raminelli and co-workers described the synthesis of aporphine **75** from amide **85**, which was converted to isoquinoline **86** through a Bischler−Napieralski reaction (Scheme 11).[34] Treatment with acetic anhydride then yielded isoquinoline **87**, which served as the nonpolar diene for the [4+2] annulation. Thus, adding **87** and benzyne precursor **88** in the presence of CsF delivered aporphine core **89** from a [4+2] reaction followed by hydrogen

Scheme 11. Raminelli's Synthesis of Aporphine

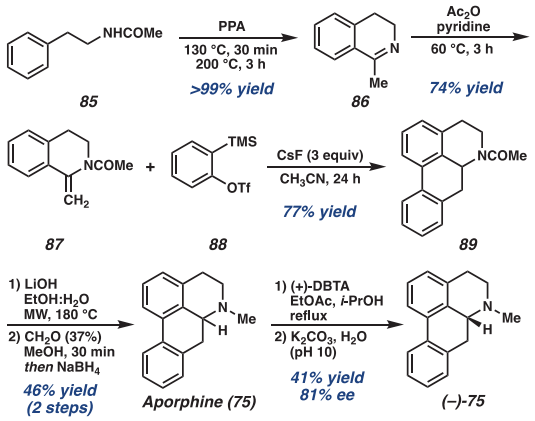

migration. Hydrolysis of **89** followed by reductive amination delivered aporphine **75**, which was then subjected to chiral resolution using (+)-DBTA to provide the enantiomer of the aporphine alkaloid. Raminelli and co-workers were further able to demonstrate the syntheses of different aporphine alkaloids using benzyne chemistry to couple isoquinoline derivatives and various silylaryl triflates, allowing rapid access to functionalized aporphine scaffolds.[35,36]

Beyond the syntheses of the classic aporphine natural product scaffold, others have targeted unique members of the aporphine alkaloids, which share the characteristic tetracyclic nucleus but with varying oxygenation patterns and bond connectivity. For instance, Nimgirawath and co-workers completed the total synthesis of telisatin A **92** and other members of the telisatin-type alkaloids that are distinguished by an oxalyl moiety fused to the THIQ core (Scheme 12).[37]

Scheme 12. Nimgirawath's Synthesis of Telisatin A

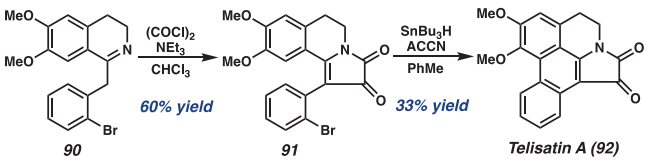

From dihydroisoquinoline **90** that was established from a Bischler−Napieralski reaction, treatment with oxalyl chloride and NEt_3 afforded dione **91** (Scheme 12). A radical cyclization using $SnBu_3H$ in the presence of 1,1′-azobis-(cyclohexanecarbonitrile) (ACCN) then delivered telisatin A **92** and other telisatin alkaloids in 30−34% yields.

Cuny and co-workers described the syntheses of C7-oxygenated aporphine alkaloids through a diastereoselective reductive cyclization followed by a Pd-catalyzed *ortho*-arylation to form the biaryl C−C bond (Scheme 13).[38,39] From

Scheme 13. Cuny's Synthesis of (−)-Artabonatine A

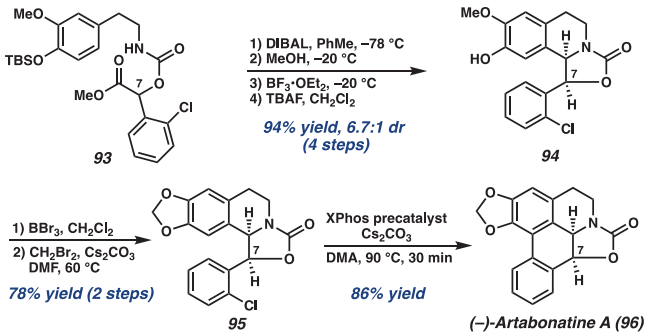

carbamate **93**, selective reduction of the methyl ester using DIBAL, followed by an acid-mediated cyclization with BF_3·OEt_2 delivered oxazolidinone **94** of both *anti*- and *syn*-diastereomers. Demethylation and formation of the dioxolane moiety with CH_2Br_2 provided **95**, which underwent an *ortho*-phenyl arylation with an XPhos precatalyst to afford (−)-artabonatine A **96**. This natural product has been revised after observing that the specific rotation and ^1H and ^{13}C NMR spectral data for the natural product possessed the *syn*-diastereomer rather than the reported structure of the *trans*-diastereomer.

Lastly, the proaporphine alkaloids are recognized as biosynthetic precursors of aporphine alkaloids that are

https://doi.org/10.1021/acs.chemrev.3c00054
Chem. Rev. 2023, 123, 9447−9496

distinguished by the spirocyclohexadienone ring system. Toward the construction of this unique spirocycle, Honda and co-workers first reported the total synthesis of stepharinine **100** and pronuciferine **101** utilizing an intramolecular aromatic oxidation of a common phenol intermediate (Scheme 14A).[40]

Scheme 14. (A) Honda's Synthesis of Stepharine and Pronuciferine; (B) Magnus's Synthesis of Stepharine

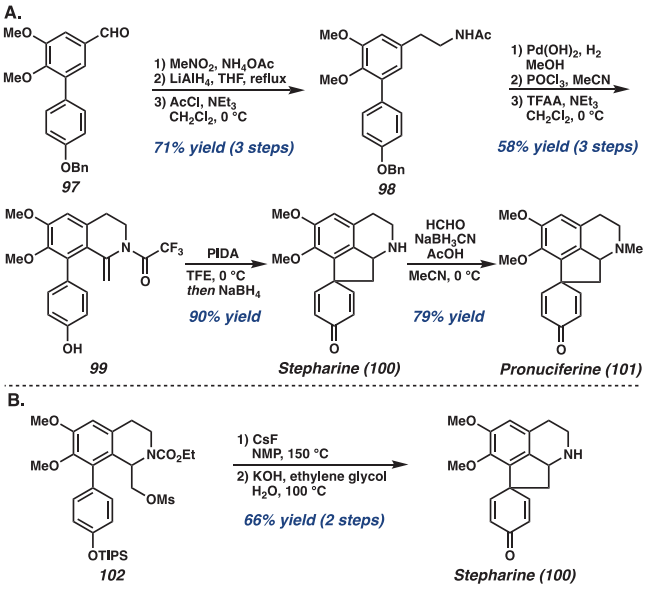

From aldehyde **97**, condensation with nitromethane, followed by reduction and acetylation, delivered amide **98**. After removal of the benzyl group, a Bischler–Napieralski reaction with $POCl_3$ and then acylation with trifluoroacetic anhydride yielded enamide **99** for the key aromatic oxidation. Ultimately, the oxidation of **99** with iodobenzene diacetate (PIDA) was successful in allowing cyclization to stepharine **100** in a 90% yield. *N*-Methylation of **100** further delivered pronuciferine **101**. Alternatively, Magnus and co-workers demonstrated that the spirocyclization could be achieved through an intramolecular displacement of a mesylate derivative **102** using CsF in NMP at 150 °C to deliver stepharine **100** as well (Scheme 14B).[41]

Takao and co-workers reported the enantioselective synthesis of a distinct proaporphine alkaloid (−)-misramine **110** utilizing their previously developed enantioselective Friedel–Crafts 1,4-addition of enones.[42,43] From phenethyl enone **103**, their key enantioselective intramolecular 1,4-addition was accomplished by using *epi*-cinchonine amine **C1** as a catalyst (Scheme 15). With enantioenriched spiroindane **104**, a Rubottom oxidation followed by treatment with camphorsulfonic acid (CSA) and trimethyl orthoformate induced an intramolecular hemiacetalization of the phenol and carbonyl to deliver tetracycle **105**. After several protecting group manipulations, benzylic oxidation with CrO_3 furnished ketone **106**. Next, to establish the THIQ core, the 2-oxoethyl group was incorporated into the benzene ring via a Claisen rearrangement to afford the C-allylated product **107**, followed by ozonolysis followed by deoxygenation to produce aldehyde **109**. Finally, reductive amination and the removal of the TBS group afforded (−)-misramine **110** as a single diastereomer.

Fagnou and co-workers further utilized the Pd-catalyzed direct arylation of aryl halides for the preparation of aporphine

Scheme 15. Takao's Synthesis of (−)-Misramine

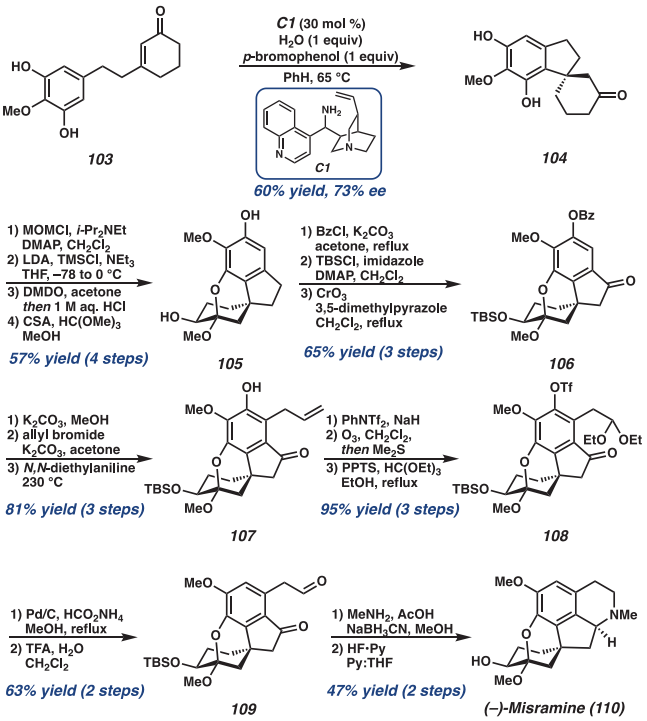

analogues, including C2-substituted aporphines and the syntheses of (*R*)-nornuciferine **122** and (*R*)-nuciferine **121** (Scheme 16).[44] First, a Bischler–Napieralski cyclization of differentially substituted amides under either $POCl_3$ or poly(phosphoric acid) yielded the dihydroisoquinoline intermediate, which was immediately reduced to THIQ **112** using $NaBH_4$ in MeOH. After protection of the secondary amine, the key direct arylation step was explored for each substrate, enabling the direct coupling of aryl bromides, chlorides, and iodides as well as different *N*-protecting groups (Scheme 16A).

Fagnou also explored various C2-substitutents by coupling aporphine derivative **115** with different nucleophilic coupling partners, installing a range of functionalities such as morpholine, pyridine, and pyrazine *N*-oxides (Scheme 16B). This strategy was also employed for the synthesis of (*R*)-nornuciferine **122** and (*R*)-nuciferine **121** by utilizing a Ru-catalyzed asymmetric transfer hydrogenation after Bischler–Napieralski cyclization to provide THIQ **118** in 99% yield and with 95% ee (Scheme 16C) Then, Pd-catalyzed arylation, followed by reduction or deprotection of the Boc group, delivered both natural products. Overall, these syntheses highlight the utility of direct arylation methodology for both target-oriented and diversity-oriented synthesis.

4.2. Bisbenzyl Thiq Alkaloids

4.2.1. General Structure and Biosynthesis. The bisbenzyltetrahydroisoquinoline alkaloids consist of two monomeric benzyl THIQ fragments linked through diphenyl ether or biphenyl bonds (Figure 10). The substitution on the arene mainly consists of hydroxyl, methoxy, or methylenedioxy groups. Over hundreds of bisbenzyl THIQ alkaloids have been isolated and characterized, with the diaryl ether linkage either involved in "tail-to-tail" coupling of the benzyl unit or "head-to-tail" coupling of the THIQ linked to the benzyl C-ring.

The bisbenzyl THIQ alkaloids have been isolated from an array of plant species, including *Chondrodendron tomentosum*

https://doi.org/10.1021/acs.chemrev.3c00054
Chem. Rev. 2023, 123, 9447−9496

Scheme 16. Fagnou's Synthesis of Aporphine Alkaloids

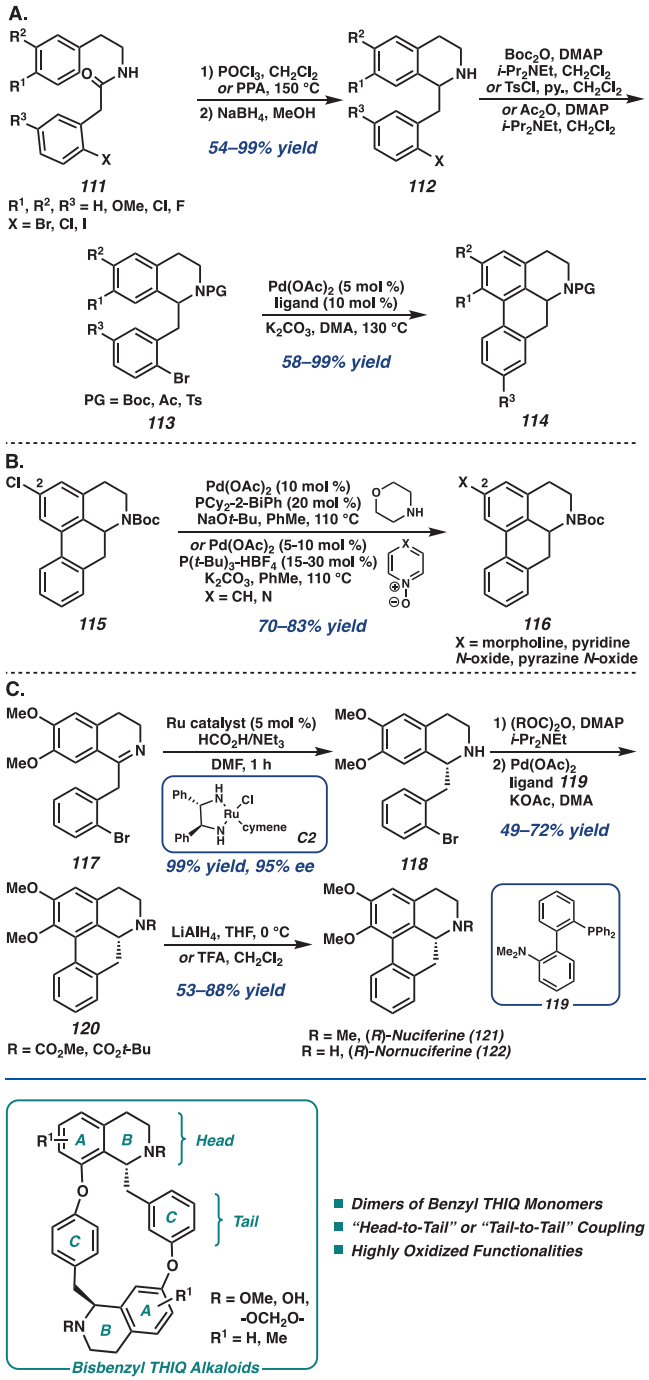

Figure 10. General structure of bisbenzyl THIQ alkaloids.

and opium poppy *Papaver somniferum*.[45] They are widely known for their dopaminergic, antitumor, and neuroprotectant properties.[46] This class of alkaloids is proposed to be formed from the coupling of two monomer units derived from *N*-methylcoclaurine (NMC) **65** in either the (*R*)- or (*S*)-configuration, catalyzed by enzyme CYP80A1 (Figure 11). First, epimerization of **65** is performed by dehydroreticuline synthase-dehydroreticuline reductase (DRS-DRR) to yield (*R*)-**65**, and then either (*R*)+(*R*) coupling or (*R*)+(*S*) coupling delivers guattegaumerine **123** or berbamunine **124**, respectively. However, dimerization of benzyl THIQs can occur either between both benzyl units or between the THIQ moiety

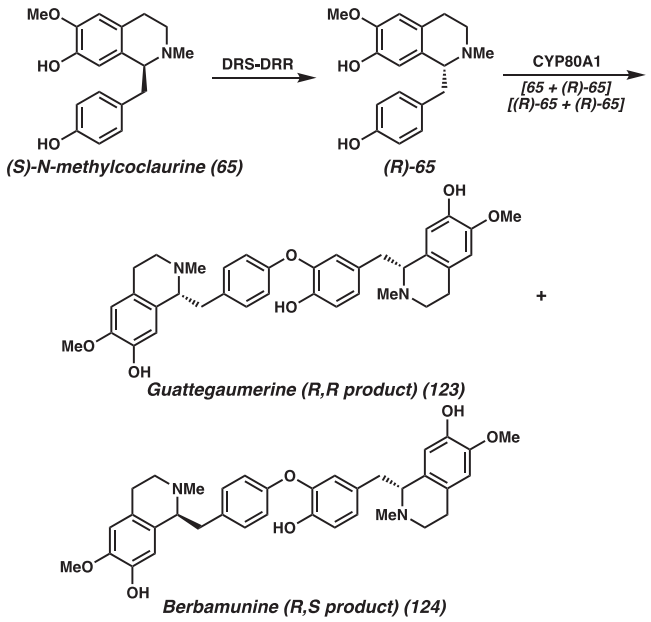

Figure 11. Proposed biosynthesis of bisbenzyl THIQ alkaloids **123** and **124**.

to a benzyl unit, and thus the structural diversity of these alkaloids is extensive.[45]

4.2.2. Total Syntheses of Bisbenzyl THIQ Alkaloids. In 2011, Opatz and co-workers described the modular syntheses of (+)-tetramethylmagnolamine **133** and (+)-*O*-methylthalibrine **132** from a common intermediate THIQ **125** (Scheme 17).[47,48] Alkylation of deprotonated aminonitrile **125** with benzyl bromide **126** and subsequent reductive methylation give THIQ monomer **127**, while bromination of **128** followed by formamide reduction yielded the other THIQ monomer **129**. Finally, an Ullman coupling of **127** forged the biaryl ether linkage with THIQ **130** to afford (+)-*O*-methylthalibrine dimer **132**, or alternatively with THIQ **129** and **131** to synthesize (+)-tetramethylmagnolamine **133**. Opatz and co-workers utilized a similar synthetic strategy for the C−O coupling of two benzyl THIQ monomers to access the macrocyclic skeleton of the curare alkaloids as well.[48]

A similar synthetic approach was described by Bracher and co-workers for the total synthesis of tetrandine **141** and isotetrandine **142**, featuring a Pictet−Spengler condensation to construct the THIQ moieties followed by an Ullmann coupling for biaryl ether formation (Scheme 18).[49] First, benzyl-THIQ **136** was constructed from a Pictet−Spengler cyclization of carbamate **134** with enol ether **135**, which further underwent C−O coupling using a copper(I) bromide-dimethylsulfide complex with Cs_2CO_3 in pyridine to yield **138**. After deprotection, a second Pictet−Spengler reaction with enol ether **139** delivered *seco*-bisbenzylisoquinoline **140** in 42−46% overall yield. A second Ullmann coupling using the same optimized conditions then afforded the macrocycle and accessed natural products tetrandine **141** and isotetrandine **142** after reduction with $LiAlH_4$.

Apart from macrocyclic bisbenzyltetrahydroisoquinoline alkaloids, several novel strategies to access *seco*-bisbenzyltetrahydroisoquinolines have been explored. In 2002, Georghiou and co-workers described the total synthesis of (−)-tejedine **154** from a key Bischler−Napieralski cyclization and diaryl ether coupling (Scheme 19).[50] One of the synthons for the key

https://doi.org/10.1021/acs.chemrev.3c00054
Chem. Rev. 2023, 123, 9447−9496

Scheme 17. Opatz's Synthesis of (+)-Tetramethylmagnolamine and (+)-*O*-Methylthalibrine

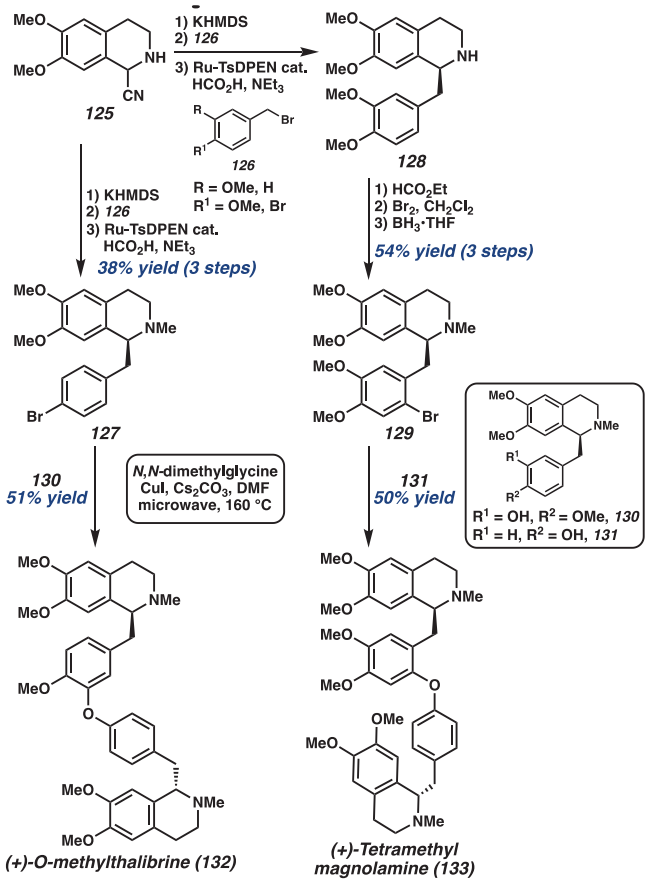

Scheme 18. Bracher's Synthesis of Tetrandine and Isotetrandine

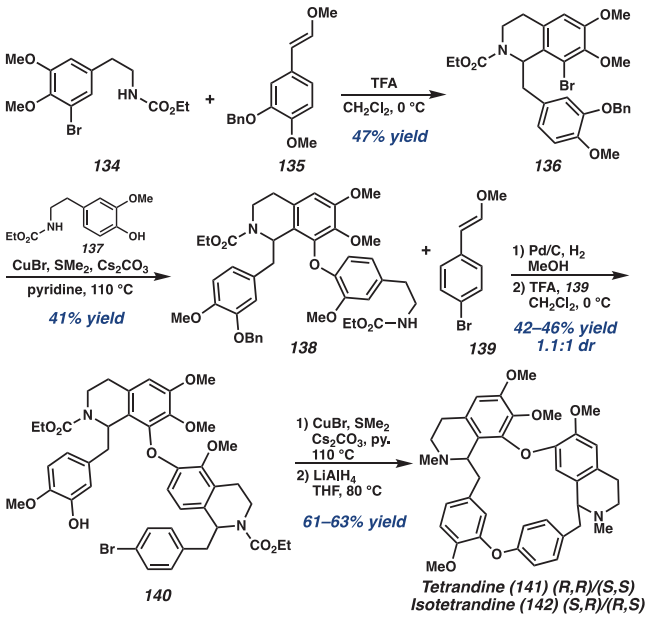

cyclization was synthesized from phenyl acetic acid **143**, which upon reaction with (*S*)-methylbenzylamine **144** delivered amide **145**, and further reduction afforded synthon **146**. The diaryl ether coupling partner was then achieved from $Cu(OAc)_2$-catalyzed C−O coupling of phenol **147** with

Scheme 19. Georghiou's Synthesis of (−)-Tejedine

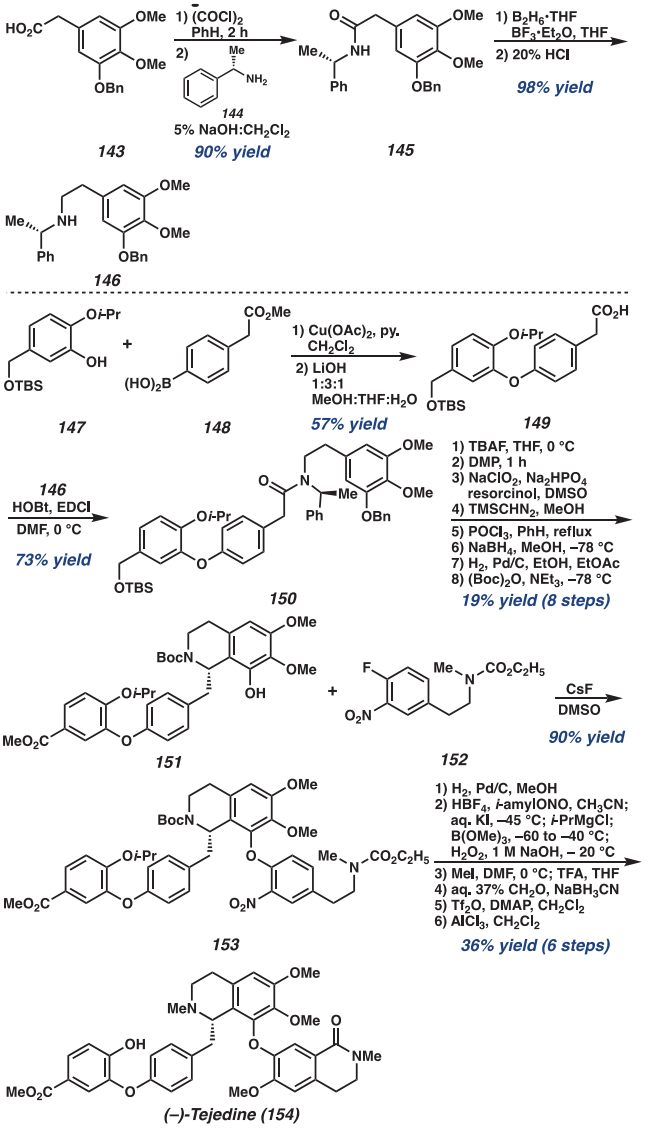

phenyl boronic acid **148**, which was then hydrolyzed to carboxylic acid **149**. With the two partners in hand, a diastereoselective Bischler−Napieralski reaction was performed using chiral auxiliary-bearing synthon **146** condensed with **149** to deliver amide **150**, followed by cyclization using $POCl_3$ and reduction to deliver THIQ **151** as a single diastereomer. Finally, the dihydroisoquinolone unit was installed from phenylethylamine **152** which underwent base-mediated S_NAr coupling with **151** to deliver **153**. After the nitro group was converted to a methoxy substituent, *N*-methylation and cyclization afforded (−)-tejedine **154**.

Toward the synthesis of (+)-*O*-methylthalibrine **161**, Nishiyama and co-workers employed an electrochemical method to construct the diaryl ether core along with a stereoselective Bischler−Napieralski reaction to establish the THIQ moieties.[51,52] First, the electrochemical halogenation of phenol **155** was optimized to deliver dichlorinated phenol **156** by using TBACl as the halogen source (Scheme 20). Then, oxidative dimerization of **156** was performed to deliver **157** in 60% yield, followed by cathodic reduction to afford the desired diaryl ether product **158**. After methylation of the phenol, catalytic hydrogenolysis delivered **159** in an 85% overall yield.

https://doi.org/10.1021/acs.chemrev.3c00054
Chem. Rev. 2023, 123, 9447−9496

Scheme 20. Nishiyama's Electrochemical Synthesis of (+)-*O*-Methylthalibrine

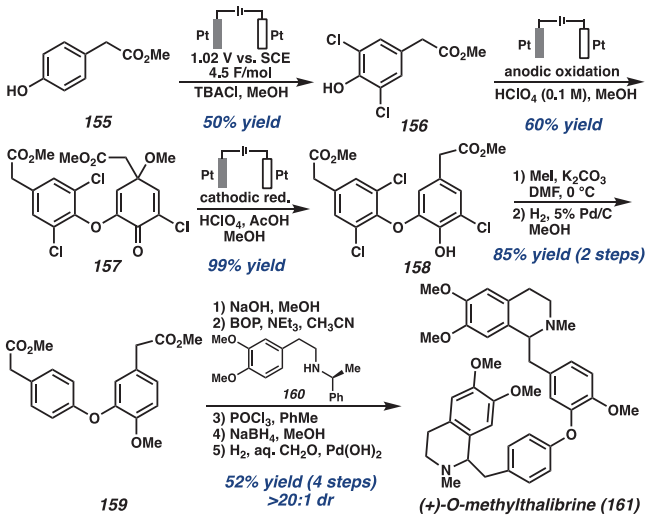

Alternatively, an electrochemical reductive dechlorination reaction was also developed by passing a methanol solution of **158** through a Pd tube (cathode) and a Pt wire (anode) in an aqueous H_2SO_4 solution outside the flow cell. Hydrogen, which was generated by electrolysis, was absorbed into the Pd tube and thus the successive reduction was conducted to give **159** in 76% yield.[51] After hydrolysis, the reaction of the resulting diacid with phenylethylamine **160** provided the corresponding bis-amide, which underwent a Bischler–Napieralski cyclization followed by reduction to deliver bis-THIQ in 75% overall yield. Finally, a one-pot conversion of removing the chiral auxiliaries and *N*-methylation afforded natural product **161**.

Alternatively, Lumb and co-workers adopted a bioinspired strategy for the synthesis of (*S*,*S*)-tetramethylmagnolamine **133** utilizing a catalytic aerobic desymmetrization of phenols.[53] From THIQ **162**, which was established from a Bischler–Napieralski cyclization followed by asymmetric reduction, a Boc protection and subsequent aerobic oxidative coupling using $CuPF_6$ and *N*,*N*′-di-*tert*-butylethylenediamine (DBED) under 1 atm of O_2 formed oxygenated radical intermediate **163** (Scheme 21). Upon treatment of another THIQ molecule **164**, radical C–O coupling afforded the desymmetrized bis-THIQ dimer **165** after reductive workup. Subsequent methylation and reduction of the Boc groups furnished tetramethylmagnolamine **133** in 7 steps with a 21% overall yield. By taking advantage of the natural product's pseudosymmetry and biosynthesis, this synthetic approach concisely assembles the target by only preparing a single coupling partner.

4.3. Protoberberine Alkaloids

4.3.1. General Structure and Biosynthesis. The protoberberine alkaloids constitute a tetracyclic ring system with varied functionalities on the arene ring. These alkaloids are derived from benzyl THIQs through phenolic oxidation and coupling with the *N*-methyl group, which serves as the "berberine bridge" carbon (Figure 12).[54]

Primarily isolated from the Papaveraceae (e.g., *Corydalis*, *Papaver*), Berberidaceae (e.g., *Berberis*, *Mahonia*), and Menispermaceae families, the protoberberine alkaloids consist of several variations of the tetracyclic ring system: the protoberberines such as berberine **166**, the tetrahydroprotoberberines like tetrahydropalmatine **167**, and C14-oxo derivatives, such as cryptopine **168**. These three distinct scaffolds are only several of the myriad number of skeleton types identified.

Scheme 21. Lumb's Synthesis of Tetramethylmagnolamine

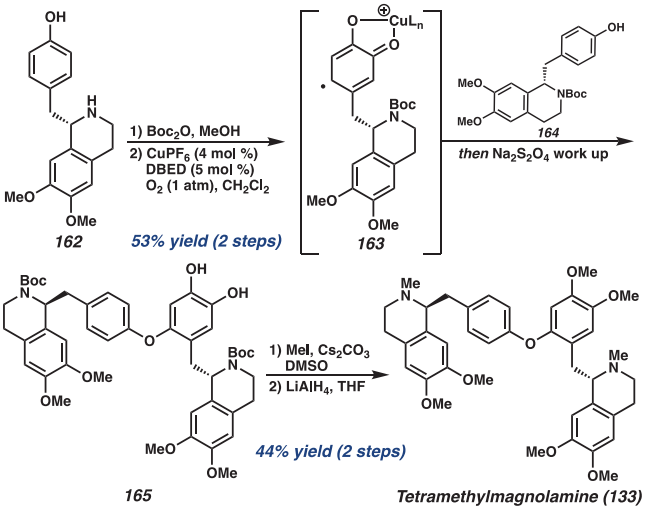

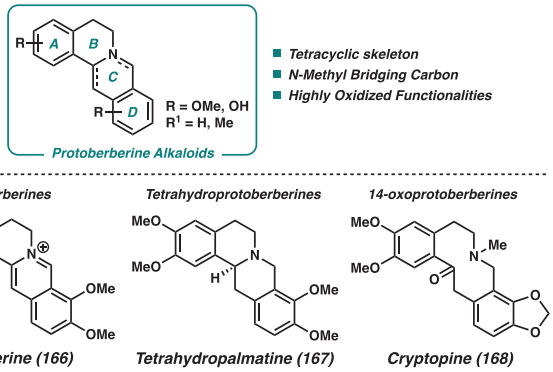

Figure 12. General structure of the protoberberine THIQ alkaloids.

Plants that contain the protoberberine alkaloids are known to be used as analgesics, sedatives, and antiseptics in traditional medicine. Both the quaternary alkaloid salts and their tetrahydroderivatives have important biological and therapeutic activity, and thus, their chemical syntheses have been extensively explored. Their biosynthesis stems from oxidation of reticuline **67** catalyzed by a berberine bridge enzyme (BBE) to generate iminium **169**, with the release of H_2O_2 as a byproduct (Figure 13).[55] Electrophilic aromatic substitution then delivers the protoberberine scaffold (*S*)-scoulerine **171**, which upon methylation by (*S*)-adenosyl methionine (SAM) forms tetrahydroprotoberberine **172**. Further oxidation of the amine by a cytochrome P450-dependent enzyme and formation of the dioxolane ring gives berberine **166**.[56]

4.3.2. Total Syntheses of Protoberberine Alkaloids. While there have been vast reports on the syntheses of the protoberberine alkaloids, some feature distinct synthetic strategies to access the natural product. In 2002, Davis and co-workers reported the synthesis of protoberberine alkaloid (−)-xylopinine **177** involving the addition of a lithiated *ortho*-tolyl nitrile into an enantiopure sulfinimine.[57,58] Using enantiopure sulfinimine **173**, which was prepared from condensation of the aldehyde with enantiopure sulfinamide, reaction with lithiated *ortho*-tolyl nitrile **174** delivered

https://doi.org/10.1021/acs.chemrev.3c00054
Chem. Rev. 2023, 123, 9447−9496

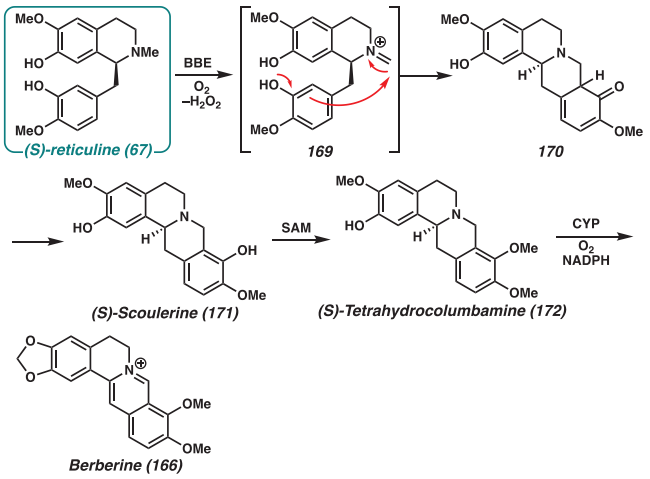

Figure 13. Proposed biosynthesis of protoberberine alkaloids **166** and **172**.

sulfinamide **175** as a mixture of diastereomers (Scheme 22A). Treatment with DIBAL followed by hydrolysis reduced the

Scheme 22. A) Davis' Synthesis of (−)-Xylopinine; B) Ruano's Synthesis of (−)-Xylopinine

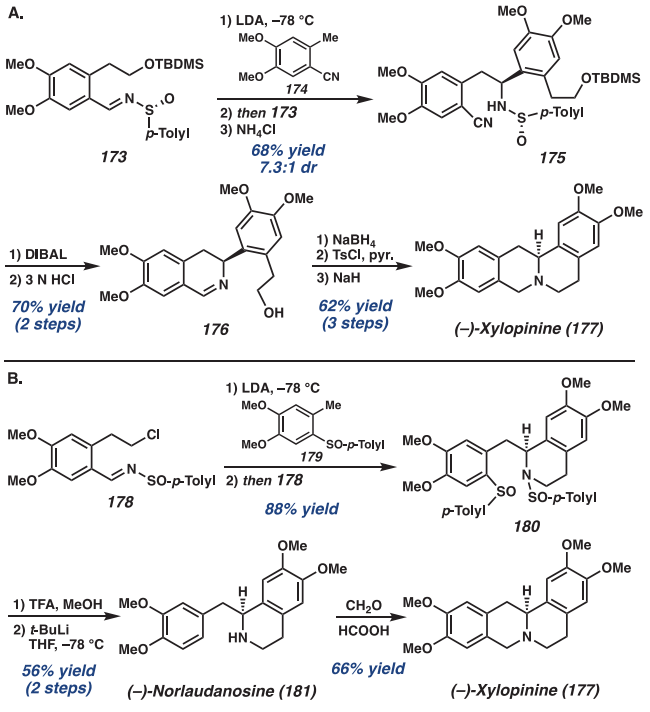

nitrile and removed the sulfinyl group to allow cyclization to afford dihydroisoquinoline **176**. Reduction of the imine, tosylation, and cyclization of the amine using NaH gave (−)-xylopinine **177** in 73% yield.

Similarly, Ruano and co-workers harnessed a similar strategy toward the synthesis of (−)-xylopinine **177**, instead using toluenesulfinamide **179** to add into *N*-sulfinylimine **178** that produced benzyl THIQ **180** in 58% yield (Scheme 22B).[59] Treatment with TFA and *t*-BuLi removed both sulfinyl groups to access (−)-norlaudanosine **181**, and a Pictet−Spengler cyclization with formaldehyde ultimately delivered (−)-xylopinine **177**. Both Yang[60] and Rozwadowska[61] have also harnessed this synthetic approach of the addition of nucleophiles to enantiopure sulfinimines to synthesize other members of the protoberberine alkaloid family.

The convergent synthetic approach of the addition of lithiated nucleophiles to dihydroisoquinolines or benzonitriles has been well explored to quickly build the protoberberine scaffold. Cho and co-workers demonstrated the convergent coupling of benzonitrile **182** and lithiated *ortho*-toluamide **183** to access isoquinolone **184** in 32% yield (Scheme 23).[62] Then, the removal of protecting groups and reaction with *p*-TsCl in the presence of K_2CO_3 delivered oxypalmatine **185**.

Scheme 23. Cho's Synthesis of Oxypalmatine

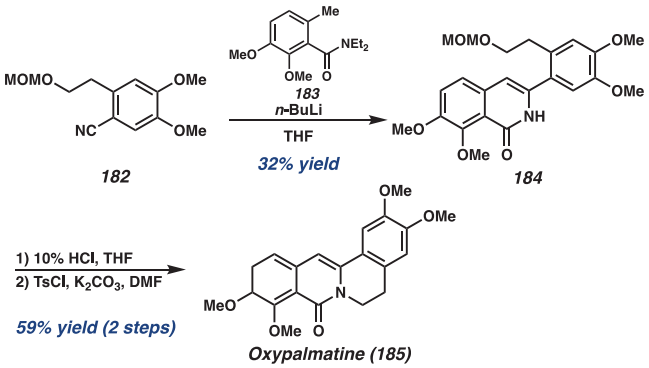

Utilizing lithiated oxazoline or oxazolidine chiral auxiliaries to add into dihydroisoquinolines, Iwao[63] and Chrzanowska[64,65] were able to synthesize both enantiomers of the protoberberine alkaloids. From enantioenriched oxazolidine **186**, treatment with *n*-BuLi generated the carbanion, followed by addition to dihydroisoquinoline **187** directly afforded oxoberbine **188** in 33% yield with 81% ee (Scheme 24A).

Scheme 24. Chrzanowska's Synthesis of A) Oxoberberine and B) (−)-Oxoxylopinine

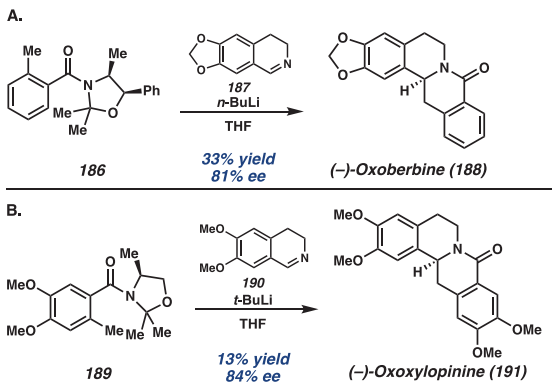

More recently, Chrzanowska and co-workers also applied the same strategy toward the synthesis of (−)-oxoxylopinine **191** from the addition of lithiated oxazolidine **189** to dihydroisoquinoline **190** (Scheme 24B).

Finally, Enders and co-workers demonstrated the addition of lithiated benzamides to enantioenriched hydrazones to assemble dihydroisoquinolones toward the synthesis of tetrahydropalmatine **167**.[66] Lithiated benzamide **192** was reacted with hydrazone **193**, which was prepared from condensation of enantiopure "SAMP" hydrazines with 3,4-dimethoxybenzaldehyde, to deliver isoquinolone **194** as a single diastereomer (Scheme 25). Then, treatment of **194** with

https://doi.org/10.1021/acs.chemrev.3c00054
Chem. Rev. 2023, 123, 9447−9496

Scheme 25. Ender's Synthesis of (−)-Tetrahydropalmatine

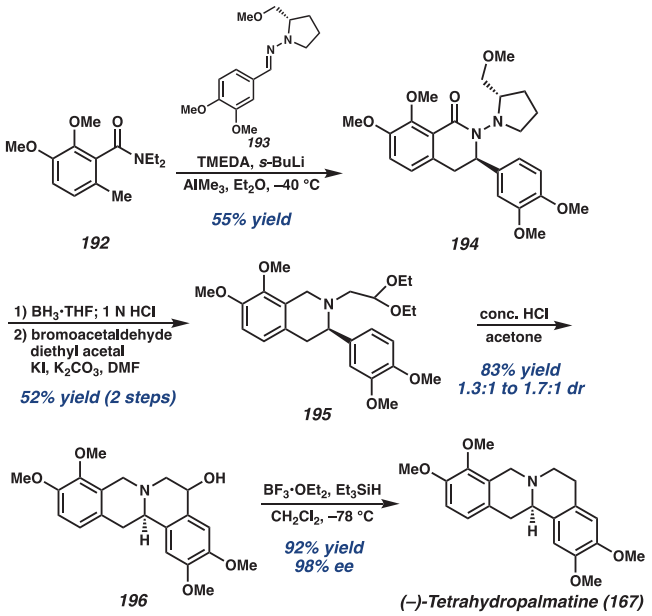

BH_3·THF cleaved the N−N bond of the chiral auxiliary, followed by the installation of the diethyl acetal moiety to afford **195**. A Pomeranz−Fritsch cyclization was then induced by using concentrated HCl to obtain protoberberine scaffold **196** as a mixture of diastereomers. Removing the hydroxyl group was achieved by using BF_3·OEt_2 and Et_3SiH to ultimately synthesize (−)-tetrahydropalmatine **167** in 92% yield with 98% ee.

More classic approaches to the protoberberine alkaloids involve electrophilic aromatic substitution chemistry to assemble the THIQ core. Both the Yang[67] and Harding[68] groups demonstrated a Bischler−Napieralski strategy toward building the THIQ core, with a tethered methyl ester allowing cyclization to the protoberberine scaffold. From amide **197**, treatment with $POCl_3$ followed by $NaBH_4$ reduction established enantioenriched THIQ **198** induced from the chiral auxiliary (Scheme 26A). Then, introduction of the methyl ester through a lithium halogen exchange and quenching with methyl chloroformate and intramolecular cyclization of the amine delivered protoberberine scaffold **199**. Yang was then able to achieve the synthesis of (−)-stepholidine **200** after carbonyl reduction and protecting group removal. Similarly, Harding utilized amide **201** with a pendent methyl ester to undergo Bischler−Napieralski cyclization and reduction to access protoberberine scaffold **202** directly (Scheme 26B). Methylation and reduction of the carbonyl then delivered isocorypalmine **203**.

Other electrophilic aromatic substitution strategies utilize formaldehyde or aldehyde equivalents to close the C-ring and access the natural product scaffold. In 2010, Georghiou and co-workers harnessed a chiral auxiliary-assisted Bischler−Napieralski cyclization and reduction of amide **204** to achieve THIQ **205**, upon which addition of formaldehyde followed by $NaBH_3CN$ reduction delivered (−)-corytenchine **206** (Scheme 27).[69]

Alternatively, Hiemstra[70] and van Maarseveen[71] and co-workers demonstrated a regioselective *ortho*- or *para*-directed Pictet−Spengler reaction to construct the THIQ core. First, a chiral phosphoric acid-catalyzed Pictet−Spengler condensation

Scheme 26. A) Yang's Synthesis of (−)-Stepholidine; B) Harding's Synthesis of Isocorypalmine

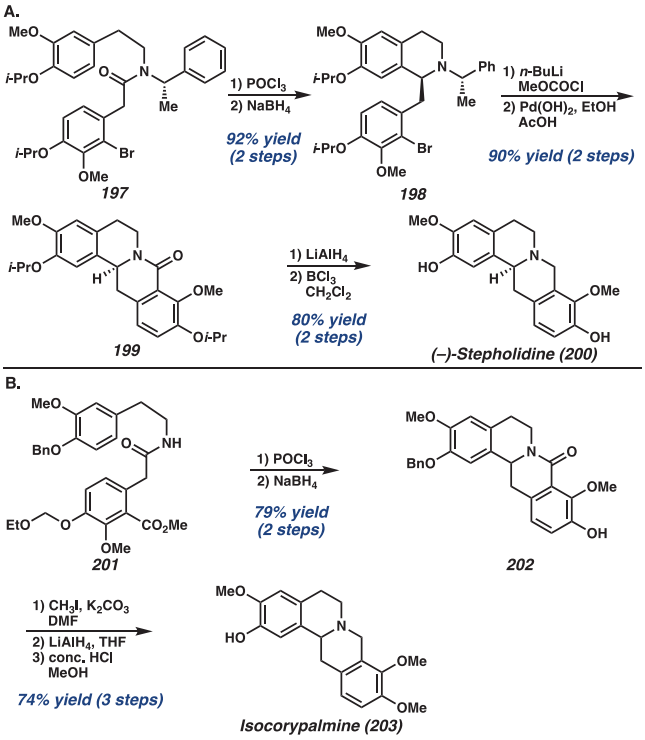

Scheme 27. Georghiou's Synthesis of (−)-Corytenchine

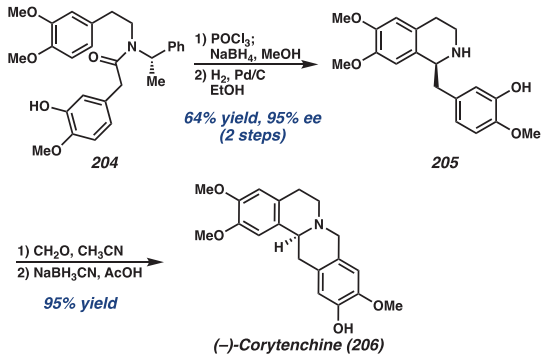

of protected amine **207** with aldehyde **208** afforded THIQ **209** in 85% yield with 90% ee (Scheme 28A). Then, a second Pictet−Spengler reaction was effected with another equivalent of aldehyde **208** to deliver either the *para*- or *ortho*-isomer depending on the solvent.

Increasing the H-bonding character of solvents such as HFIP and trifluoroethanol increased the ratio of *para*-substituted product **212**, while aprotic, apolar solvents such as toluene gave the highest selectivity of *ortho*-isomer **211**. Treatment with BBr_3 led to the formation of *para*-isomer (+)-javaberine A **213** and (+)-javaberine B **214**. van Maarseveen and co-workers demonstrated an *ortho*-selective Pictet−Spengler reaction using aldehyde **216** with equimolar amounts of **215** in toluene as the solvent to achieve the *ortho*-isomer **217** in good selectivity (Scheme 28B). Debenzylation and cyclization of the C-ring using formaldehyde under acidic conditions produced (−)-govaniadine **218** in 61% yield, allowing access to several other *ortho*-oxygenated alkaloids as well.

https://doi.org/10.1021/acs.chemrev.3c00054
Chem. Rev. 2023, 123, 9447−9496

Scheme 28. A) Hiemstra's Synthesis of (+)-Javaberine A and (+)-Javaberine B; B) van Maarseveen's Synthesis of (−)-Govaniadine

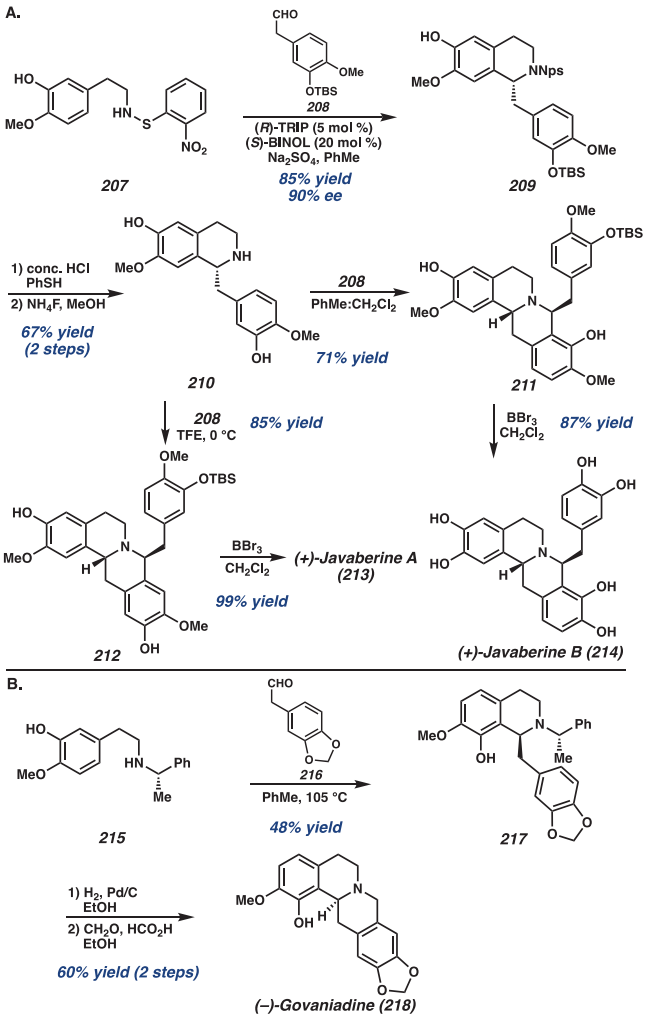

Apart from the classical synthetic approaches to the protoberberine alkaloids, Opatz and co-workers utilized a Stevens rearrangement of ammonium ylides to synthesize the protoberberine alkaloids.[72] From common synthetic intermediate THIQ **219**,[73] reaction with dibromide **220** delivered spirocyclic ammonium salt **221**, which upon deprotonation induced a Stevens rearrangement followed by reduction with $NaCNBH_3$ to obtain xylopinine **177** (Scheme 29A). This was further optimized to a one-pot cascade synthesis of pseudopalmatine **222** from **219** and **220** using DIPEA as a base, and aromatization under air to protoberberine alkaloid **222** (Scheme 29B).[74]

Several transition-metal-catalyzed annulations have been developed to apply toward the synthesis of the protoberberine alkaloids. In 2014, Donohoe and co-workers described a Pd-catalyzed enolate arylation of aryl bromides and ketones to generate masked 1,5-dicarbonyl intermediates that could readily cyclize with a source of NH_3 to an array of isoquinolines.[75] The coupling of ketone **223** and aryl bromide **224** was achieved using $Pd(amphos)_2Cl_2$ and Cs_2CO_3 to access ketone **225** in 93% yield (Scheme 30). Then, a one-pot aromatization and cyclization using NH_4Cl in ethanol and water delivered palmatine **226**. This protocol was successfully

Scheme 29. A) Opatz's Synthesis of Xylopinine and B) Pseudopalmatine

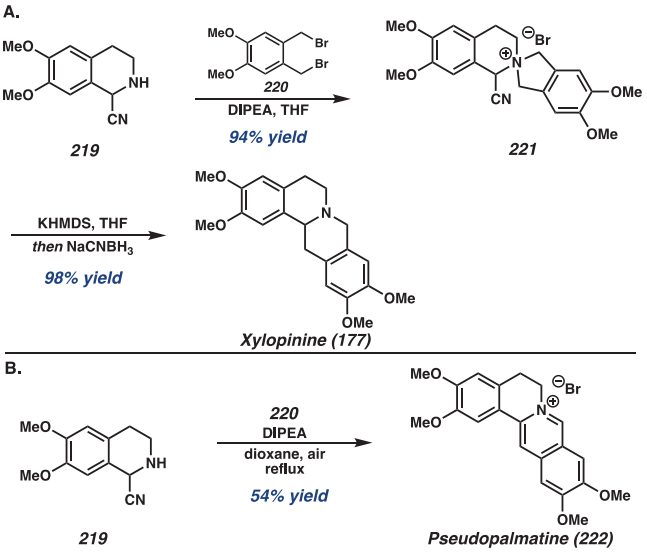

Scheme 30. Donohoe's Synthesis of Palmatine

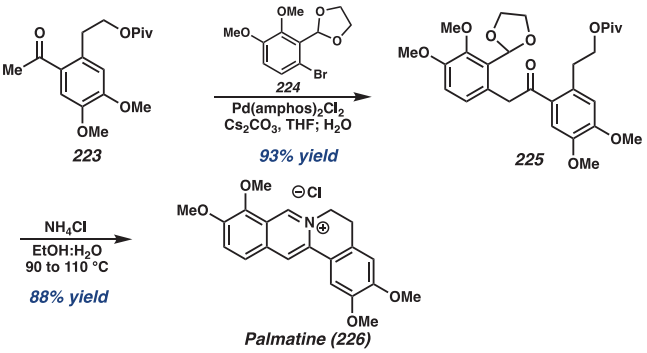

utilized for a variety of substituted aryl bromides and ketones for the rapid synthesis of protoberberine alkaloids.

Alternatively, Mhaske and co-workers employed a Pd-catalyzed intramolecular tandem olefin amidation and C−H activation method for the synthesis of the protoberberine core.[76] From amide **227**, iodination and Stille coupling with vinyl tributyltin afforded key precursor **228** (Scheme 31). Using $Pd(OAc)_2$ as a catalyst and $Cu(OAc)_2{\cdot}H_2O$ and O_2 as an oxidant, **228** first underwent amidation to assemble the THIQ, followed by C−H activation of the arene to allow cyclization to oxotetrahydropalmitine **229** in 55% yield.

Scheme 31. Mhaske's Synthesis of Oxotetrahydropalmitine

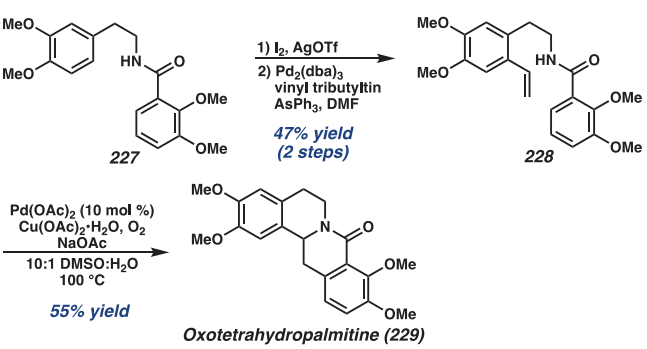

https://doi.org/10.1021/acs.chemrev.3c00054
Chem. Rev. 2023, 123, 9447−9496

In 2016, Cheng and co-workers developed a general Rh-catalyzed C−H activation and annulation method to afford various natural and unnatural protoberberine alkaloids.[77] An array of substituted benzaldehydes, such as **230**, were coupled with alkyne **231** using $[RhCp^*(CH_3CN)_3][SbF_6]_2$ as a catalyst with $Cu(BF_4)_2{\cdot}6H_2O$ and O_2 as an oxidant to deliver protoberberine alkaloid corysamine **232** in 92% yield (Scheme 32). This one-pot transformation was successfully employed

Scheme 32. Cheng's Synthesis of Corysamine

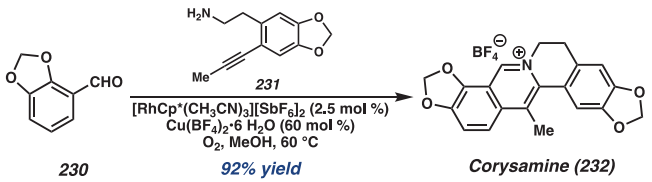

for a variety of benzaldehydes and alkyne amines to provide a library of protoberberine salts in good yield and selectivity.

Glorius and co-workers also reported a C−H activation annulation approach of substituted benzamides to install the oxyprotoberberine core.[78] Using $Cp^*Co(CO)I_2$ as a catalyst, benzamide **233** underwent alkyne insertion, reductive C−N bond formation, and N−O bond cleavage to achieve isoquinolone **234** in a single transformation (Scheme 33). A

Scheme 33. Glorius' General Synthesis of Protoberberine Alkaloids

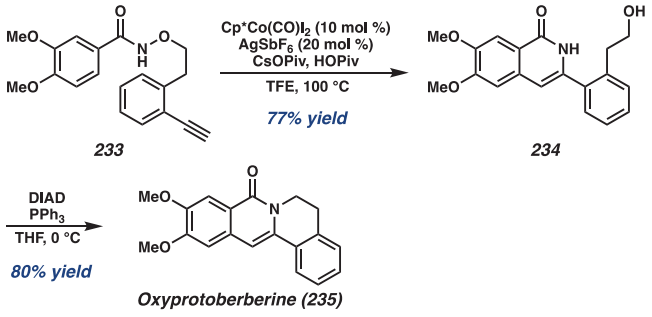

Mitsunobu reaction then constructed the oxyprotoberberine scaffold **235** in 80% yield, which could be further elaborated into protoberberine or tetrahydroprotoberberine alkaloids.

Harnessing a Cu-catalyzed three component coupling reaction of an amine, aldehyde, and alkyne, Tong and co-workers optimized a general annulation strategy that enabled the syntheses of over 30 natural protoberberine alkaloids.[79,80] To this end, THIQ **236**, benzaldehyde **237**, and trimethylsilylacetylene were employed in a three component condensation reaction to afford THIQ **238** in 81% yield (Scheme 34). Then, a Pd-catalyzed reductive carbocyclization reaction successfully provided the desired tetracycle **239** of the protoberberine core. Hydrogenation of the *exo*-olefin delivered natural product thalictricavine **240** as a single diastereomer. A Rh-catalyzed isomerization of **239** with concomitant oxidation under air also provided the protoberberine salt dehydrothalictricavine **241** in 65% yield. With this highly efficient synthetic route, a variety of 13-methyl-protoberberine alkaloids were synthesized for the first time, including their analogues in excellent overall yields.

Finally, Ward and co-workers employed a novel chemoenzymatic cascade toward the synthesis of the tetrahydroprotoberberine alkaloids.[81] From dopamine **61**, first a Pictet−Spengler condensation using a transaminase enzyme (TAm) from CV2025 *Chromobacterium violaceum* and a norcoclaurine synthase enzyme (NCS) delivered THIQ **242** in 87% yield with 99% ee (Scheme 35). Then, the addition of formaldehyde induced a second Pictet−Spengler reaction to deliver tetrahydroprotoberberine alkaloid **243** in 64% yield.

Scheme 34. Tong's Synthesis of Thalictricavine and Dehydrothalictricavine

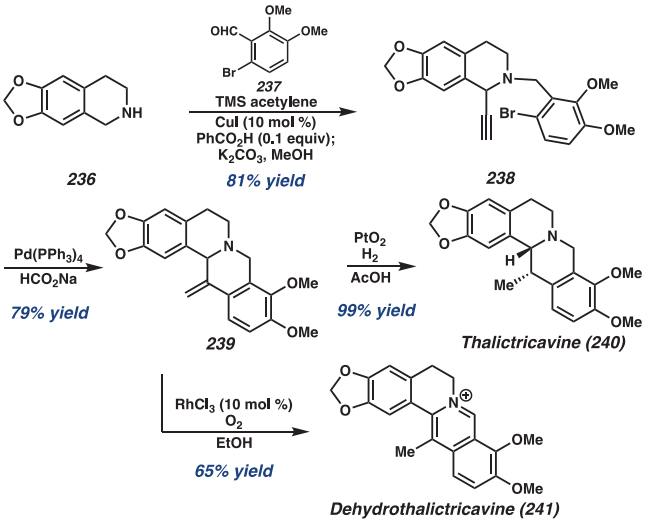

Scheme 35. Ward's Chemoenzymatic Synthesis of Tetrahydroprotoberberine Alkaloid

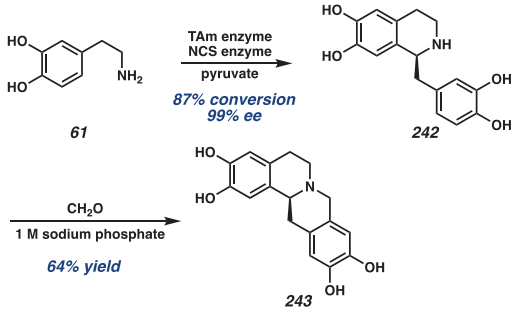

4.4. Morphinan Alkaloids

4.4.1. General Structure and Biosynthesis. The morphinan alkaloids are distinguished by their phenanthrene core with a bridging piperidine ring and a fused benzodihydrofuran moiety. They are famous THIQ-derived natural products well-known for their analgesic and anesthetic bioactivity. Morphine **244** is commonly used to treat severe pain, while other members such as naltrexone **245** and naloxone **246** are commercially produced for treatment of opiate overdoses and alcohol addiction (Figure 14).[82] Isolated primarily from opium poppy *Papaver somniferum*, the global production of opium poppy concentrate is estimated to be around 8700 tons per year, of which morphine and codeine are the principal ingredients.[83]

The biosynthesis of morphine and its related congeners stems from key intermediate reticuline **67**, which is converted to the (*R*)-enantiomer by 1,2-dehydroreticuline reductase (Figure 15).[82] Then, an oxidative phenol coupling catalyzed by salutaridine synthase (CYP719B1) establishes the morphinan

https://doi.org/10.1021/acs.chemrev.3c00054
Chem. Rev. 2023, 123, 9447−9496

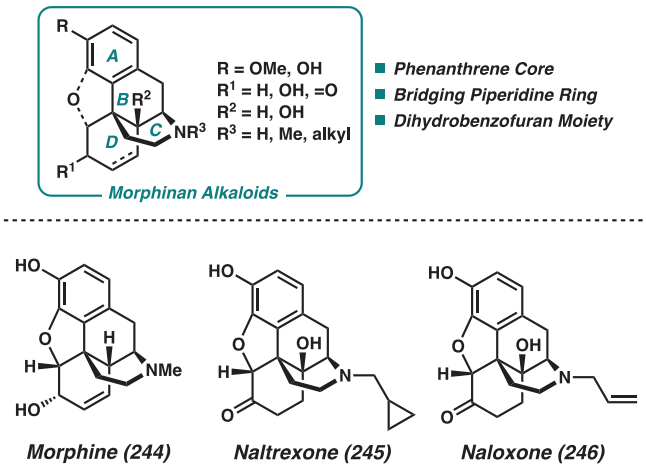

Figure 14. General structure of the morphinan THIQ alkaloids.

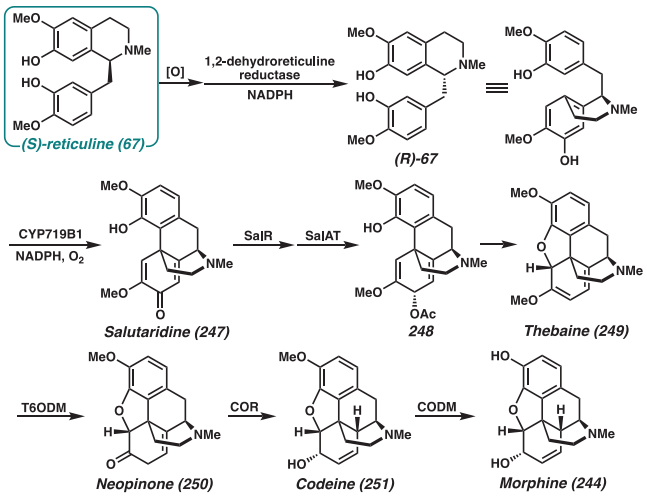

Figure 15. Proposed biosynthesis of morphine **244** and related members of the morphinan alkaloids.

skeleton in salutaridine **247**. Tetracycle **247** is then reduced by salutaridine reductase and acetylated by salutaridinol acetyltransferase to deliver salutaridinol-7-*O*-acetate **248**. An S_N2'-type cyclization then occurs to establish the dihydrobenzofuran moiety in thebaine **249**. Thebaine-6-*O*-demethylase (T6ODM) cleaves off the methyl group to give neopinone **250**, which can undergo isomerization and reduction of the carbonyl by codeinone reductase (COR) to yield codeine **251**.[84] Finally, demethylation catalyzed by codeine *O*-demethylase (CODM) produces morphine **244**.

4.4.2. Total Syntheses of Morphinan Alkaloids. Since Gates' first synthesis of morphine in 1952, many others have pursued the synthesis of this alkaloid and other related natural products from this family.[85] The continuing interest in the morphinan alkaloids as synthetic targets has resulted in numerous reviews in the total synthesis of these alkaloids, and thus this section will only cover the most recent syntheses from the past decade.[86−89]

A myriad of strategies for the synthesis of morphine have been well explored in the past several decades. In particular, Fukuyama and co-workers have disclosed several syntheses of morphine featuring an intramolecular Mannich cyclization to construct the THIQ core.[90−92] However, their most recent synthesis of (−)-morphine utilizes chiral substrate **252** to construct the morphine skeleton via a Friedel−Crafts cyclization and dehydration to deliver **253** (Scheme 36).[93]

Scheme 36. Fukuyama's Synthesis of (−)-Morphine

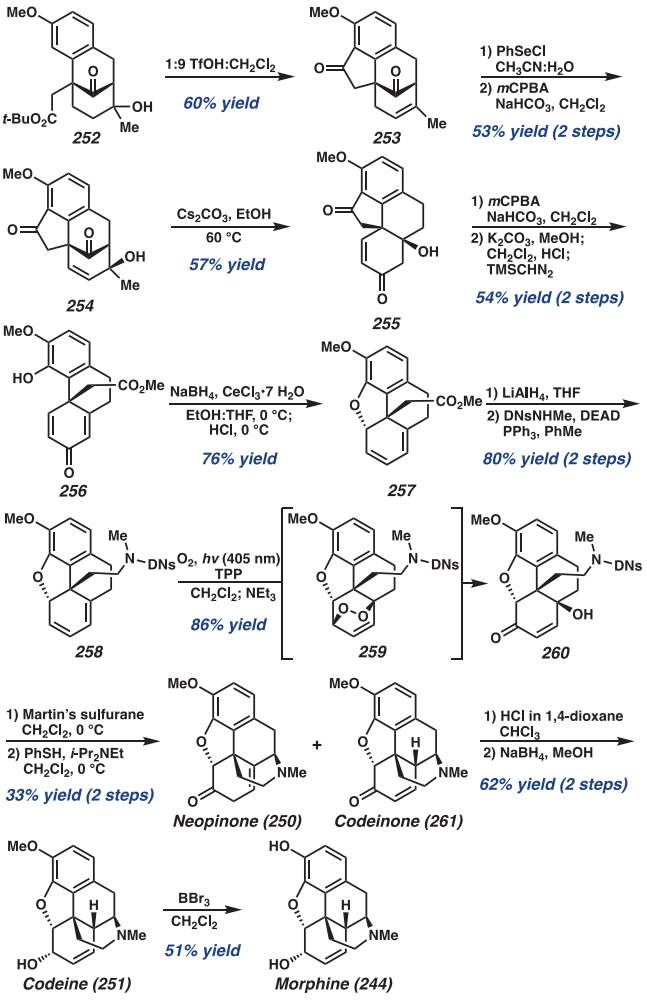

Hydroxyselenenylation of the resulting olefin followed by oxidation and elimination generates allylic alcohol **254**, which undergoes a retro-aldol/aldol sequence to furnish enone **255**. Construction of the dihydrofuran ring commenced with Baeyer−Villiger oxidation and methanolysis of the lactone to afford dienone **256**. Luche reduction of the enone followed by treatment with HCl then caused the formation of a dienyl cation and interception with the phenol to furnish the dihydrofuran ring **257**. With the tetracyclic scaffold in place, functional manipulations with the pendent methyl ester moiety to the protected tertiary amine **258** were set up for oxidation with singlet oxygen to give endoperoxide **259**. Treatment with triethylamine induced cleavage of the O−O bond to afford hydroxyenone **260**, with dehydration of the alcohol and removal of the DNs group facilitating 1,6-addition to access natural products neopinone **250** and codeinone **261**, with further reduction to deliver codeine **251** and morphine **244**.

In an alternative fashion, Chida and co-workers sought to access (−)-morphine **244** through an elegant sequential Claisen rearrangement of an allylic vicinal diol, resulting in the stereoselective formation of two C−C bonds and two contiguous stereocenters in a single operation (Scheme 37).[94] Starting from allylic vicinal diol **262**, a Johnson-type Claisen

https://doi.org/10.1021/acs.chemrev.3c00054
Chem. Rev. 2023, 123, 9447−9496

Scheme 37. Chida's Formal Synthesis of (−)-Morphine

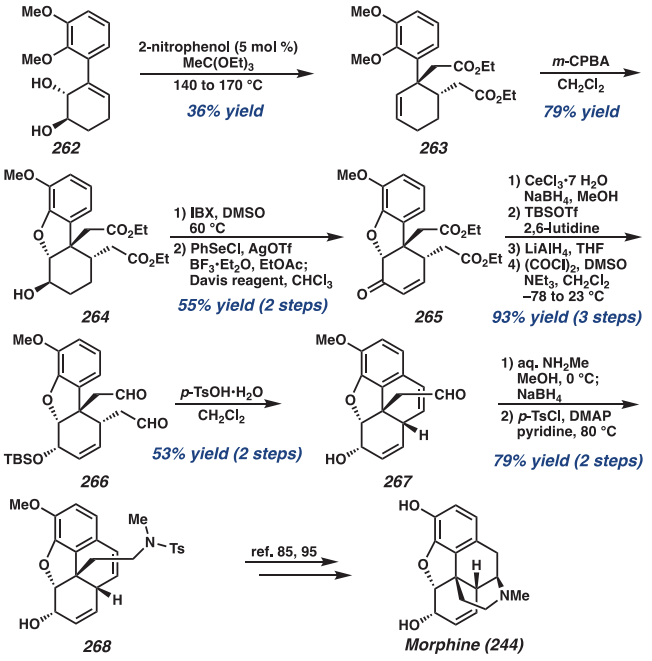

Scheme 38. Smith's Total Synthesis of (±)-Morphine

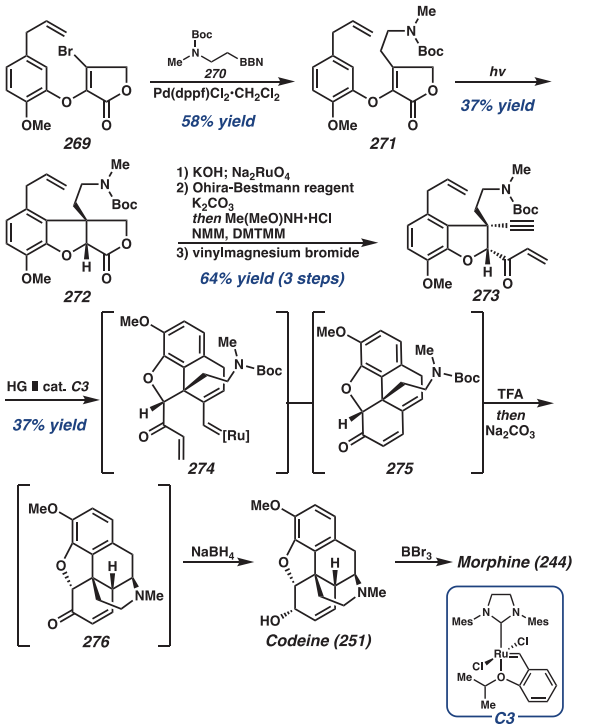

rearrangement with $MeC(OEt)_3$ in the presence of 2-nitrophenol initiated the sequential Claisen/Claisen rearrangement to provide **263**. In this transformation, both the vicinal quaternary and tertiary stereocenters were installed in a single transformation. Construction of the benzofuran moiety then was accomplished by treatment of **263** with *m*CPBA, inducing demethylative etherification of the epoxide to deliver **264**. Further oxidative manipulations afforded enone **265**, and following reduction, protection of the resulting alcohol, global reduction, and Swern oxidation, dialdehyde **266** was accessed to construct the tetracyclic scaffold. A Friedel−Crafts cyclization using *p*-TsOH·H_2O allowed for the installation of the tetracycle **267** with concomitant removal of the TBS group. Finally, reductive amination and protection of the secondary amine generated late-stage intermediate **268**, which was only two steps away from the natural product synthesis.[85,95]

Toward the synthesis of (±)-morphine, Smith and co-workers utilized a diastereoselective light-mediated cyclization to establish the benzofuran moiety, and a cascade ene-yne-ene ring closing metathesis to forge the tetracyclic scaffold (Scheme 38).[96] First, a challenging sp^3-sp^2 Suzuki−Miyaura cross-coupling of vinyl bromide **269** with *β*-amino borane derivative **270** was accomplished using $Pd(dppf)Cl_2{\cdot}CH_2Cl_2$ as a catalyst. Photocyclization of **271** then proceeded smoothly to deliver *cis*-fused **272** as the sole product. After subsequent functional group manipulations to install the terminal alkyne and vinyl ketone in **273**, the cascade ene-yne-ene metathesis was accomplished using the Hoveyda−Grubbs II catalyst (**C3**). It is proposed that the transformation proceeded via the reaction of the ruthenium catalyst with the allyl component of **273** first, followed by an intramolecular reaction with the alkyne to generate alkylidene intermediate **274**. Ring closing metathesis with the vinyl ketone then afforded tetracycle **275**, which was subjected further to deprotection of the amine and 1,6-addition to afford the morphine scaffold **276**. Diastereoselective reduction of the ketone delivered codeine **251** as a single diastereomer as well as morphine **244** after demethylation.

Most recently, Tu and co-workers disclosed an enantioselective synthesis of (−)-morphine harnessing a catalytic enantioselective Robinson annulation to rapidly construct the benzofuran moiety of the natural product.[97] From enone **277**, which was prepared in four steps from commercially available materials, an intramolecular Michael addition, followed by Robinson annulation, was thoroughly investigated and optimized. Ultimately, spiropyrrolidine catalyst **C4** with triisopropylbenzoic acid as an additive proved to be the most effective in delivering tricycle **279** in 66% yield with 94% ee (Scheme 39). This key transformation performed well on up to a 5 g scale to rapidly build stereochemical complexity toward the morphine scaffold.

With large amounts of **279** in hand, prenylation followed by ozonolysis and treatment with a catalytic amount of poly(phosphoric acid) induced a Friedel−Crafts cyclization to afford tetracycle **281**. After selective epoxidation and the Wharton reaction to achieve allylic alcohol **282**, cleavage of the benzyl group and an intermolecular Mitsunobu reaction deliver amine **283**. Inversion of the allylic alcohol stereocenter and deprotection of the tosyl group promoted the hydroamination reaction to access (−)-codeine **251**, and subsequent demethylation was used to synthesize (−)-morphine **244**.

Toward the synthesis of other related morphine alkaloids, Fukuyama and co-workers disclosed the synthesis of oxycodone **295**, which is distinguished from morphine by the ketone and additional hydroxyl functionality.[98] Their synthetic approach commenced with the alkylation of arene **284** with the enolate derived from imide **285** to furnish **286** as a single diastereomer (Scheme 40).

Removal of the chiral auxiliary and subsequent methylation of the acid delivered **287** to set up for direct arylation. Thus, treatment of **287** with $Pd(OAc)_2$ resulted in arylation to

https://doi.org/10.1021/acs.chemrev.3c00054
Chem. Rev. 2023, 123, 9447−9496

Scheme 39. Tu's Total Synthesis of (−)-Morphine

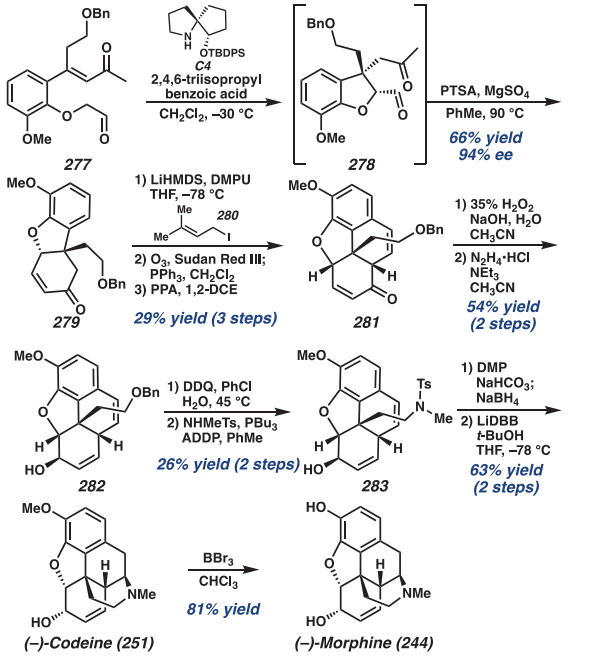

Scheme 40. Fukuyama's Total Synthesis of (−)-Oxycodone

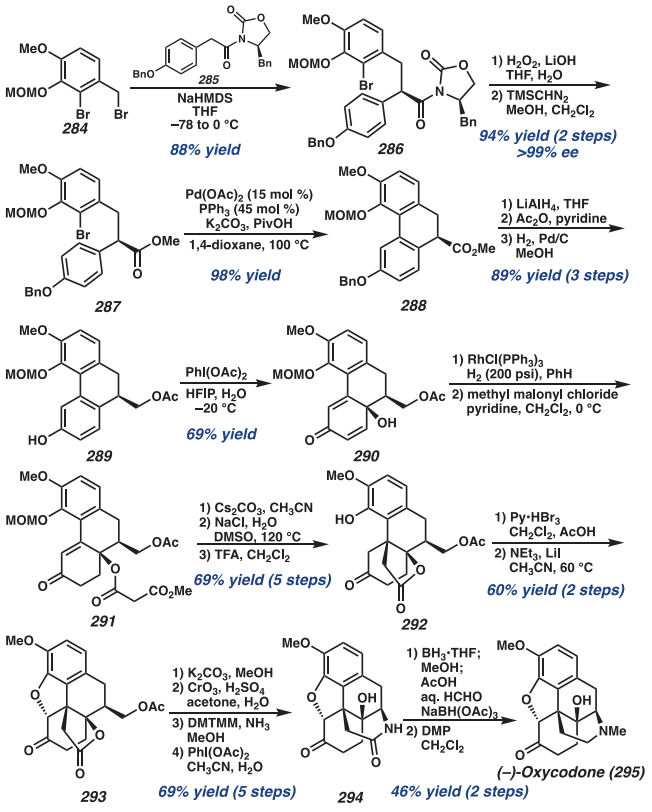

establish the tricycle, which upon reduction of the ester, acetylation, and debenzylation gave phenol **289**. Next, a key oxidative dearomatization was attempted to install the hydroxyl group. Reaction of **289** with $PhI(OAc)_2$ afforded the desired intermediate **290** in 69% yield, followed by selective hydrogenation and acylation to deliver enone **291**. Upon treatment with Cs_2CO_3, an intramolecular Michael addition proceeded to deliver the desired lactone **292** after two additional manipulations. Selective α-bromination of the ketone allowed the formation of benzofuran moiety **293** by displacement with the phenol. Functionalization of the acetate to the amide set up for a Hofmann rearrangement, followed by hydrolysis of the resulting isocyanate to the primary amine and amidation to form the desired lactam **294**. Finally, reduction of the lactam, *N*-methylation, and oxidation of the secondary alcohol furnished (−)-oxycodone **295**.

Other approaches toward the synthesis of oxycodone include a desymmetrization-based strategy reported by Chen and co-workers.[99] To this end, an oxidative dearomatization of phenol **296** under hypervalent iodine conditions afforded hydroxy dienone **297** that could rapidly build tricycle **298** by using an intramolecular Heck cyclization (Scheme 41).

Scheme 41. Chen's Total Synthesis of (+)-Oxycodone

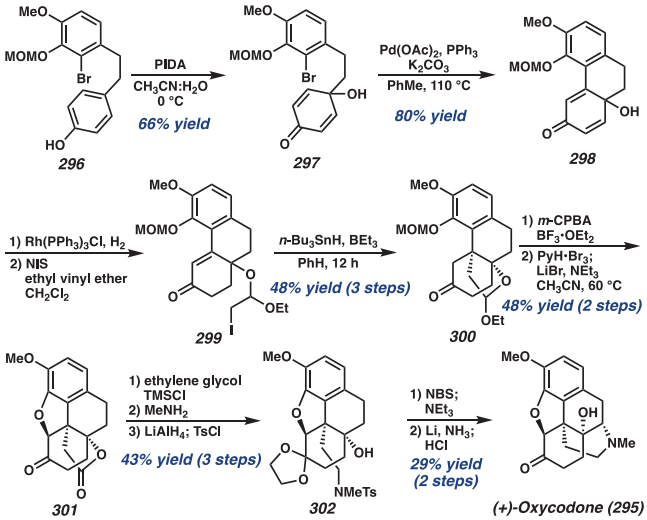

Installation of the all-carbon quaternary stereocenters was accomplished through a radical cyclization of iodoacetal **299** to deliver lactol **300**, which could then be further oxidized to deliver the morphinan scaffold **301**. Protection of the ketone, followed by amidation and reduction, led to the formation of amine **302**, which furnished oxycodone **295** after desaturation and deprotection steps. This developed sequence demonstrated a shorter step-count in comparison to the original Fukuyama synthesis.

Chen and co-workers' alternative synthetic approach to the morphinan family of natural products was developed from their method of oxidative dearomatization of atropisomerically pure biaryl phenols to achieve complex intramolecular Diels–Alder products such as **303**.[100] To demonstrate the synthetic utility of these intermediates, **303** was elaborated into lactam **305** via Beckmann rearrangement of oxime **304** (Scheme 42). Reduction of the amide, followed by Hoffmann elimination, induced further cleavage of the bridgehead C–N bond to furnish amine **306**. Selective reduction, deoxygenation, and demethylation were sequentially performed to deliver the key intermediate **308**. Then, phenolic demethylation followed by treatment with pyridinium tribromide established dihydrobenzofuran ring **309**, with subsequent olefin isomerization and detosylation to synthesize dihydrocodeinone **310**. **310** serves as a valuable intermediate to access a variety of morphinan alkaloids including codeine, morphine, thebaine, and oxycodone.

https://doi.org/10.1021/acs.chemrev.3c00054
Chem. Rev. 2023, 123, 9447–9496

Scheme 42. Chen's Total Synthesis of (+)-Dihydrocodeinone

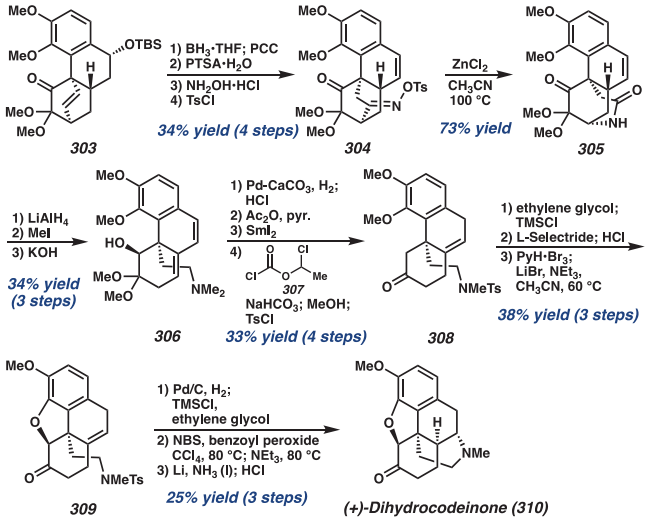

In 2014, Opatz and co-workers have also disclosed a general strategy toward the enantioselective synthesis of (−)-dihydrocodeine **318** and other related morphinan alkaloids (Scheme 43).[101] Their key intermediate is prepared from

Scheme 43. Opatz's Total Synthesis of (−)-Dihydrocodeine

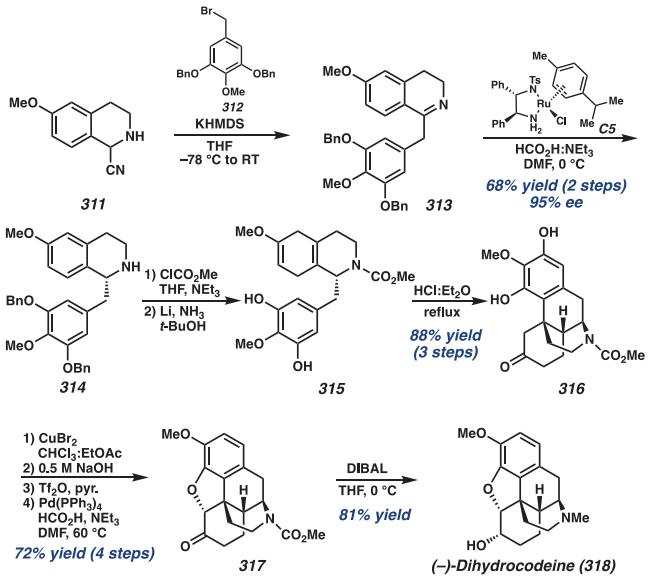

aminonitrile **311**, which upon deprotonation with KHMDS furnished a stabilized α-aminocarbanion, which was alkylated with benzyl bromide **312** to deliver **313** upon spontaneous dehydrocyanation.

Enantioselective reduction of **313** using Noyori's asymmetric hydrogenation catalyst **C5** delivered THIQ **314** with 95% ee. With the C1 stereocenter established, the secondary amine was protected, followed by Birch reduction furnishing carbamate **315**, which was immediately set up for a Grewe cyclization to establish two new stereogenic centers of the tetracycle **316**. α-Bromination and treatment with NaOH closed the dihydrobenzofuran ring, with subsequent triflation and Pd-catalyzed detriflation furnishing **317** in 80% yield. Treatment with DIBAL ultimately reduced both the ketone and carbamate, accessing dihydrocodeine **318** in 81% yield. Intermediate **318** also constitutes the formal synthesis of thebaine **249**, while **317** served as a precursor for the synthesis of codeine and morphine.

This synthetic strategy toward the morphinan alkaloids as well as their biosynthesis also further inspired the development of an electrochemical oxidative coupling of benzyl THIQs.[102,103] Toward the synthesis of thebaine **249**, Opatz and co-workers optimized an electrochemical oxidative coupling of THIQ **319** using Pt electrodes in an undivided cell, achieving tetracycle **320** regio- and diastereoselectively (Scheme 44A). With this developed methodology, they

Scheme 44. A) Opatz's Optimized Electrochemical Oxidative Coupling; B) Application Toward the Total Synthesis of (−)-Thebaine

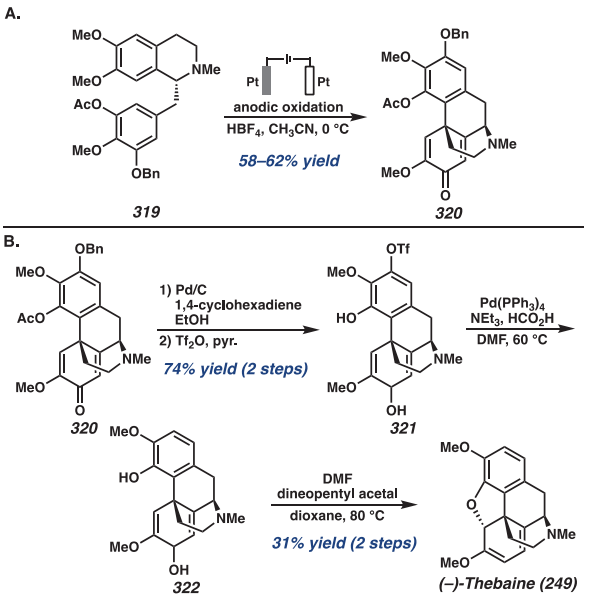

demonstrated the synthesis of both racemic and (−)-thebaine **249** through several functional group manipulations and a biomimetic S_N2', involving activation of the allylic alcohol **322** with *N*,*N*-dimethylformamide dineopentyl acetal to close the dihydrobenzofuran ring (Scheme 44B). This electrochemical coupling strategy has also been applied toward the total synthesis of (−)-oxycodone **295** from tetracycle **320**.[103]

The synthesis of the morphinan alkaloids, and in particular oxycodone, has been extensively explored by Hudlicky and co-workers for more than 25 years. Several generations of the chemoenzymatic synthesis of *ent*-oxycodone have been reported, featuring a key Heck cyclization to achieve the dihydrobenzofuran ring and ultimately a keto-nitrone coupling to establish the natural product scaffold.[104] The final synthetic route began with the enzymatic dihydroxylation of phenethyl acetate by whole-cell fermentation with *E. coli* JM109 (pDTG601A) to produce *cis*-diol **324**, which was subsequently reduced and protected as a silyl ether to deliver **325** (Scheme 45). A Mitsunobu coupling of the allylic alcohol with phenol **326** then afforded intermediate **327**, which upon an intramolecular Heck reaction constructed dihydrobenzofuran ring **328**. Dihydroxylation of the olefin, followed by DBU-mediated elimination via formation of an intermediate lactol furnished ketone **329** in 63% yield. Oxidative manipulations to transform the acetate to a methyl ester delivered intermediate **330**, and

https://doi.org/10.1021/acs.chemrev.3c00054
Chem. Rev. 2023, 123, 9447−9496

Scheme 45. Hudlicky's Total Synthesis of (+)-Oxycodone

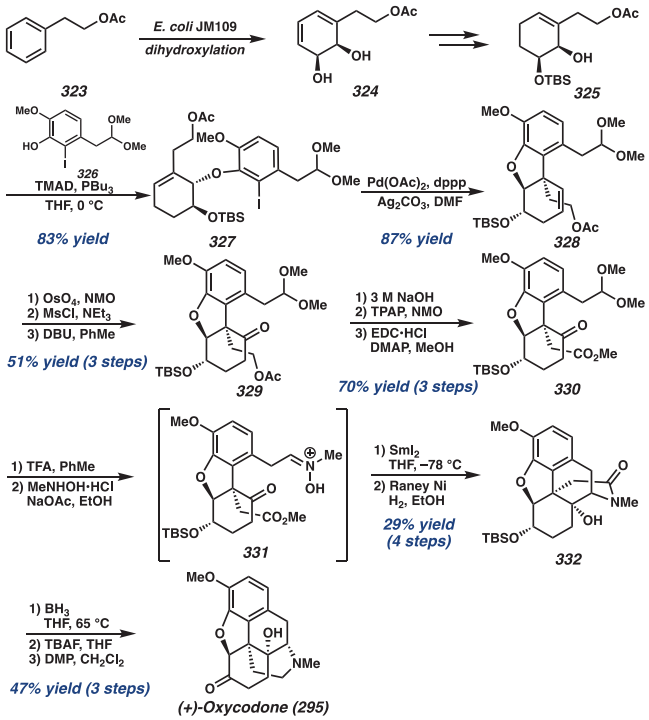

Scheme 46. Zhang's Total Synthesis of Codeine

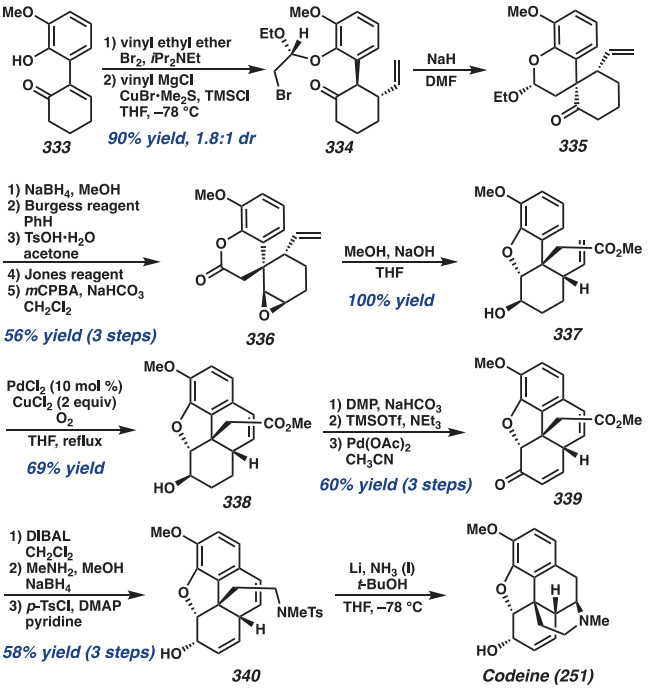

then deprotection of the acetal afforded an aldehyde intermediate, which was treated with *N*-methyl hydroxylamine to provide nitrone **331**. Treatment with SmI_2 then induced cyclization to the lactone with the desired stereochemistry, which upon Raney nickel reduction furnished lactam **332**. Finally, further reduction of the amide carbonyl and oxidation of the alcohol delivered *ent*-oxycodone **295**. Overall, the fourth-generation synthesis of oxycodone was accomplished in 11 steps from phenethyl acetate via a key nitrone intermediate to achieve the correct stereochemistry.

More recent synthetic approaches to the morphinan alkaloids harness C−H activation strategies to efficiently establish the natural product scaffold. For instance, Zhang and co-workers report the total synthesis of codeine and morphine featuring a cascade cyclization to construct the dihydrofuran ring, and an intramolecular Pd-catalyzed C−H olefination of an unactivated alkene to install the morphinan skeleton (Scheme 46).[105] Starting from phenol **333**, which was quickly accessed by Suzuki coupling, treatment with ethyl vinyl ether followed by Michael addition with vinyl magnesium bromide in the presence of copper(I) bromide delivered ketone **334** in 1.8:1 dr relative to the ketal center. The undesired diastereomer could be converted to **334** upon treatment with 2 N HCl. Treatment of **334** with NaH afforded spiroketone **335** as a single diastereomer, with subsequent manipulations of the ketone to give epoxide **336**. Then, the key cascade cyclization was accomplished using MeOH in the presence of NaOH by opening the lactone ring and attacking the epoxide to deliver **337**. Next, an intramolecular Pd-catalyzed C−H alkenylation was performed to deliver **338** with high regioselectivity. With the tetracycle established, **338** was eventually converted to the natural product using oxidative manipulations to achieve enone **339**, DIBAL reduction, and reductive amination to furnish amine **340**, and a radical cyclization to synthesize codeine **251**.

Ellman and co-workers alternatively devised a Rh-catalyzed C−H alkenylation and electrocyclization cascade strategy to synthesize the THIQ framework toward the total synthesis of (−)-naltrexone **245** (Scheme 47).[106] From imine **341**, which was prepared in 8 steps from commercial starting materials, a Rh(I)-catalyzed C−H activation of the olefin was initiated, followed by alkyne insertion to deliver an azatriene intermediate **342**. Triene **342** undergoes rapid electrocyclization *in situ* to access dihydropyridine **343**, which was subsequently reduced to deliver THIQ **344**. Treatment of **344** with dilute H_3PO_4 then afforded morphinan scaffold **346** in a 66% yield. They propose that this transformation likely proceeded through removal of the silyl and acetonide protecting groups, followed by allylic alcohol ionization and a hydride shift to provide ketone **345**. A Grewe cyclization then established the desired morphinan skeleton. Treatment of **346** with Br_2 then afforded a dibrominated intermediate due to facile bromination of the electron-rich aromatic ring, followed by nucleophilic displacement to establish the dihydrofuran ring. Triflation of the phenol followed by dehydrogenation of the ketone using $Pd(TFA)_2$ installed enone **347**. Finally, a late-stage C−H hydroxylation of enone **347** was performed to access the natural product. Using pyridine as the solvent and ketoglutaric acid to reduce the peroxide intermediate, treatment of **347** with $CuSO_4$ and O_2 successfully installed the hydroxyl group with the correct stereochemistry to yield **348**. Removing the bromide and triflate groups, reduction of the enone, and demethylation with BBr_3 ultimately afforded (−)-naltrexone **245**.

In 2020, Metz and co-workers described the total synthesis of thebainone A **357**, harnessing an intramolecular nitrone cycloaddition and a Heck cyclization to construct the natural product scaffold (Scheme 48).[107] From ester **349**, which was accessed in 4 steps from isovanillin, a Heck cyclization using $Pd_2(dba)_3$ and Ag_2CO_3 induced formation of spirolactone **350** in 83% yield. Deprotection of the ketone and aldehyde, followed by treatment with *N*-methylhydroxylamine induced a

https://doi.org/10.1021/acs.chemrev.3c00054
Chem. Rev. 2023, 123, 9447−9496

Scheme 47. Ellman's Total Synthesis of (−)-Naltrexone

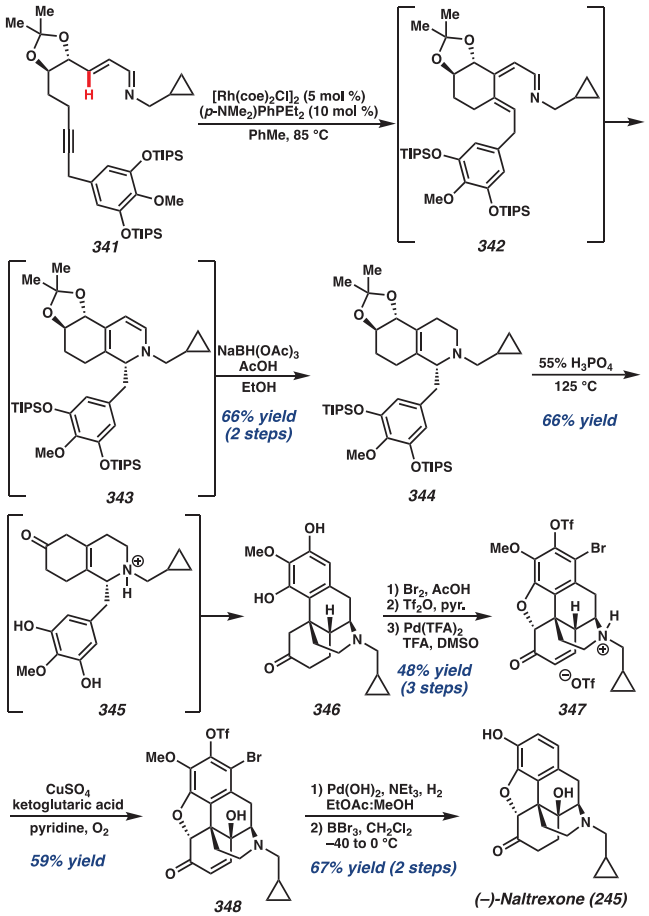

Scheme 48. Metz's Total Synthesis of Thebainone A

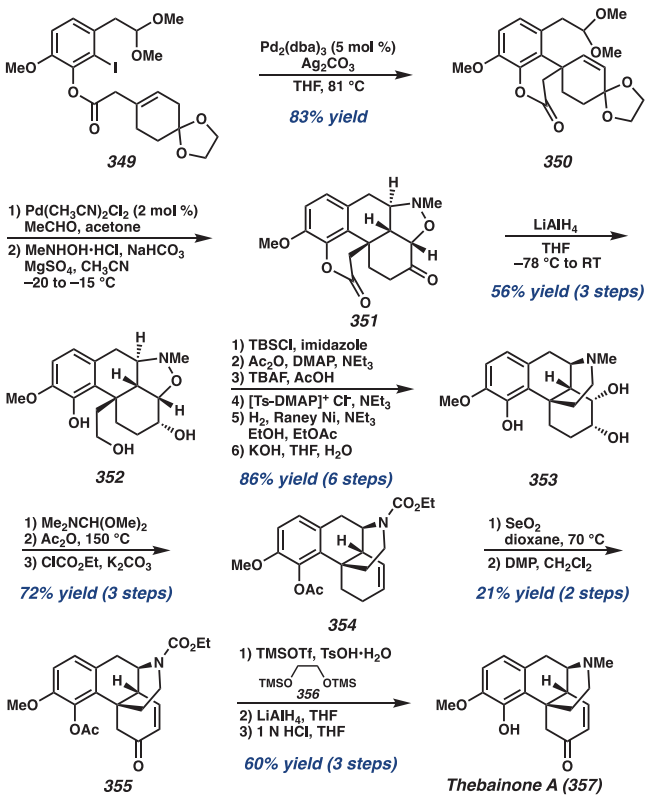

diastereoselective nitrone cycloaddition to achieve isoxazolidine **351**.

Since this ketolactone was rather unstable, subsequent reduction with $LiAlH_4$ delivered **352**, and conversion of the primary alcohol to a tosylate was then followed by reductive cleavage of the heterocycle with concomitant nucleophilic substitution to generate **353**. To install the enone moiety, the *cis*-diol was reductively eliminated by formamide acetal pyrolysis with subsequent acetylation and ethyl carbamate formation to give **354**. Allylic oxidation followed by DMP oxidation then successfully installed enone **355** in 21% yield over two steps. Finally, protection of the ketone was required to reduce the carbamate and acetate groups, and deprotection with 1 N HCl ultimately provided thebainone A **357**.

4.5. Pavine and Isopavine Alkaloids

4.5.1. General Structure and Biosynthesis. The pavine and isopavine alkaloids contain a characteristic tetracyclic tetrahydroisoquinoline core structure consisting of a dibenzo-9-azabicyclo[3.3.1]nonane and dibenzo-9-azabicyclo[3.2.2]-nonane, respectively (Figure 16).[108] They are mainly found

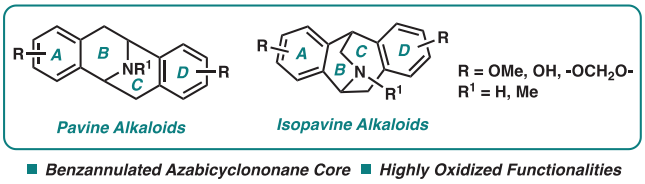

Figure 16. General structure of the pavine and isopavine THIQ alkaloids.

in four plant families, the Papaveraceae, Berberidaceae, Lauraceae, and Ranunculaceae families.[108] These alkaloids have been shown to possess interesting bioactivity for the treatment of nerve system disorders such as Alzheimer's, Parkinson's disease, and Huntington's chorea.[109]

Although the complete biosynthesis of the pavine and isopavine alkaloids has not been entirely elucidated, there are some speculations about their biogenetic precursors. It is likely that they are derived from benzyl THIQ reticuline **67** or a similar analog thereof, which undergoes cyclization at either the C3 or C4 position of the THIQ ring to achieve the pavine or isopavine scaffold, respectively.[110] For the isopavine alkaloids, a 4-hydroxybenzyl THIQ is postulated as a precursor that could undergo dehydration and cyclization to achieve the azabicyclo[3.2.2]nonane core.[111] Alternatively, it has been suggested that pavine alkaloids are derived from a similar intermediate such as 4-hydroxynorlaudanosoline, from which a dehydration reaction and cyclization at the C3 position would yield the pavine skeleton.[110] More recently, Ng and co-workers elucidated the structure of an *N*-methyltransferase enzyme (pavine NMT) that is involved in the *N*-methylation of the pavine alkaloids.[112]

4.5.2. Total Syntheses of Pavine and Isopavine Alkaloids. In 2004, Marazano reported the synthesis of (−)-argemonine **363**, enabled by a key enantioselective transformation of isoquinolinium salt **358** to 1-benzyl isoquinoline derivative **361** (Scheme 49).[113] Isoquinolinium salt **360** was prepared in two steps from salt **358**, and the reduction of **360** with $LiAlH_4$ formed tertiary amine **361**. Cyclization of **361** in the presence of formic acid and H_3PO_4 supplied benzylamine **362** with a 93:7 dr. Hydrogenolysis with Pd/C (10 mol %) and H_2 cleaved the chiral auxiliary, which

https://doi.org/10.1021/acs.chemrev.3c00054
Chem. Rev. 2023, 123, 9447−9496

Scheme 49. Marazano's Enantioselective Synthesis of (−)-Argemonine

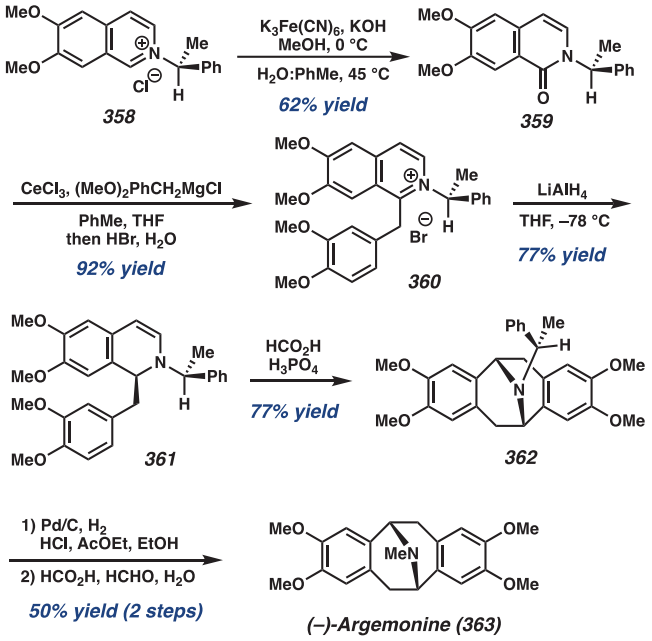

was dissolved in formic acid and aqueous formaldehyde to furnish the methylated natural product (−)-argemonine **363**.

Nishigaichi and co-workers also developed a modular synthesis of argemonine **363** and eschscholtzidine **371** from the coupling of isoquinolines and electron-rich potassium trifluoroborate reagents (Scheme 50).[114] After the synthesis of

Scheme 50. Nishigaichi's Synthesis of Argemonine and Eschscholtzidine

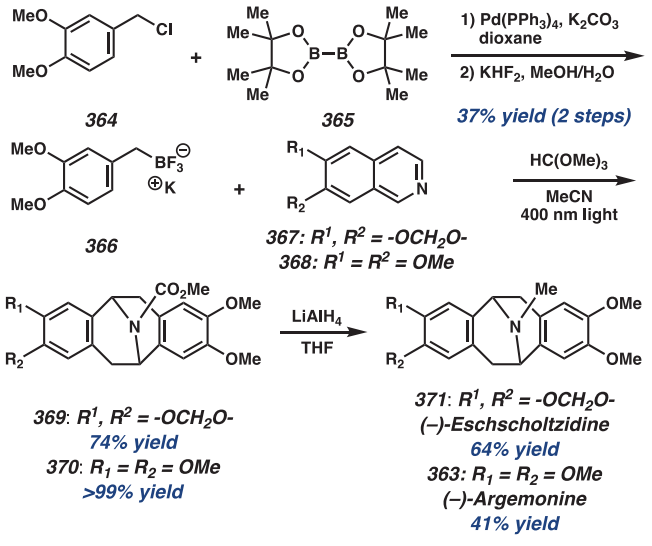

potassium trifluoroborate reagent **366** from benzyl chloride **364**, treatment of **366** with isoquinolines **367** and **368** under thermal or photochemical conditions followed by reduction with $LiAlH_4$ resulted in the concise syntheses of argemonine **363** and eschscholtzidine **371**.

Jiang and co-workers reported a general approach to access isopavines, including (−)-amurensinine, (−)-reframidine, (−)-reframine, and other non-natural isopavine derivatives within five or six steps with >95% ee.[115] Their retrosynthetic strategy began with the formation of bridging C−N and C−C bonds through the Pictet−Spengler reaction of an amino dimethyl acetal **375** (Scheme 51). From aldehyde **372**, a

Scheme 51. Jiang's Enantioselective Synthesis of (−)-Amurensinine

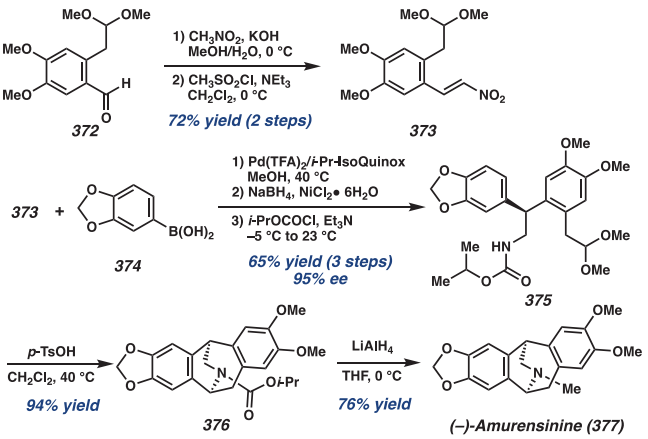

Henry reaction with nitromethane, followed by dehydration with methanesulfonyl chloride and excess trimethylamine, delivered *β*-nitrostyrene **373**. A Pd-catalyzed asymmetric addition of **373** with aryl boronic acid **374**, followed by reduction and conversion to the carbamate, yielded **375**. The Pictet−Spengler reaction of carbamate **375**, followed by reduction of carbamate **376**, formed (−)-amurensinine **377**.

In 2006, Stoltz and co-workers reported the enantioselective total synthesis of amurensinine **377**.[116,117] They envisioned to apply their developed Pd-catalyzed oxidative kinetic resolution methodology to rapidly access the isopavine core in a modular fashion (Scheme 52).[117] To this end, (3,4-dimethoxyphenyl)-acetic acid **378** was treated to form a diazoester compound and then subjected to a $Rh_2(OAc)_4$-catalyzed C−H insertion to produce *β*-ketoester **379** in 91% yield over 6 steps. Coupling of *β*-ketoester **379** and aryne precursor **380** in the presence of CsF afforded a net C−C insertion to form the central carbocyclic ring of ketoester **381**. Diastereoselective reduction of ketoester **381** and protection of the primary alcohol provided **382**. Oxidative kinetic resolution using Pd-(sparteine)Cl_2 and (−)-sparteine as the chiral ligand provided enantioenriched (−)-**382** with 99% ee. Conversion of the alcohol to the azide with inversion using $(PhO)_2P(O)N_3$ (DPPA) produced azido alcohol (−)-**383** with no loss of optical purity. After oxidation of the alcohol, reduction of the azide delivered the desired lactam (+)-**384**. Reductive methylation produced (+)-amurensinine **377** with 99% ee.

In 2007, Martin utilized a four-component reaction to rapidly access roelactamine **389** in a racemic fashion from piperonal **385**.[118] The condensation of piperonal with methylamine provided an imine *in situ* that was then reacted sequentially with benzyl Grignard **387** and acid chloride **386** to furnish amide **388** (Scheme 53). Treatment of **388** with a concentrated 2:1 mixture of HCl:MeOH allowed the amide to undergo sequential cyclizations to produce roelactamine **389**.

Finally, the first synthesis of a pavine alkaloid with C7 functionalization was reported by Nakagawa-Goto.[119] From amine **390**, which was prepared in three steps, amidation with carboxylic acid **391** using carbonyldiimidazole (CDI) provided amide **392** (Scheme 54). A Bischler−Napieralski reaction with

https://doi.org/10.1021/acs.chemrev.3c00054
Chem. Rev. 2023, 123, 9447−9496

Scheme 52. Stoltz's Enantioselective Synthesis of (+)-Amurensinine

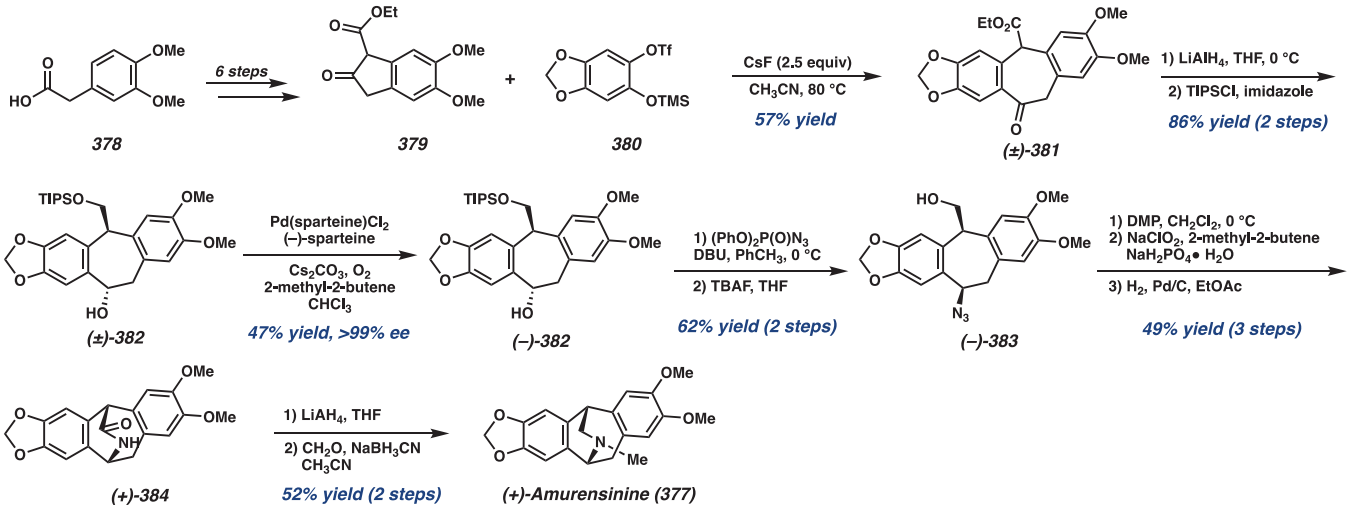

Scheme 53. Martin's Synthesis of (±)-Roelactamine

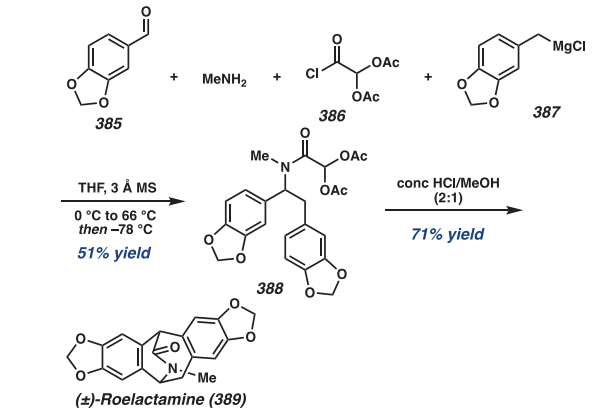

Scheme 54. Nakagawa-Goto's Synthesis of (±)-Neocaryachine

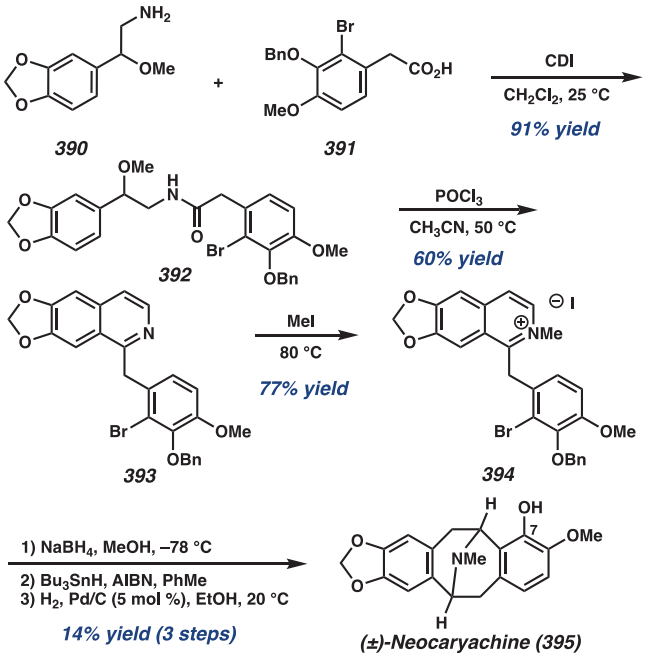

$POCl_3$ formed benzylisoquinoline **393**. Treatment of **393** with methyl iodide delivered the isoquinolinium salt **394**. Subsequent reduction with $NaBH_4$ to the enamine, followed by radical cyclization and removal of the benzyl group, yielded (±)-neocaryachine **395**.

5. THIQ ALKALOIDS FROM THE SAFRAMYCIN FAMILY

The saframycin family is the largest subclass of tetrahydroisoquinoline alkaloids consisting of saframycins, safracins, ranieramycins, and ecteinascidins. The core structure of natural products in this family features the intricate pentacyclic skeleton, having five six-membered rings condensed into the core scaffold (Figure 17). Well known for their potent anticancer/antitumor activities, natural products in this family have been popular targets in numerous synthetic endeavors.

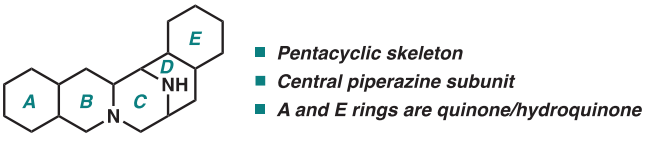

Figure 17. Core skeleton of THIQ alkaloids in the saframycin family.

5.1. Saframycin Alkaloids

5.1.1. General Structure and Biosynthesis. The very first set of saframycins, namely, saframycins A–E, were isolated in 1977 from bacteria *Streptomyces lavendulae*.[120] In the ensuing studies, four additional saframycins (F, G, H, and R) were isolated from the same species of bacteria,[121,122] and later in 1988, it was disclosed that myxobacteria *Myxococcus xanthus* strain Mx x48 produced saframycins MX1 and MX2.[123] In addition to the "natural" saframycins, six new saframycins (Y3, Yd-1, Yd-2, Ad-1, Y2b, and Y2b-d) were obtained by a directed biosynthesis through the supplementation of different amino acids.[124]

Among the currently known saframycin alkaloids, the shared structural motif is the amide side chain, which is appended to the B-ring at the C1 position (Figure 18). Additionally, the A-ring of all saframycins is in the quinone oxidation state, while the E-ring can be in various oxidation levels, in the range of phenol, hydroquinone, and quinone. The amino nitrile or

https://doi.org/10.1021/acs.chemrev.3c00054
Chem. Rev. 2023, 123, 9447–9496

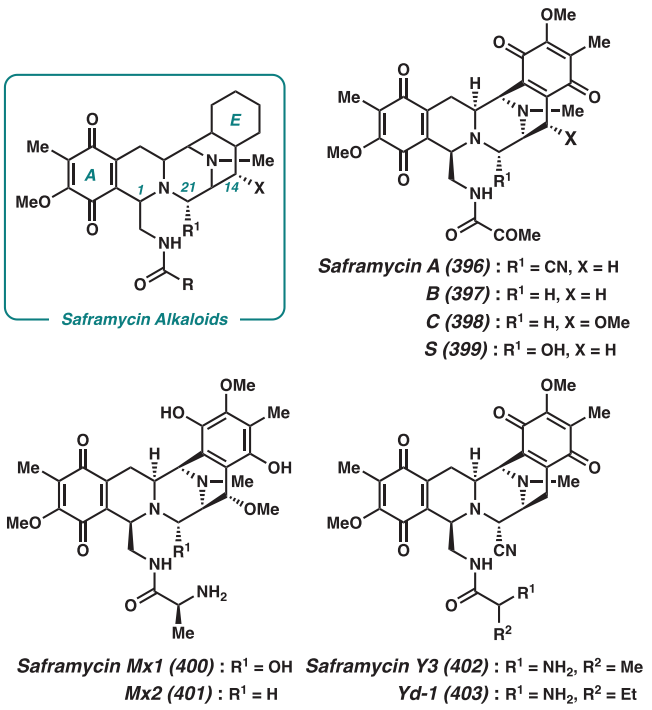

Figure 18. General structure and representative examples of saframycin alkaloids.

carbinol amine functionality on the central piperazine subunit functions as a latent electrophilic iminium species, which can alkylate DNA, and is largely responsible for saframycins' potent antitumor/antimicrobial activity.[125] Saframycins voided of a leaving group at C21 typically exhibit significantly lower biological activities.[120]

Early biochemical studies of saframycins were conducted via feeding/isotope-labeling experiments, and the results suggest that one alanine, one glycine, and two tyrosine derivatives constitute the backbone of saframycin A.[126] By exploiting the cloned biosynthetic gene cluster and its sequence analysis, it was later proposed that the pentacyclic backbone is assembled by a nonribosomal peptide synthetase (NRPS).[127] Specifically for saframycin A, the NRPS comprises three modules (SfmA, SfmB, and SfmC) in which the first two are responsible for the production of dipeptidyl intermediate **A** from alanine and glycine (Scheme 55A). As for the last module, intriguing multistep transformations catalyzed by SfmC were discovered by Oikawa and co-workers in 2010.[128,129] The notable domains in this module are a) the Pictet–Spengler reaction domain (PS), which catalyzes two successive Pictet–Spengler reactions to construct the bis-tetrahydroisoquinoline (bis-THIQ) intermediate, and b) the reduction domain (Red), which reduces the thioester intermediates and releases aldehyde precursors (**B**, **E**, and **F**) for the following reactions.

Interestingly, they also noted that the relatively less strict substrate specificity of the PS domain might allow for the incorporation of synthetic aldehydes into the core skeleton. Once the pentacycle is constructed, late-stage tailoring modifications, including hydroquinone oxidation, *N*-methylation, and hydrolysis of the fatty acid chain, proceed to afford saframycin A.[130] This thorough understanding of the biosynthetic mechanism serves as a foundation for future developments of a chemoenzymatic total synthesis of saframycin alkaloids and their related analogs (*vide infra*).

Scheme 55. A) Domain Organization of Saframycin A NRPS; B) Proposed Biosynthetic Mechanism for the Construction of Saframycin A's Pentacyclic Skeleton

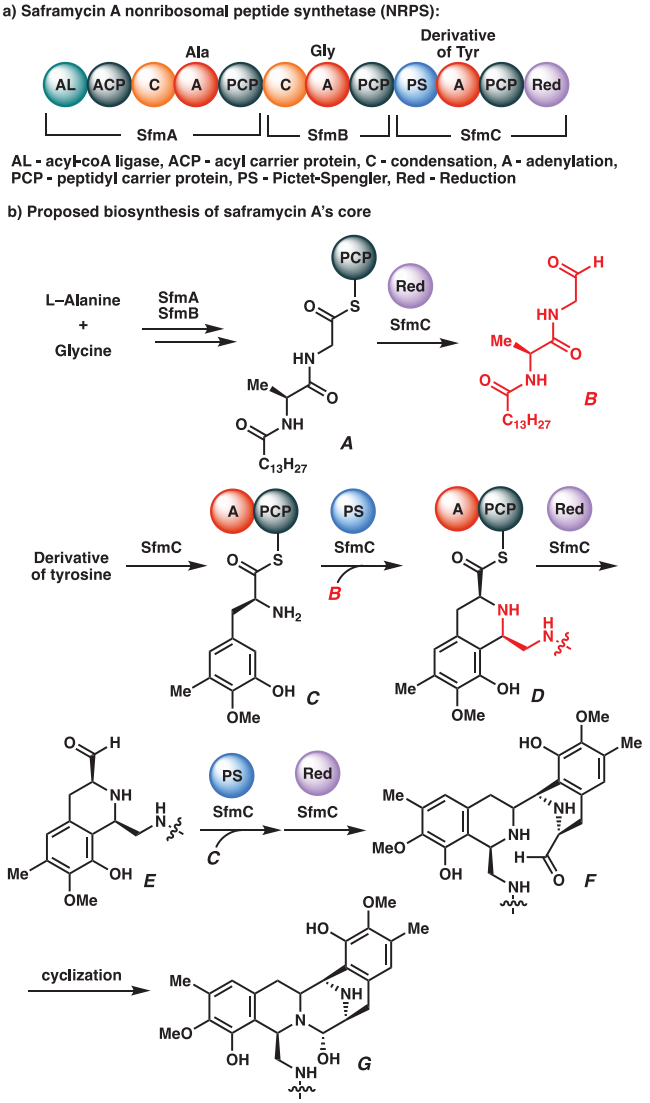

5.1.2. Total Syntheses of Saframycin Alkaloids. After the publication of a comprehensive review by William in 2002,[3] there have been only three reports detailing the synthesis of saframycin alkaloids, all of which targeted saframycin A.

In 2011, Liu employed L-tyrosine as a chiral building block in the preparation of (−)-saframycin A (Scheme 56).[131] They commenced their synthetic studies by converting L-tyrosine methyl ester into the desired amino acid **405** in 12 steps and tetrahydroisoquinoline **404** in 11 steps, which served as the eastern and western portions of the natural product, respectively. Although the regioselectivity issue for monohydroxy phenol substrate is a common problem in the Pictet–Spengler cyclization reaction,[132] they noted that the selectivity, in this case, can be controlled by carefully maintaining the reaction temperature at 0 °C with a slow addition of the aldehyde starting material, furnishing THIQ **404** in 86% yield.

With both halves in hand, they coupled them together to give amide intermediate **406**. Subsequent functional group manipulations and an intramolecular Pictet–Spengler cyclization with triflic acid (TfOH) afforded pentacycle **407**. It is

https://doi.org/10.1021/acs.chemrev.3c00054
Chem. Rev. 2023, 123, 9447−9496

Scheme 56. Liu's Total Synthesis of (−)-Saframycin A

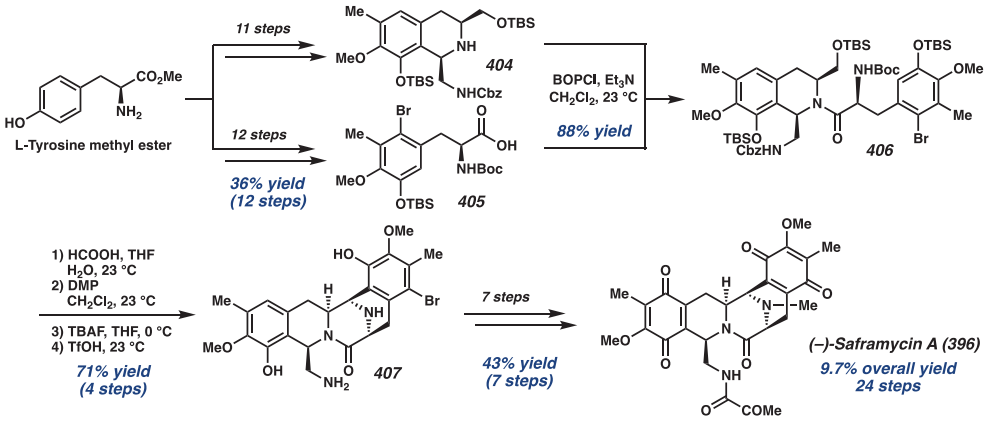

Scheme 57. Saito's Total Synthesis of (±)-Saframycin A

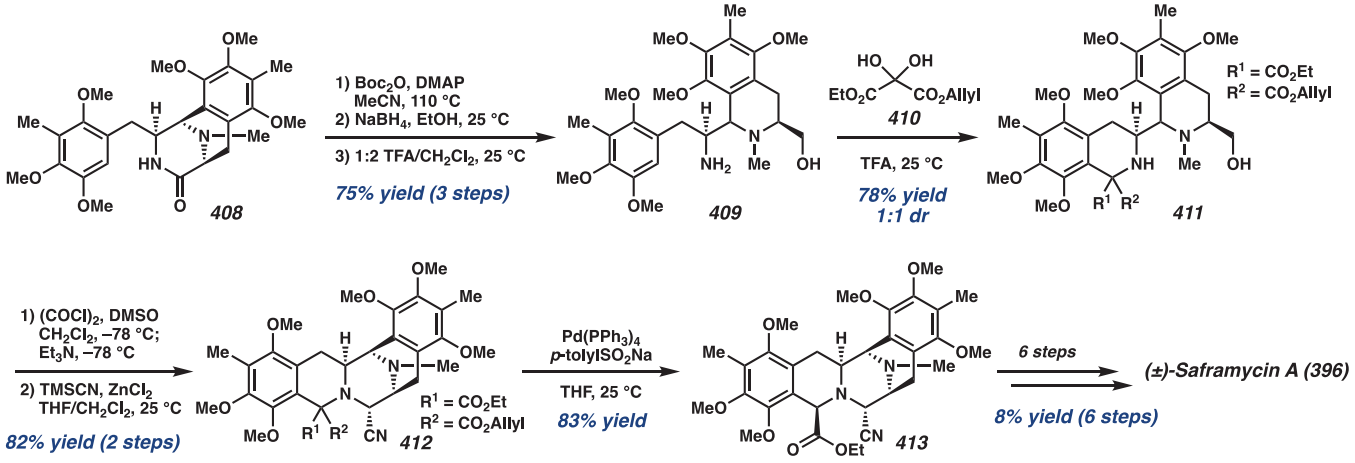

worth noting here that the second Pictet−Spengler cyclization requires a bromine atom on the eastern half of the molecule to function as a blocking group and provide the correct regiochemical outcome for the cyclization. They further advanced this intermediate to the targeted natural product via a seven-step peripheral modification, concluding a 24-step total synthesis of (−)-saframycin A **396** in an overall 9.7% yield. Of note, the key synthetic strategy in this report is reminiscent of Corey's approach to prepare the pentacyclic core of ecteinascidin and phthalascidin where an amide coupling is used to merge the western and eastern halves of the molecule.[133]

In 2018, Saito and co-workers published a racemic synthesis of saframycin A **396** (Scheme 57), which is a follow-up study to correct the stereochemistry at the C1 position of the western THIQ.[134] The tricyclic lactam **408**, which was prepared in 14 steps from commercially available material,[135,136] first underwent reductive cleavage and Boc removal to provide hydroxymethyl isoquinoline **409**. This compound served as a Pictet−Spengler substrate, and cyclization with allyl ethyl oxomalonate ester (**410**) delivered bis-THIQ **411**. From this intermediate, the pentacyclic core **412** was constructed via Swern oxidation of the primary alcohol to afford the aldehyde, which underwent ring-closure to generate the hemiaminal C-ring. By subjecting TMSCN to the same pot, the amino nitrile formation proceeded to furnish the desired product **412** in 82% yield over 2 steps. They subsequently performed decarboxylation and stereoselective protonation to correctly install the stereochemistry at the C1 position of the western THIQ (**413**). In the final stage, the ethyl ester in **413** was converted to the pyruvamide through a four-step sequence, consisting of a) $LiBH_4$ reduction, b) Mitsunobu reaction with phthalimide, c) removal of phthalimide to reveal the free amine, and d) acylation of amine with pyruvic acid. Finally, selective demethylation and ceric ammonium nitrate (CAN) oxidation were performed to deliver (±)-saframycin A **396** in an overall 27 steps for the longest linear sequence.

The most recent total synthesis of saframycin A is a merger of chemical and biosynthesis.[137] Based on the proposed nonribosomal peptide synthetase (NRPS) responsible for the construction of the pentacyclic skeleton (*vide supra*), Oikawa and Oguri specifically designed substrates that successfully participated in the SfmC-catalyzed multistep enzymatic conversion (Scheme 55). Once the core skeleton was obtained, they exploited chemical synthesis to further manipulate functional groups and finally deliver not only saframycin A, but also jorunnamycin A and *N*-Fmoc saframycin Y3. This hybrid strategy is highly efficient and allows for rapid access to the elaborated pentacyclic scaffolds only in a single day.

5.2. Safracin Alkaloids

5.2.1. General Structure and Biosynthesis. Isolated from *Pseudomonas fluorescens*,[138] safracins are structurally similar to the saframycins, except for having a phenol E-ring instead of a quinone/hydroquinone (Figure 19). Optimization of the fermentation process of this bacteria resulted in a

https://doi.org/10.1021/acs.chemrev.3c00054
Chem. Rev. 2023, 123, 9447−9496

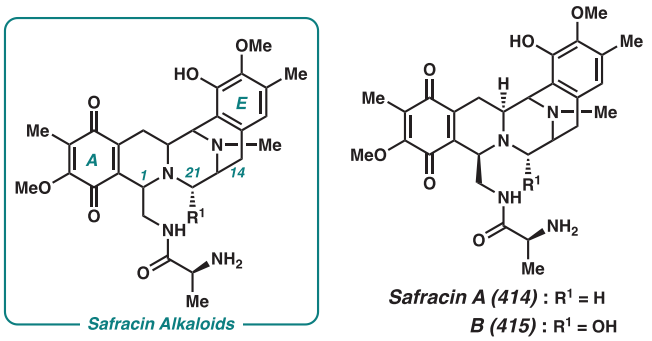

Figure 19. General structure and structure of safracin alkaloids.

multikilogram isolation of cyanosafracin B, having a nitrile moiety at the C21 position, which served as an inexpensive precursor to prepare ecteinascidin 743 (Et-743), an anticancer drug.[139]

Biosynthetically, the pentacyclic core of safracins is believed to be assembled from one alanine, one glycine, and two functionalized tyrosine via the nonribosomal peptide synthetase (NRPS), resembling the mechanism reported for the saframycins.[140] In the most recent study, Tang and co-workers essentially established the entire safracin biosynthetic pathway by investigating post-NRPS modifications. These include the A-ring oxidation, *N*-methylation, and removal of the fatty acyl chain.[141]

5.2.2. Total Syntheses of Safracin Alkaloids. Despite extensive research in the area of safracin biosyntheses, to the best of our knowledge, there is still no report of a chemical total synthesis of any safracin alkaloid. Since the initial disclosure of efforts toward safracin A by Kubo and co-workers in 1995,[142] not much progress has been reported. This could perhaps be attributed to the ample quantities of safracins obtained from the isolation process.

5.3. Renieramycin Alkaloids

5.3.1. General Structure and Biosynthesis. The general structure of renieramycins is highly similar to that of the saframycin alkaloids. The main difference is at the C1 position, where renieramycins possess an ester or alcohol functionality instead of an amide side chain found in the saframycins (Figure 20).

Renieramycin alkaloids are typically isolated from marine organisms, such as different species of blue sponges and nudibranchs, collected in various parts of the world. Before 2002, only the structures of renieramycins A−G and I, cribrostatin 4 (or renieramycin H), and jorumycin were disclosed. However, in the past 20 years, more than 20 new renieramycins were reported.[143] These new compounds are mostly artifacts resulting from attempts to improve the stability of renieramycin alkaloids.

In 2003−2004, the structures of renieramycins J−O, and Q−S were isolated from the Thai sponge *Xestospongia sp.* pretreated with potassium cyanide (KCN) by Saito, Suwanborirux, and co-workers.[144−146] They found that the addition of KCN helps stabilize the labile amino alcohol moiety via the conversion to a more stable amino nitrile and improves the isolated yields of renieramycins by approximately 100-fold. This developed isolation protocol also allowed for the discovery of minor components of renieramycins in

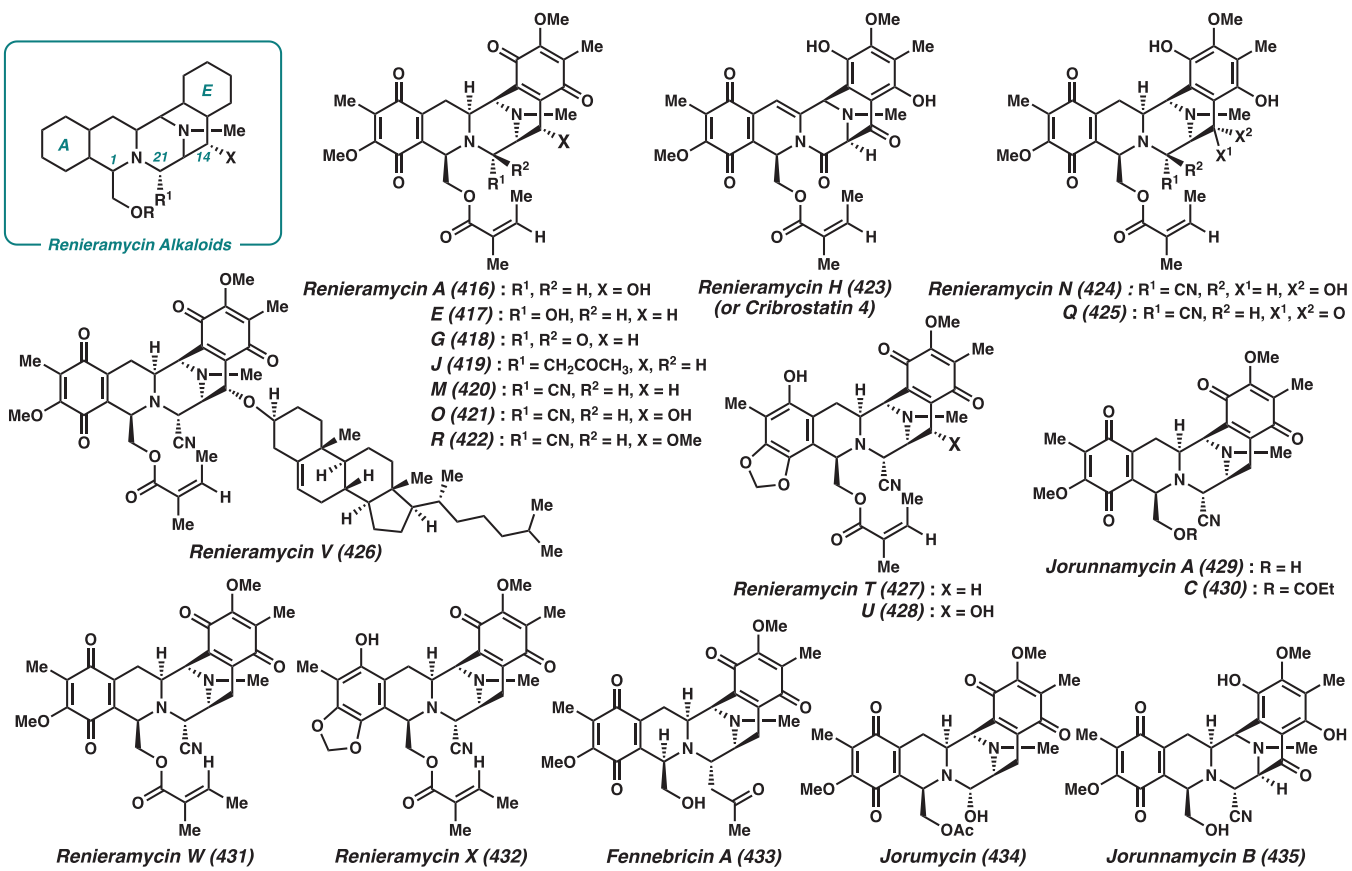

Figure 20. General structure and representative examples of renieramycin alkaloids.

https://doi.org/10.1021/acs.chemrev.3c00054
Chem. Rev. 2023, 123, 9447−9496

Xestospongia sp., including renieramycins T−U, which possess an ecteinascidin-renieramycin hybrid structure,[147] as well as renieramycin V, which contains a sterol unit appended to the C14 position.[148] Additionally, jorunnamycins A−C were isolated from the aqueous KCN-pretreated *Jorunna funebris* collected in Thailand.[149]

The Saito and Concepcion groups later reported three novel renieramycin-type alkaloids, namely, renieramycins W−Y, which were isolated from the KCN-pretreated *Xestospongia sp.* collected in the Philippines.[150] Structurally, renieramycins W and X are the first to have tiglic acid ester functionality instead of the angelate ester or the alcohol. Most recently, Guo and co-workers successfully isolated and disclosed the structures of fennebricins A−D from the South China Sea nudibranch *J. funebris*.[151,152]

Biosynthetically, the core pentacyclic skeletons of renieramycins were also reported to be assembled through a nonribosomal peptide synthetase (NRPS) pathway, similar to the NRPS system of saframycin A.[153] Donia and co-workers recently discovered that there are three NRPS modules, namely, RenE, RenF, and RenK, which are responsible for the production of the renieramycin E core structure (Scheme 58A). The first two modules (RenK and RenE) promote the formation of aldehyde building block **436**, while RenF catalyzes multistep transformations to ultimately deliver pentacycle **438** (Scheme 58B). Of note, the RenK module is missing an adenylation domain (A) consistent with the fact that renieramycin E is one amino acid shorter than saframycin A.

Scheme 58. A) Domain Organization of Renieramycins NRPS; B) Proposed Biosynthetic Mechanism for the Construction of Renieramycin E's Pentacyclic Skeleton

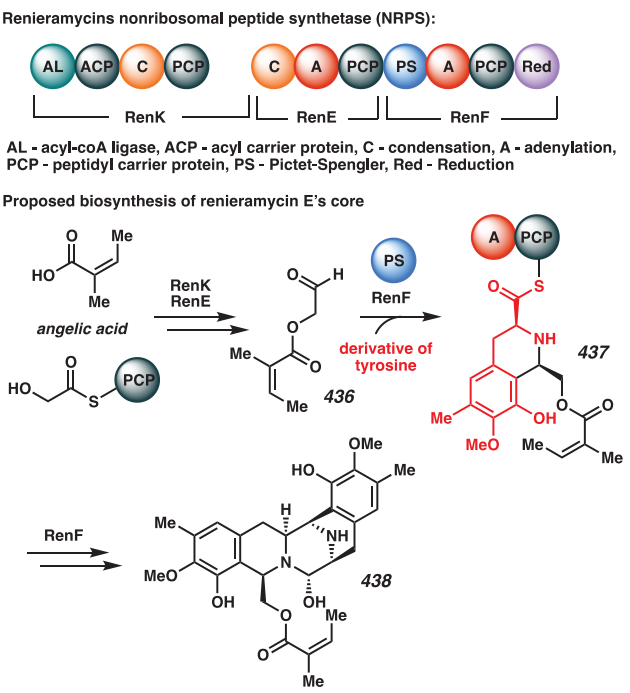

5.3.2. Total Syntheses of Renieramycin Alkaloids. In the past 20 years, chemical syntheses of renieramycins have been an active research area, with a number of synthetic studies toward these molecules and >10 reports successfully preparing naturally occurring renieramycin alkaloids. The first total synthesis of (−)-cribrostatin 4 (**423**, aka renieramycin H) was disclosed by Danishefsky and co-workers in 2005 utilizing asymmetric reductions as key transformations to prepare both western and eastern halves of the molecule (Scheme 59).[154] With the two enantioenriched fragments in hand, they convergently coupled them together through an amide coupling, followed by a "lynchpin Mannich" cyclization to deliver pentacycle **442**. Of note, the stereochemistry at the C3 position is opposite to that existing in the saframycin-like backbone. Nonetheless, this is inconsequential because the targeted natural product has a C3=C4 benzylic olefin. Accordingly, the ketone functionality at the C4 position was reduced and subsequently eliminated, affording intermediate **443**.

Finally, the last steps of the total synthesis involve the adjustment of oxidation levels of the A- and E-rings, the installation of the ketone at C14, and the introduction of the angeloyl group. By first converting intermediate **443** to monoquinone **444**, regioselective benzylic oxidation with SeO_2 proceeded smoothly, followed by DMP oxidation and quinone reduction to generate bis-hydroquinone **445**. Despite the difficulty encountered in their initial attempts to perform analogueation on a similar substrate, they adjusted the A-ring oxidation state and were able to perform esterification on this specific intermediate using analogue chloride **446**, followed by TBS deprotection to prepare **447**. Selective air oxidation of the ring A hydroquinone eventually provided cribrostatin 4 (**423**) in 34 steps for the longest linear sequence from commercially available 2,3-dimethoxytoluene. They additionally noted that the high stability of the E-ring hydroquinone can be attributed to the presence of the C14 ketone, while the resting state of the A-ring is at the quinone oxidation level.

With a longstanding interest in the chemistry and biology of the THIQ antitumor antibiotics, the Williams laboratory also developed an asymmetric total synthesis of (−)-cribrostatin 4 (**423**) (Scheme 60).[155] By exploiting a sequential asymmetric Staudinger/Pictet−Spengler cyclization reaction, which was first developed in a separate study,[156] the *β*-lactam-fused THIQ **448** was prepared to serve as the western portion of the molecule. On the other hand, the enantioenriched tyrosine derivative **449** was synthesized using a chiral glycine template as a chiral auxiliary. The assembly of these two molecules was then performed through an acid chloride intermediate to provide amide **450** without detectable epimerization at the C13 position. Treatment of **450** with TBAF resulted in the removal of both the TBS and Fmoc protecting groups to give **451**.

Following this, the $LiEt_3BH$ reduction of *β*-lactam **451** initiated a cyclization/elimination cascade, which established the pentacyclic skeleton of cribrostatin 4. Although there are two possible pathways for this transformation, the authors postulated that the formation of an *o*-quinone methide intermediate to be operative. Finally, the advancement of pentacycle **452** to cribostatin 4 consists of a) debenzylation with $PdCl_2$, b) oxidation of both phenols to bisquinone **453** with PIFA, c) esterification to generate the angelated intermediate, and d) double oxidation to install a ketone functionality at the C14 position. It is worth noting here that the order of this sequence proves critical to the success of this synthesis, as Danishefsky previously found that the pentacyclic alcohol (deangelated cribrostatin 4) was highly unstable, and attempts to perform esterification on this particular intermediate all led to decomposition of the starting material.[154]

https://doi.org/10.1021/acs.chemrev.3c00054
Chem. Rev. 2023, 123, 9447−9496

Scheme 59. Danishefsky's Total Synthesis of (−)-Cribrostatin 4

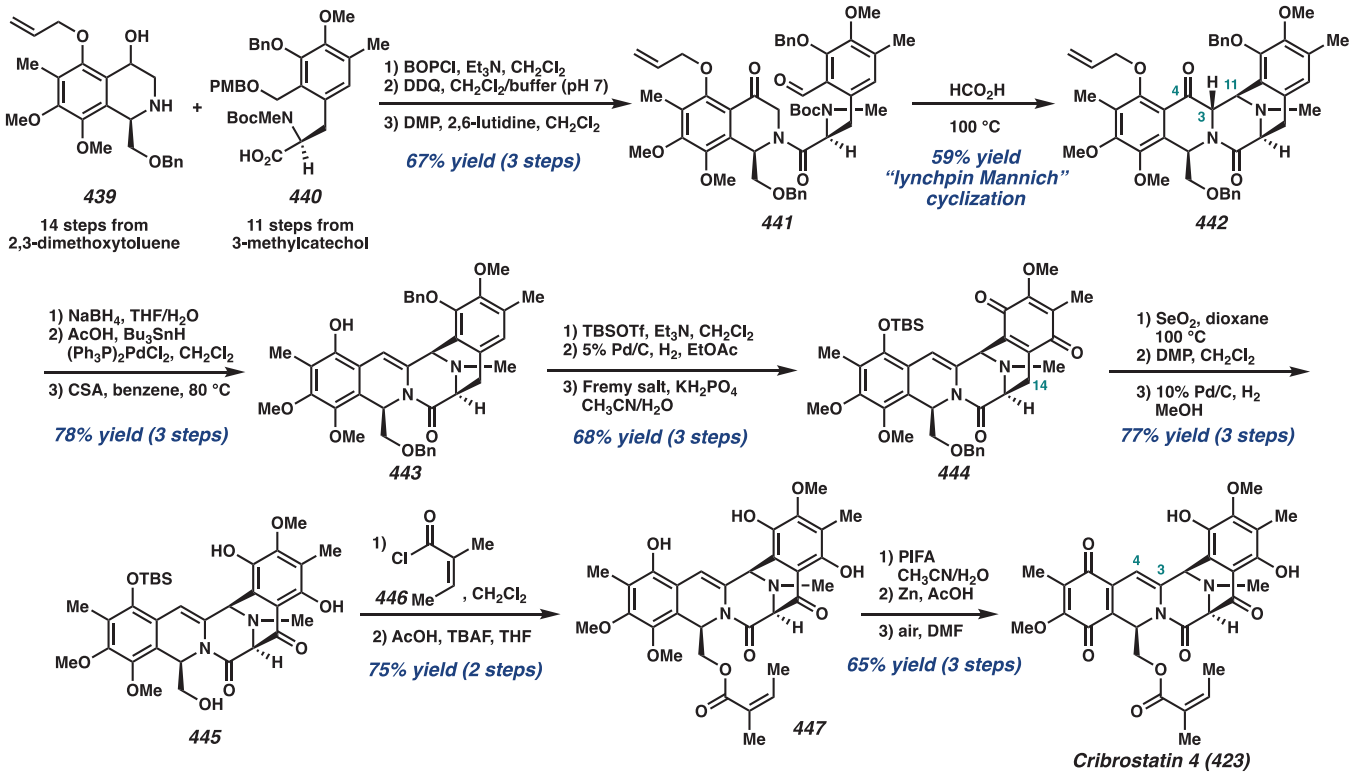

Scheme 60. Williams' Total Synthesis of (−)-Cribrostatin 4

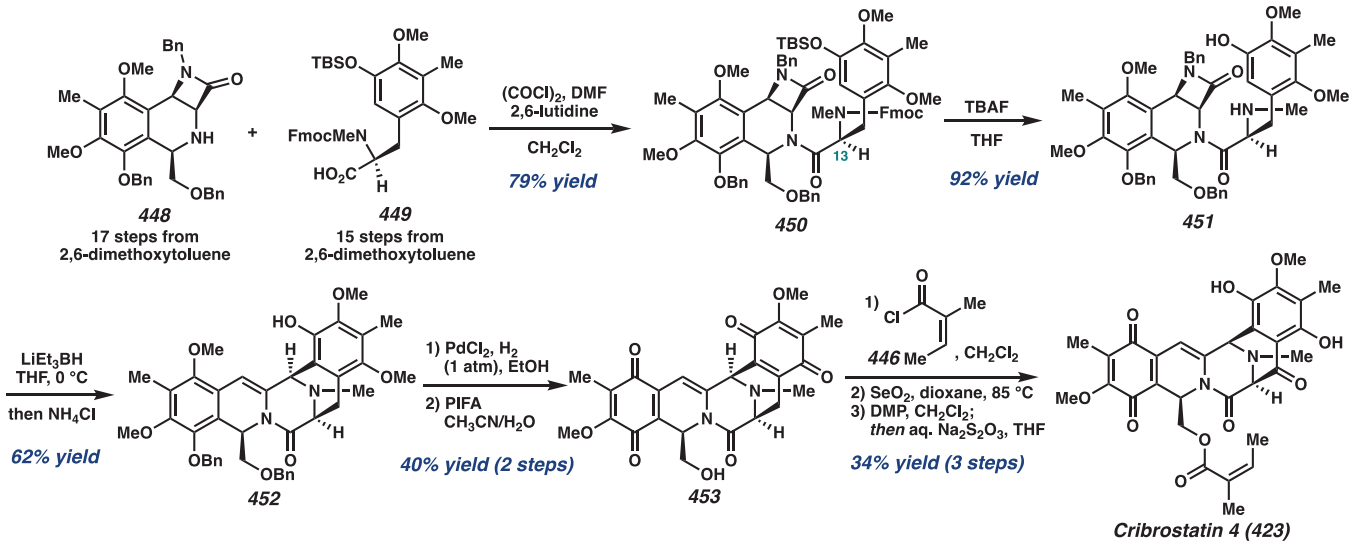

Overall, Williams and co-workers completed a 25-step (longest linear sequence) asymmetric total synthesis of (−)-cribostatin 4 (**423**), starting from commercially available 2,6-dimethoxytoluene.

Within the same year, Zhu and co-workers described the third asymmetric total synthesis of (−)-cribrostatin 4 (**423**).[157] The key synthetic strategy to access the pentacyclic skeleton (**460**) features a domino sequence involving the formation of iminium ion **457**, followed by β-elimination and Pictet−Spengler cyclization, which greatly resembles Williams' strategy (Scheme 61). In Zhu's case, the thiol group at the C4 position acts as a leaving group to unveil α,β-unsaturated iminium ion **459**. This intermediate then underwent cyclization to form pentacycle **460** and its constitutional isomer, arising from the undesired regioselectivity, in 51% and 15% yield, respectively. The desired isomer (**460**) was transformed into cribrostatin 4 (**423**) following a strategy similar to that for previous syntheses, providing the natural product in the longest linear sequence of 26 steps from commercially available starting material.

More recently, Saito reported a racemic total synthesis of cribrostatin 4 from commercial material.[158] Instead of building the pentacyclic core from an amide coupling to join the two halves of the molecule, they completed the synthesis by employing diketopiperazine as a central building block and consequently constructing the B- and D-rings to generate the

https://doi.org/10.1021/acs.chemrev.3c00054
Chem. Rev. 2023, 123, 9447−9496

Scheme 61. Zhu's Strategy to Prepare the Pentacyclic Skeleton of (−)-Cribrostatin 4

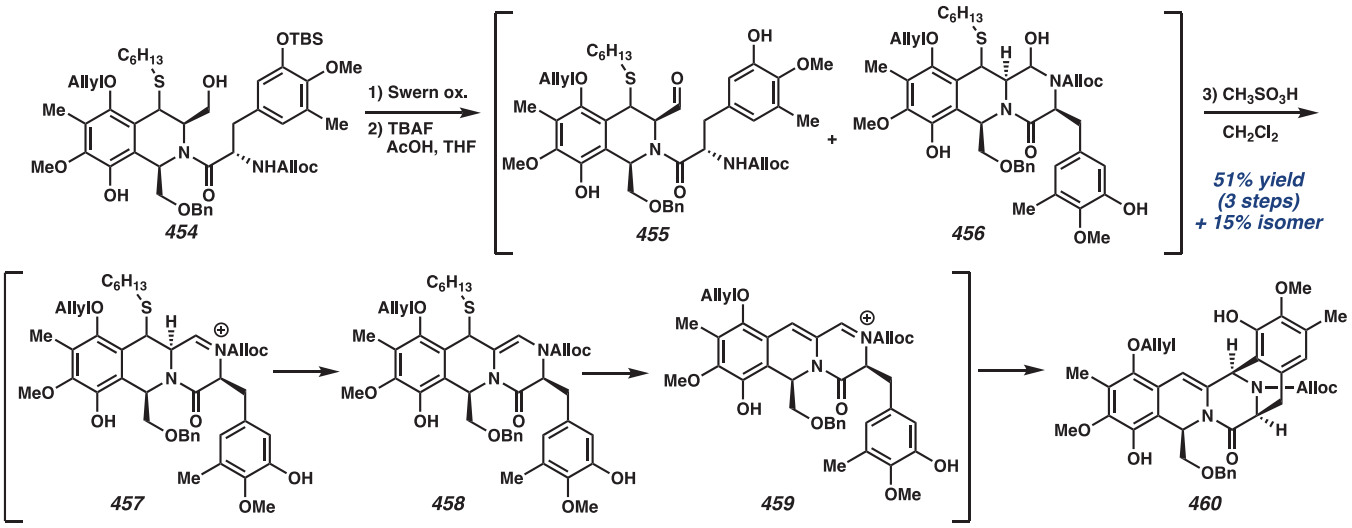

Scheme 62. Williams' Total Synthesis of (−)-Renieramycin G, (−)-Jorumycin, 3-*epi*-Renieramycin G, and 3-*epi*-Jorumycin

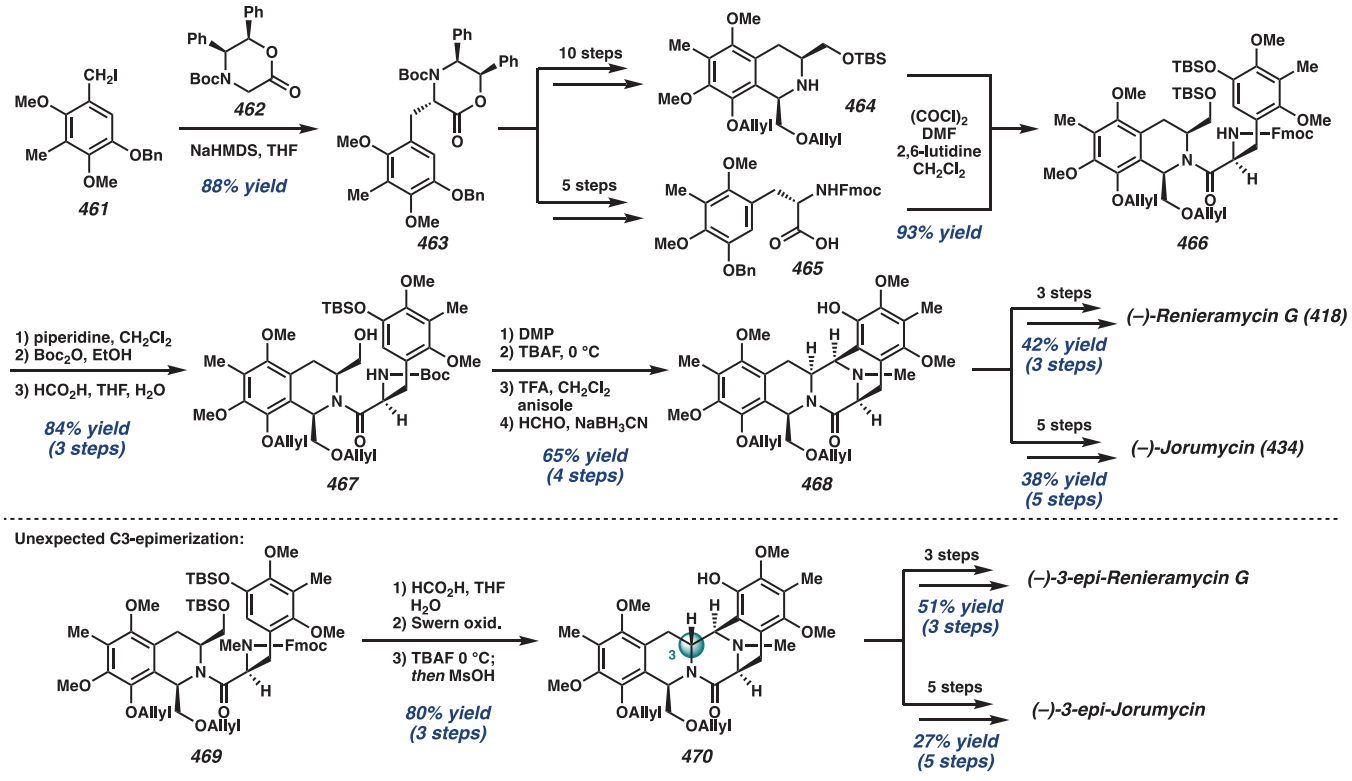

pentacyclic framework. The endgame of this synthesis follows the sequence reported by Williams.[155] The Saito group also realized an alternative synthetic plan to cribrostatin 4 in 2015,[159] where they slightly modified the order of transformations in the early stage to prepare the pentacyclic skeleton. With this improved strategy, they were able to perform reactions on a larger scale and prepared 81 mg of cribrostatin 4 with 8.3% overall yield in addition to renieramycin I, which contains a methoxy substituent at the C14 position.

Apart from cribrostatin 4 (or renieramycin H), renieramycin G (**418**) has also been a popular target, attracting interest from the groups of Williams, Magnus, Zhu, Saito, and Yang to complete its total synthesis. In 2005, Williams and co-workers disclosed the first asymmetric total synthesis of renieramycin G along with another structurally similar natural product, jorumycin (**434**) (Scheme 62).[160] They elegantly took advantage of the intrinsic symmetry of the molecule to prepare only one building block (**461**) that can be employed as both western and eastern fragments. The use of chiral glycine template **462** as a chiral auxiliary allows for the preparation of benzylated oxazinone **463**, which can be further transformed into enantioenriched 1,3-*cis*-THIQ **464** over 10 steps and tyrosine derivative **465** over 5 steps.

The coupling of these two molecules via an acid chloride intermediate proceeded smoothly to deliver amide **466** in a

https://doi.org/10.1021/acs.chemrev.3c00054
Chem. Rev. 2023, 123, 9447−9496

Scheme 63. Magnus' Total Synthesis of (±)-Renieramycin G

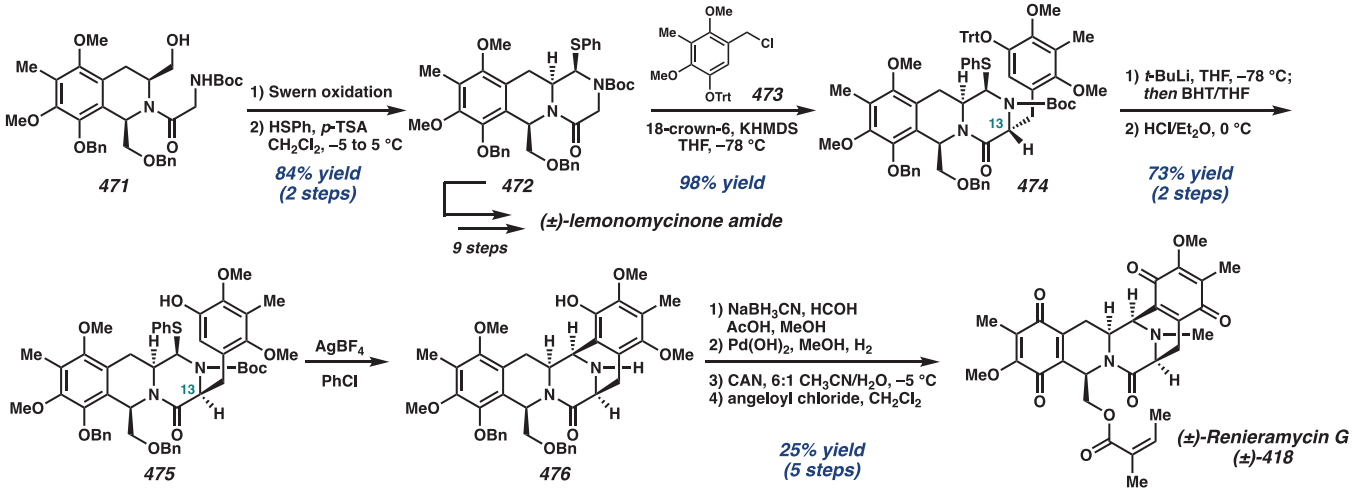

Scheme 64. Zhu's Total Syntheses of (−)-Renieramycins G, M, (−)-Jorunnamycin A, and (−)-Jorumycin

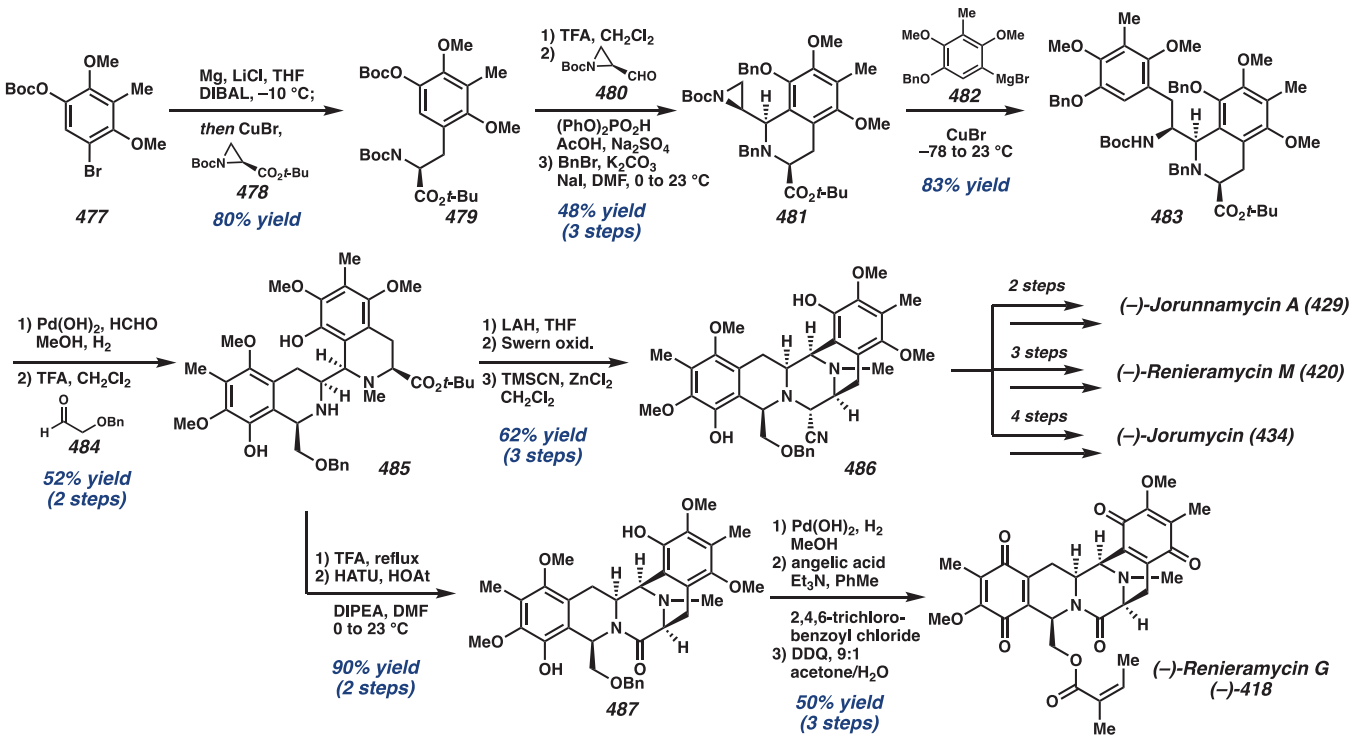

93% yield. Fmoc removal with piperidine, reprotection of the free amine with a Boc protecting group, and selective removal of the TBS group were followed to provide alcohol **467**. The pentacycle was then obtained after the oxidation of the primary alcohol, formation of the carbinol amine, and Pictet−Spengler cyclization to construct the D-ring. Reductive amination afforded intermediate **468** that is a precursor to both (−)-renieramycin G (**418**) and (−)-jorumycin (**434**). Interestingly, the use of different protecting groups on the eastern nitrogen atom, which require basic conditions for deprotection, resulted in the generation of the C3-*epi* variant (**470**) through epimerization. They, nonetheless, successfully advanced this unexpected epimer to 3-*epi*-renieramycin G and 3-*epi*-jorumycin for further biological evaluation studies.

At the same time, Magnus independently developed racemic total syntheses of renieramycin G (**418**) and a lemonomycinone analog (Scheme 63).[161,162] The A- and B-rings of both molecules were initially prepared through a modified Larock isoquinoline synthesis, followed by an addition at the C1 position, a reduction of the C3=C4 olefin, and silyl-activated amide coupling to deliver 1,3-*cis*-THIQ **471**. This THIQ intermediate (**471**) then underwent cyclization and functional group interconversion to thioaminal **472**. At this stage, thioaminal **472** serves as a diverging point to access renieramycin G or lemonomycinone amide, where a lactam enolate alkylation with benzyl chloride **473** was performed for the synthesis of renieramycin G. This provided the undesired epimer of tetracycle **474** at the C13 position as a single diastereomer, which they were able to correct via a diastereoselective reprotonation with *in situ* trityl removal to deliver **475**. Treatment of this intermediate (**475**) with $AgBF_4$ then triggered cyclization to generate the D-ring in pentacycle

https://doi.org/10.1021/acs.chemrev.3c00054
Chem. Rev. 2023, 123, 9447−9496

Scheme 65. Saito's Total Synthesis of (±)-Renieramycin G

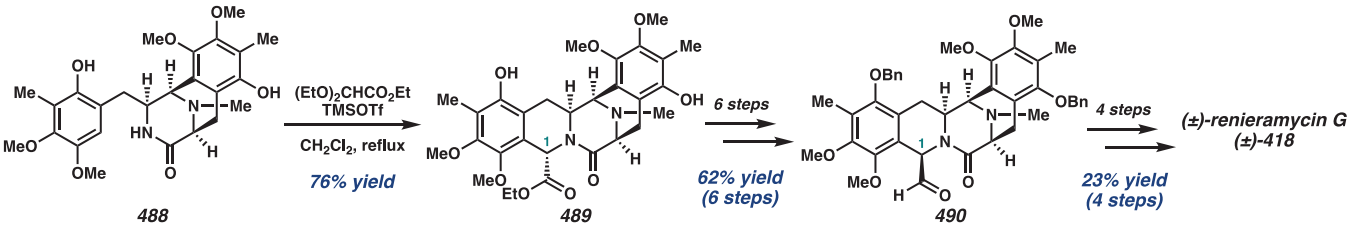

Scheme 66. Yang's Strategy to Assemble the Pentacyclic Core of Renieramycin Alkaloids

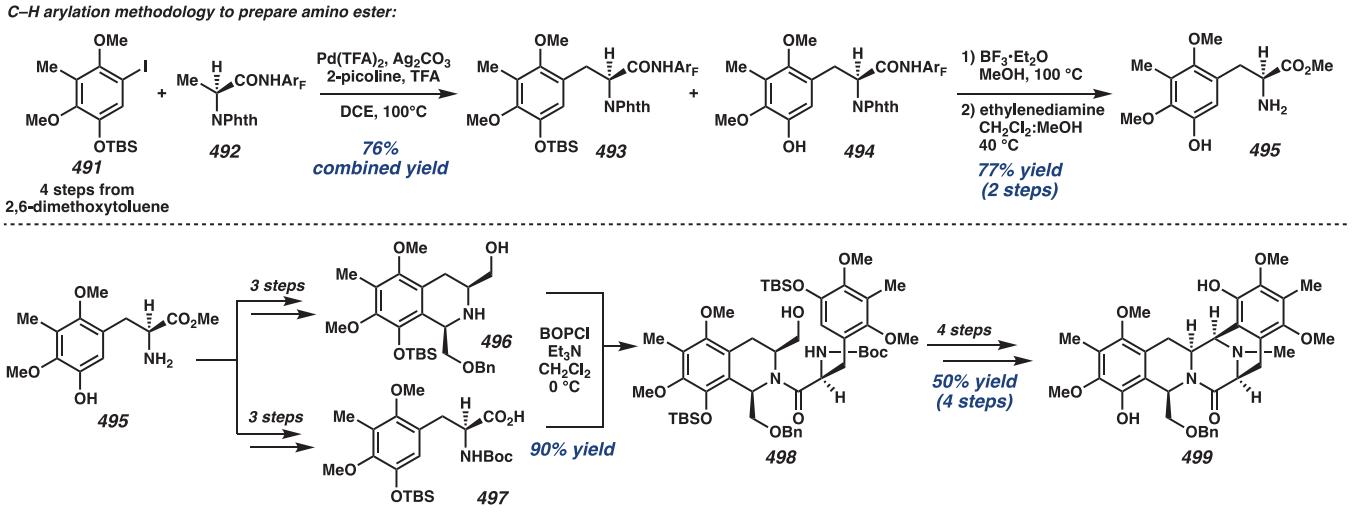

476. Finally, reductive amination, hydrogenolysis, ceric ammonium nitrate (CAN) oxidation, and esterification afforded racemic renieramycin G (**418**). In this same report, lemonomycinone amide was also prepared by adapting this synthetic strategy.

Zhu and co-workers disclosed the asymmetric total syntheses of (−)-reinieramycins G, M, (−)-jorunnamycin A, and (−)-jorumycin in 2009 (Scheme 64).[163] By employing aziridine as a lynchpin, they took a different approach to constructing the pentacyclic skeleton. Instead of relying on the amide coupling to merge the western and eastern parts of the molecule, they exploited aziridine ring-opening to forge the desired pentacycle. Starting with a CuBr-mediated ring-opening of enantioenriched aziridine **478**, which was prepared from a chiral pool starting material (*N*-trityl-L-serine methyl ester), the Boc-protected amino ester **479** was formed in 80% yield. Following Boc removal, the Pictet−Spengler cyclization of the free amine with formyl aziridine **480** and global benzylation were performed to afford the eastern THIQ building block (**481**). From here, another CuBr-promoted aziridine ring-opening was utilized, and a sequence consisting of a debenzylation with *in situ* methylation and tandem Boc removal/Pictet−Spengler reaction delivered the key bis-THIQ (**485**). This intermediate was then subjected to two different synthetic sequences to prepare a variety of renieramycin alkaloids. First, conversion of the ester to the aldehyde and a Strecker reaction provided pentacycle **486**. This intermediate can be further advanced to jorunnamycin A (**429**), renieramycin M (**420**), and jorumycin (**434**) over 2, 3, and 4 steps, respectively. On the other hand, renieramycin G (**418**) was obtained via a) an amide coupling to form pentacycle **487**, b) hydrogenolysis with Pearlman's catalyst, c) angelation of the primary alcohol, and c) DDQ oxidation of the bis-phenols.

By exploiting the common strategy in the construction of the bis-THIQ pentacyclic scaffold, i.e., the amide coupling with subsequent elaboration of the C−E rings through Pictet−Spengler cyclization, the Liu group reported an asymmetric total synthesis of (−)-renieramycin G (**418**).[164] The use of L-tyrosine methyl ester as a chiral pool starting material, similar to their total synthesis of saframycin A (*vide supra*), allows for diastereocontrol in ensuing transformations, which ultimately resulted in the successful preparation of enantiopure (−)-renieramycin G in 21 steps for the longest linear sequence. After the disclosure of this report, the group extended this synthetic strategy to prepare 15 analogs of renieramycin G with varying groups at the angelate ester,[165] 15 analogs of jorumycin with varying groups at the primary alcohol,[166] as well as 3 additional stereoisomers of renieramycin G.[167] These analogs were biologically evaluated for their cytotoxic activities against multiple cancer cell lines.

In 2011, Saito and co-workers reported the total synthesis of (±)-renieramycin G (Scheme 65),[168,169] in which the synthetic strategy closely followed their previously reported pathway for the synthesis of saframycin B.[170] From tricyclic lactam **488**, they performed a Pictet−Spengler cyclization with diethoxyacetate, delivering pentacycle **489** in 76% yield, albeit with the opposite stereochemistry at the C1 position. By converting the pendent ester to the aldehyde **490**, they were able to correct this stereochemical problem via base-mediated epimerization over a total of 6 steps. Finally, the racemic renieramycin G (**418**) was obtained by performing a reduction of the aldehyde to the alcohol, followed by debenzylation, CAN oxidation, and angelation.

Most recently, Yang and co-workers accomplished the total syntheses of the renieramycin alkaloids by a unified strategy (Scheme 66).[171] The key transformations to construct the

https://doi.org/10.1021/acs.chemrev.3c00054
Chem. Rev. 2023, 123, 9447−9496

Scheme 67. Yokoya's and Williams' Total Synthesis of (−)-Renieramycin T

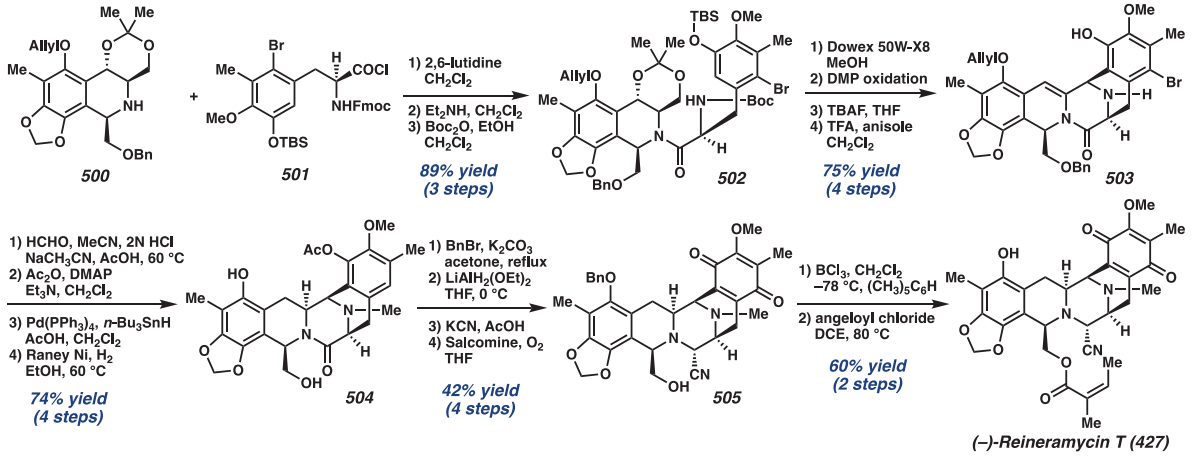

Scheme 68. Chen's Total Synthesis of (−)-Renieramycin T

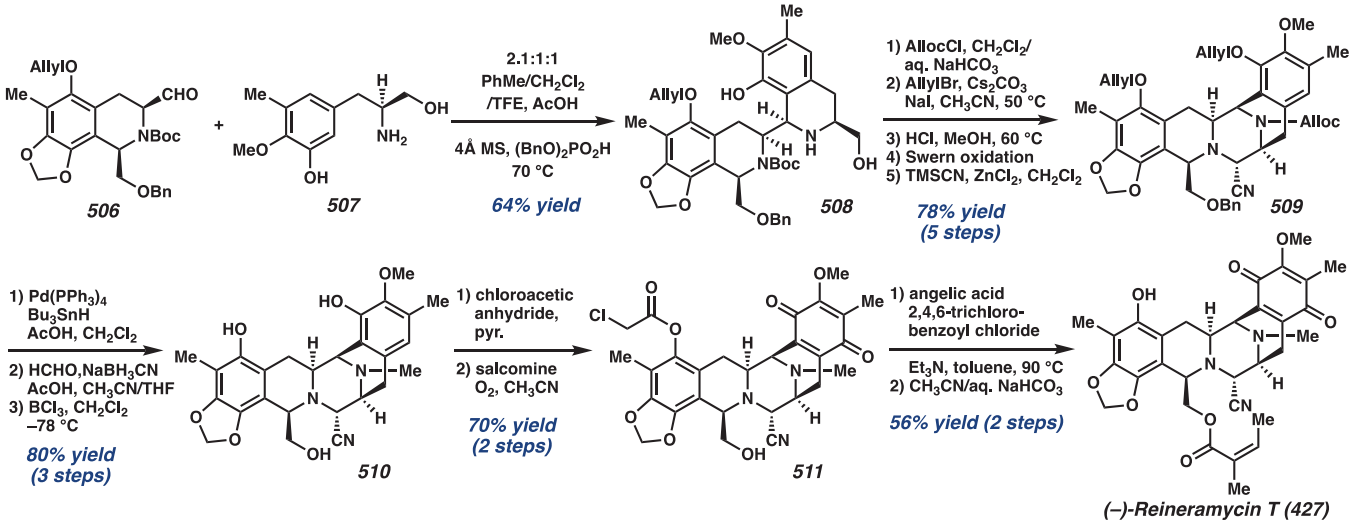

pentacycle are not significantly different from those of previous reports (i.e., the amide coupling with subsequent formation of the C- and D-rings); however, they were able to expediently prepare tyrosine derivatives **493** and **494** through the utilization of a C−H functionalization methodology. Inspired by Yu's C−H arylation, they performed the coupling of alanine derivative **492** with aryl iodide **491**.[172] This reaction proceeded smoothly to provide a 76% combined yield of arylated products **493** and **494**, which were transformed into the same amino ester **495** via the removal of the $CONHAr_F$ directing group and phthalimide protecting group, respectively. Amino ester **495** was used to prepare both the western (**496**) and eastern (**497**) fragments of the renieramycin alkaloids.

Treatment of 1,3-*cis*-THIQ **496** and Boc-protected amino acid **497** with BOPCl and Et_3N provided the amide product **498** in 90% yield. With **498** in hand, pentacycle **499** was obtained from DMP oxidation, removal of the phenolic TBS protecting groups, acid-promoted intramolecular Pictet−Spengler cyclization, and reductive amination. Subsequently, enantioenriched (−)-renieramycins G, M, J, (−)-jorunnamycin A, and (−)-fennebricin A were prepared from this same pentacycle **499**. Of note, this research represents the first asymmetric total syntheses of renieramycin J and fennebricin A.

The recently isolated renieramycin T (**427**), which features a hybrid structure of ecteinascidin−renieramycin, was also a target for a total synthetic endeavor by Yokoya and Williams.[173] By adapting the strategy used in their total synthetic studies of Et-743,[174,175] they completed the synthesis of (−)-renieramycin T through the use of L-tyrosine as a chiral pool starting material (Scheme 67). Amide coupling of highly decorated THIQ **500** and Fmoc-protected amino acid chloride **501**, followed by swapping of amine protecting groups, provided amide **502** in 89% overall yield. Removal of the acetonide, then Dess−Martin oxidation, and intramolecular Pictet−Spengler cyclization delivered pentacycle **503** in 75% yield over 4 steps. From this key intermediate, they performed several functional group manipulations to obtain phenol **504**. This phenolic hydroxyl group was benzyl protected prior to the partial reduction of the central amide, cyanation of the *in situ* generated iminium ion, and oxidation of the eastern phenol to afford monoquinone **505**. Finally, debenzylation with BCl_3 and subsequent esterification with angeloyl chloride completed the total synthesis of renieramycin T (**427**). This natural product along with other compounds in this synthetic sequence was evaluated for their cytotoxicities and revealed to exhibit moderate activities against human cancer cell lines.

https://doi.org/10.1021/acs.chemrev.3c00054
Chem. Rev. 2023, 123, 9447−9496

Scheme 69. Stoltz's Total Syntheses of (−)-Jorunnamycin A and (−)-Jorumycin

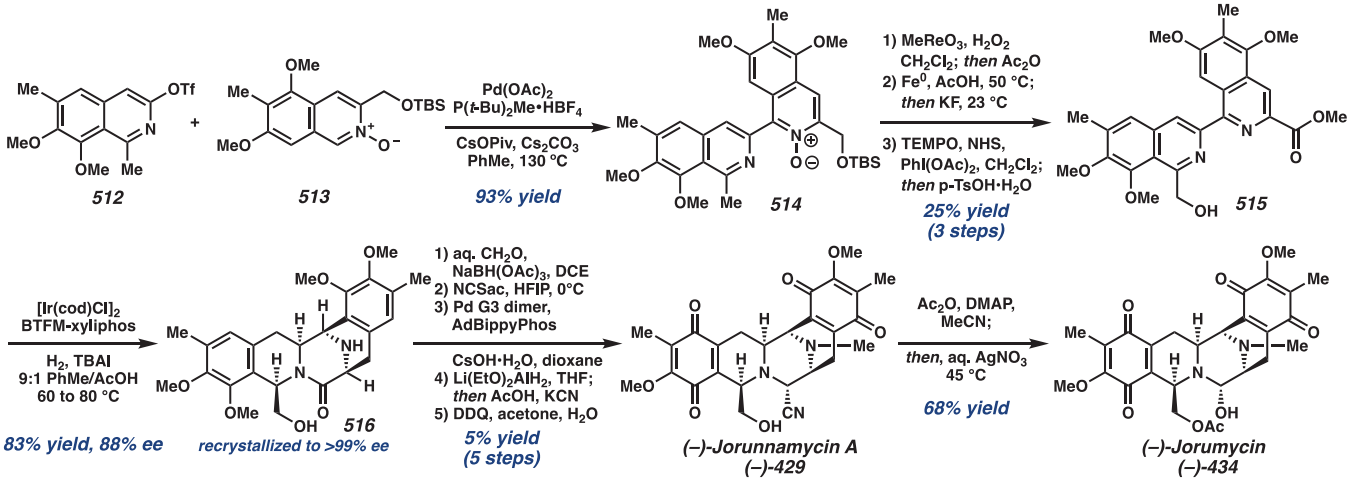

Seeking to develop an alternative strategy for the production of renieramycin T, Saito and co-workers applied the stereoselective decarboxylative reprotonation strategy previously discovered in the synthesis of saframycin A (Scheme 57, *vide supra*) in the context of this natural product.[176] To this end, the group completed a formal synthesis of renieramycin T by concluding at intermediate **505** as reported by Yokoya and Williams.

The Chen group also achieved a total synthesis of (−)-renieramycin T in 2016.[177] By mimicking the reported biosynthesis of Et-743,[178] they performed a Pictet−Spengler cyclization under a unique ternary solvent system (PhMe, CH_2Cl_2, and 2,2,2-trifluoroethanol) to construct the D-ring of bis-THIQ intermediate **508** (Scheme 68). Protection/deprotection chemistry was followed, and then a Swern oxidation with a subsequent $ZnCl_2$-promoted Strecker reaction eventually closed the C-ring, forming pentacycle **509** in 78% yield over 5 steps. With this intermediate in hand, they discovered that the chloroacetyl protecting group needed to be chemo- and regioselectively installed on the A-ring phenol (**511**) prior to oxidation and installation of the angeloyl group. Accordingly, they successfully prepared (−)-renieramycin T (**427**) in an additional 4 steps with 39% yield. Overall, this asymmetric total synthesis consists of 22 steps for the longest linear sequence with a 6.2% overall yield from known starting materials. Apart from (−)-renieramycin T, the Chen group successfully prepared three other renieramycin-type alkaloids: (−)-jorunnamycin A, (−)-jorunnamycin C, and (−)-jorumycin through this similar synthetic strategy.[179]

Aiming to devise a complementary synthetic route to prepare bis-THIQ alkaloids that specifically avoids the Pictet−Spengler reaction, the Stoltz group completed a synthetic study toward jorumycin (**434**) via a two-part strategy, consisting of a cross-coupling reaction for the convergent construction of the requisite carbon-based skeleton and an enantioselective hydrogenation to install all of the key stereochemistry (Scheme 69).[180] Specifically, we successfully exploited the *N*-oxide C−H functionalization developed by Fagnou and co-workers in the coupling of the eastern (**513**) and western (**512**) isoquinoline fragments. With the coupled product **514** in hand, the advancement of this intermediate to the bis-isoquinoline hydrogenation precursor (**515**) was performed through isoquinoline oxidation/mono-*N*-oxide rearrangement, followed by N−O bond cleavage and oxyl-mediated oxidation.

Another key transformation in this synthetic strategy is the sequential stereoselective hydrogenation to construct the pentacyclic scaffold of bis-THIQ molecules. The use of $[Ir(cod)Cl]_2$ in conjunction with an electron-poor Josiphos BTFM-xyliphos ligand was found to promote the desired hydrogenation-lactamization cascade, providing the pentacycle (**516**) as a single diastereomer in 83% yield and with 88% ee. Furthermore, this intermediate was recrystallized from a slowly evaporating acetonitrile solution to enantiopurity. The relative and absolute stereochemistry of the product was confirmed via X-ray crystallographic analysis.

The final stage of the synthesis consists of a 5-step sequence. First, reductive amination was employed to methylate the piperazinone N−H. Bis-chlorination of the A- and E-rings with *N*-chlorosaccharin (NCS) was then followed, and the subsequent C−O bond coupling provided a dihydroxylated compound. Lastly, partial reduction of the central lactam with cyanide trapping and DDQ oxidation delivered jorunnamycin A (**429**). Conversion of jorunnamycin A (**429**) into jorumycin (**434**) was achieved in one additional step, concluding the 16-step total synthesis. As a result of this unique approach, access to electronically modulated aromatic substitution patterns is readily attainable.

5.4. Ecteinascidin Alkaloids

5.4.1. General Structure and Isolation. The ecteinascidin alkaloids are known to be extremely potent antitumor agents, with Et-743 **2** (Yondelis) approved for clinical use for the treatment of advanced soft tissue sarcoma.[181] Apart from other THIQ alkaloids, these agents are unique in their structure, with the pentacyclic skeleton linked to a 10-membered lactone bridge through a benzylic sulfide linkage (Figure 21). Most ecteinascidin alkaloids contain an additional THIQ ring attached to the lactone bridge as a spirocycle, which is a key distinguishing feature from other THIQ natural product families.

Early biosynthetic studies of the ecteinascidins revealed that tyrosine and cysteine are the two amino acid building blocks specifically for the synthesis of Et-743.[182] More recently, with the advancement of next-generation sequencing technology, Sherman and co-workers exploited a meta-omic approach to identify the biosynthetic gene cluster responsible for the production of Et-743.[183] In this study, three putative modules of nonribosomal peptide synthetase (NRPS) are reported to

https://doi.org/10.1021/acs.chemrev.3c00054
Chem. Rev. 2023, 123, 9447−9496

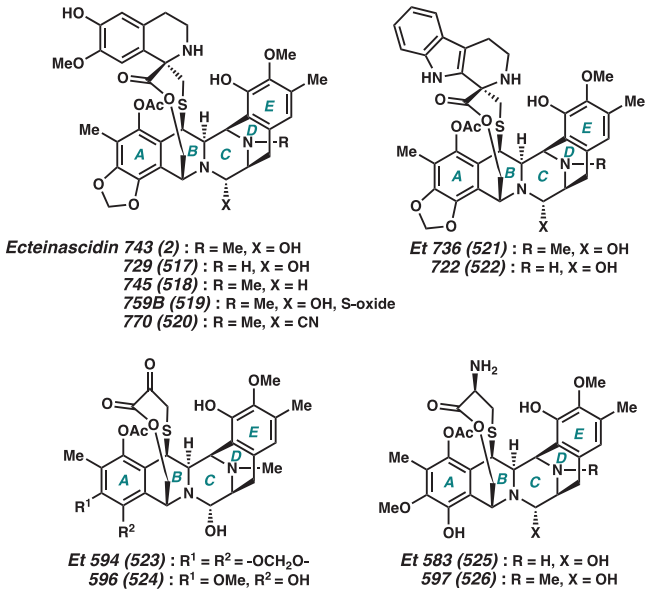

Figure 21. Ecteinascidin natural products.

promote transformations for the construction of the pentacyclic core (Scheme 70). Similar to the NRPS system of saframycin A (*vide supra*), EtuA2 is a homologue of SfmC that iteratively incorporates two molecules of tyrosine derivatives into the core structure. After the reductive release, also through the EtuA2 module, the aldehyde intermediate undergoes cyclization to generate the C-ring. Hydrolysis of the pendent *N*-acyl moiety subsequently proceeds, and the 10-membered lactone bridge is proposed to be assembled via the tailoring EtuO module. This produces Et-583 (**525**) as a late-stage intermediate, leading to other isolable ecteinascidins (Et-597, Et-596, and Et-594) and finally Et-743.

5.4.2. Total Synthesis of Ecteinascidin Alkaloids. Approaches to the chemical syntheses of these natural products generally utilize electrophilic aromatic substitution strategies for the construction of the THIQ motifs. After Corey's seminal total synthesis of Et-743 (**2**) in 1996, scientists at Pharma Mar disclosed a semisynthetic approach to prepare Et-743 and phthalascidin Pt-650 from cyanosafracin B in 2000. Despite being highly efficient and scalable, the structural diversity of analogs prepared using this semisynthetic tactic is inherently limited by the structure of the isolated compound. As a result, other groups have attempted to target this molecule and its congeners with distinct disconnections, resulting in six additional total syntheses of ecteinascidin alkaloids reported between 2002 and 2020.[184,185]

In 2002, Fukuyama and co-workers reported the second total synthesis of **2**.[186] With two functionalized fragments **533** and **534**, a Ugi four-component condensation reaction assembled intermediate **536** in high yield, which formed the diketopiperazine C-ring of the core in four subsequent steps (Scheme 71). After protection of the phenol and lactam nitrogen of **537**, partial reduction of the carbonyl with $NaBH_4$, and dehydration of the hemiaminal intermediate afforded the desired intermediate **538** for Heck cyclization. Using 5 mol % of $Pd_2(dba)_3$ and 20 mol % of the $P(o\text{-tol})_3$ ligand, an intramolecular Heck reaction proceeded smoothly to install the D-ring of the natural product scaffold **539** in 83% yield.

After several functional group manipulations, the key aldehyde intermediate **540** then underwent hydrogenolysis of

Scheme 70. A) Domain Organization of Et-743 NRPS; B) Proposed Biosynthetic Mechanism for the Construction of Et-743's Pentacyclic Skeleton

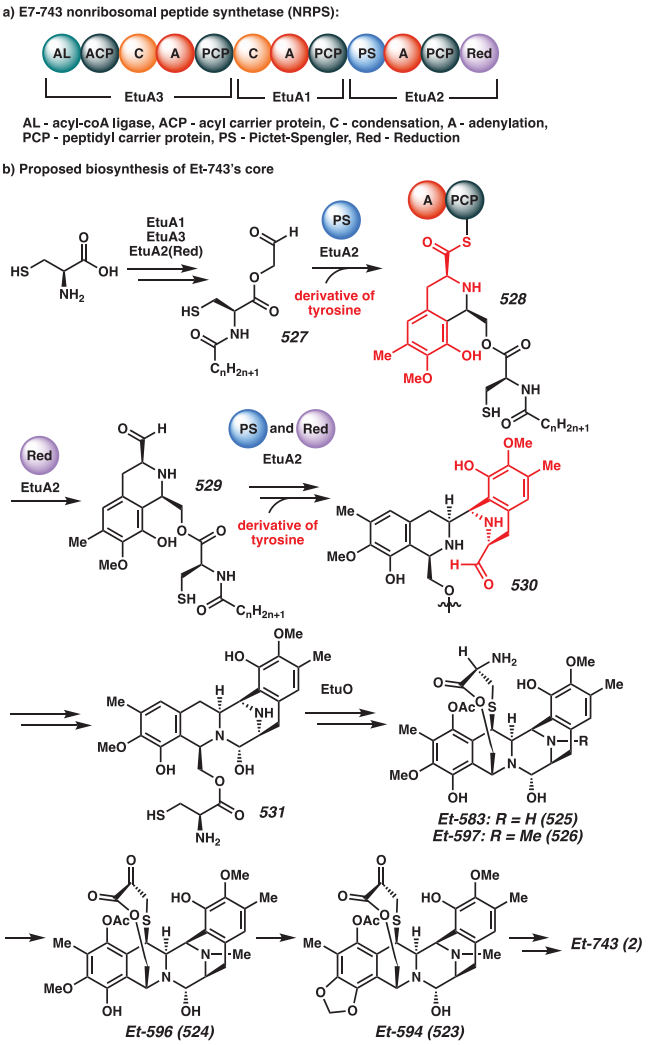

the benzyl ether to induce spontaneous cyclization and deliver the desired pentacycle **541**. With the desired oxidation already in place at the C4 position, condensation of the alcohol with L-cysteine derivative **542** furnished ester **543**, which smoothly formed the lactone bridge **544** under acidic conditions. A biomimetic transamination reaction afforded α-ketolactone **545** to undergo a subsequent Pictet–Spengler reaction with **546** to install the third THIQ moiety. Generating the labile hemiaminal last with $AgNO_3$ in CH_3CN and H_2O completed natural product **2** in 93% yield.

Since their completed total synthesis of **2** in 2002, Fukuyama and co-workers have revised their strategy to render its synthesis more efficient and practical.[187] They instead envisioned accessing intermediate **549** from dihydropyrrole **548**, assembled via a Heck reaction between amine **547** and enamide **548** (Scheme 72). Construction of the B-ring and the 10-membered lactone bridge proceeded according to their initial synthetic strategy. With the functionalized fragments in hand, treatment of **547** with *tert*-butyl nitrite and $BF_3{\cdot}OEt_2$ generated the diazonium salt *in situ* to undergo the key intermolecular Heck reaction with **548** in the presence of a palladium catalyst. Dihydroxylation of **549** and oxidative cleavage of the resulting 1,2-diol with H_5IO_6 formed

https://doi.org/10.1021/acs.chemrev.3c00054
Chem. Rev. 2023, 123, 9447−9496

Scheme 71. Fukuyama's Total Synthesis of Ecteinascidin 743

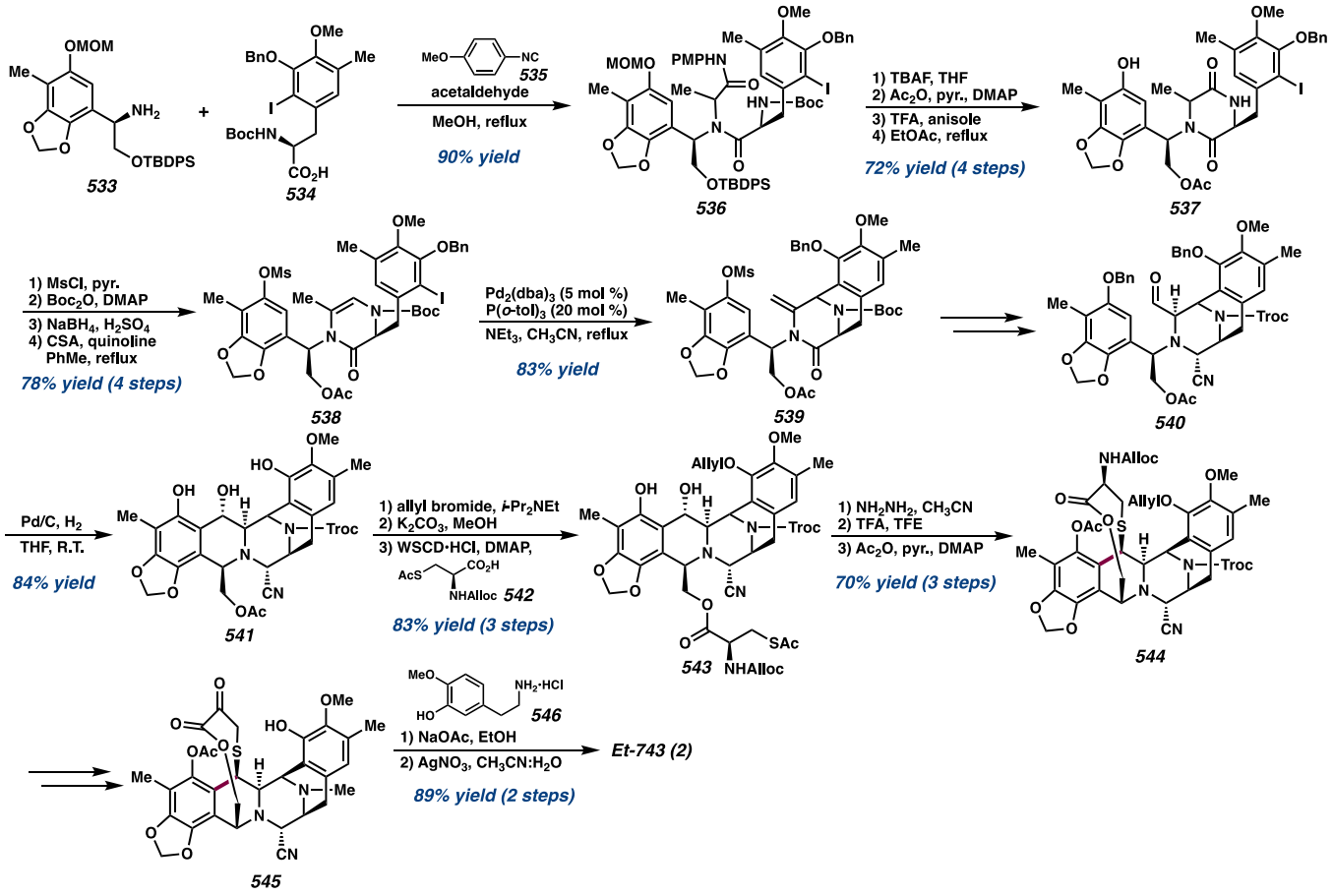

Scheme 72. Fukuyama's Revised Total Synthesis of Ecteinascidin 743

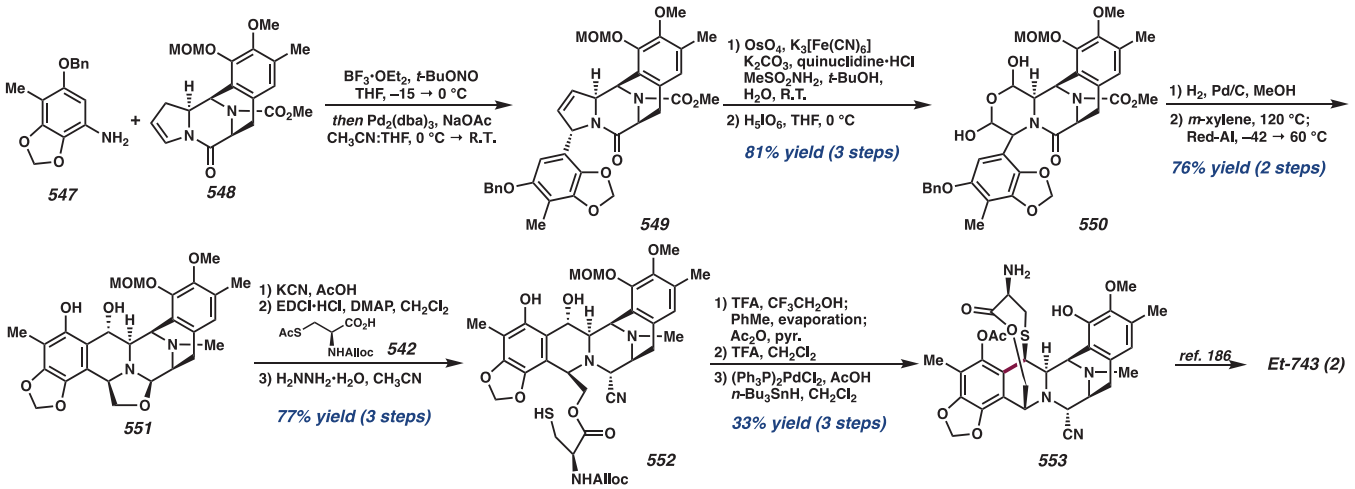

dialdehyde intermediate **550**, which could then be liberated by heating in *m*-xylene and trapped intramolecularly by the electron-rich arene to establish the THIQ B-ring and deliver **551**. Substitution at the C1 position of **552** was then elaborated to construct the 10-membered cyclic sulfide and access the natural product based on the previous synthetic strategy. Overall, the synthetic route to **2** was successfully shortened to 28 steps (as compared to 45 steps in their previous study) and 1.1% overall yield by efficiently constructing the B-ring.

Other synthetic strategies to construct the THIQ B-ring of Et-743 (**2**) were reported in 2006, wherein Danishefsky and co-workers demonstrated a novel vinylogous Pictet–Spengler cyclization from an *ortho*-hydroxystyrene intermediate **554** (Scheme 73).[188] Treatment of **556** with DMDO then oxidized the C4 position, which produced alcohol **558** as the major product through either a concerted rearrangement or a 1,2-hydride migration from epoxide **557**. After installation of the nitrile functionality, the MOM group was cleaved to reveal the

https://doi.org/10.1021/acs.chemrev.3c00054
Chem. Rev. 2023, 123, 9447–9496

Scheme 73. Danishefsky's Formal Total Synthesis of Ecteinascidin 743

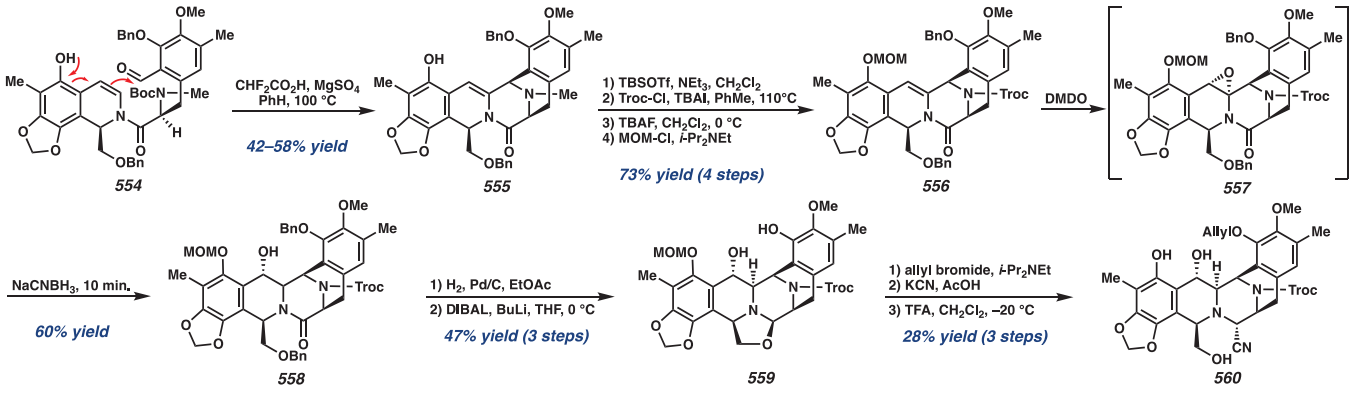

Scheme 74. Zhu's Total Synthesis of Ecteinascidin 770 and Ecteinascidin 743

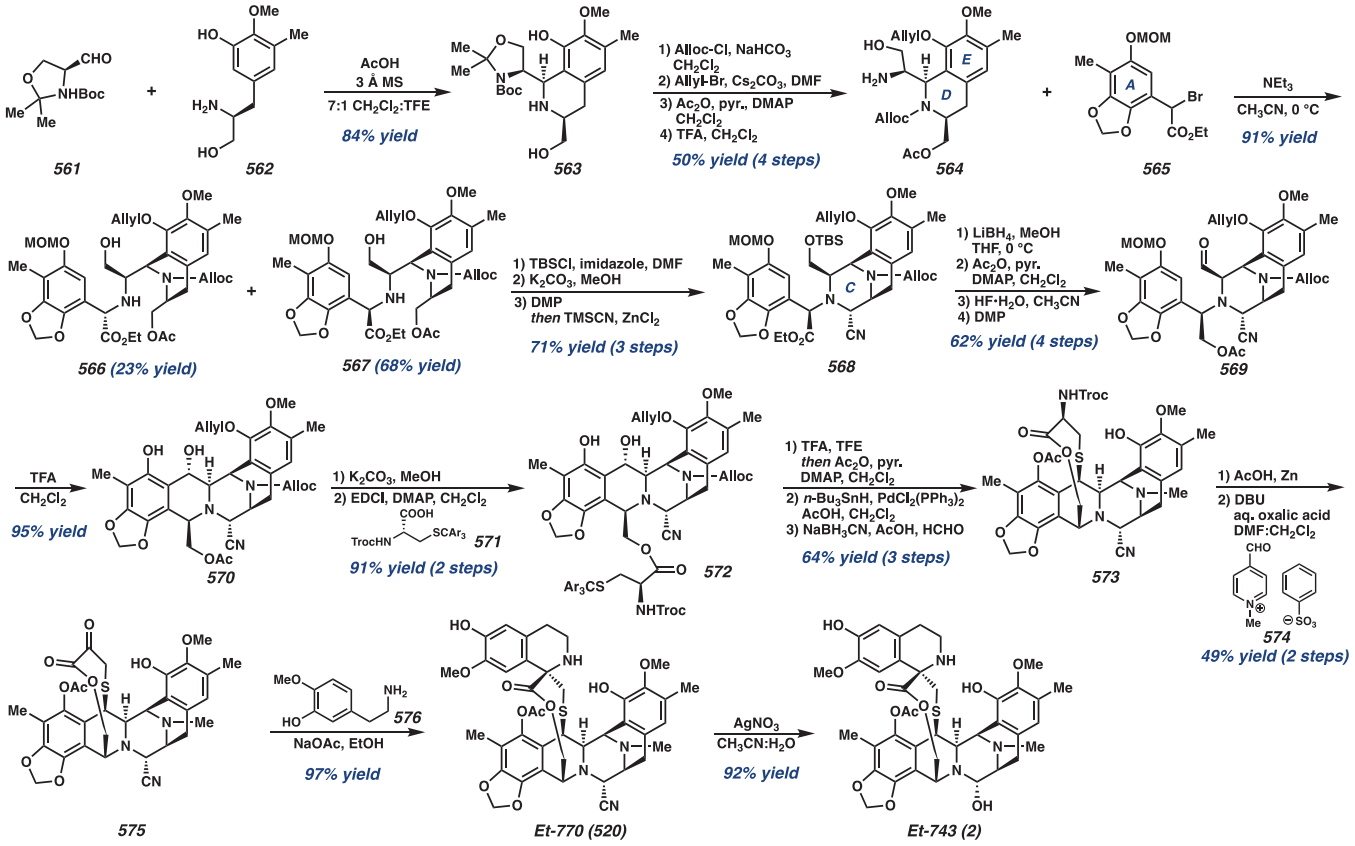

final intermediate **560**, which constituted a formal total synthesis of Et-743 (**2**).

On the other hand, Zhu and co-workers reported the total synthesis of Et-743 (**2**) by retrosynthetically disconnecting the molecule into four building blocks of similar size (Scheme 74).[189] Synthesis of the D- and E-rings of **2** commenced with condensation of aldehyde **561** with phenylalanol **562**, providing access to THIQ **563** in 84% yield as a single diastereomer. Masking the secondary amine as the *N*-allyloxycarbamate, followed by chemoselective protection of the alcohol and removal of the masked amino alcohol, delivered **564**. Assembly of this key intermediate with benzyl bromide **565** under CH_3CN in the presence of triethylamine delivered two coupled products, **566** and **567** that were isolated in 23 and 68% yield, respectively. The desired diastereomer **567** was carried forward to access the C-ring through a zinc-chloride-catalyzed Strecker reaction that provided amino nitrile **568** as a single diastereomer. After several oxidative manipulations to deliver aldehyde **569**, cyclization under acidic conditions afforded **570** with the concomitant removal of the MOM-protecting group. After the installation of the side chain at the C1 position to deliver **572**, the 10-membered lactone bridge was installed from dissolving **572** in TFE containing 1% TFA through *in situ* generation of an *ortho*-quinone methide, followed by an intramolecular Michael addition to access the key C−S bond in **573**. Following Corey's protocol, installation of the final THIQ was accomplished via oxidation to the ketoester **575** and Pictet−Spengler cyclization with **575** to provide Et-770 (**520**) in 97% yield.[184] Treatment of Et-770 with $AgNO_3$ in a mixture of CH_3CN and H_2O provided Et-743 (**2**) in 92% yield. Within the same year, Zhu and co-workers reported a similar synthetic

https://doi.org/10.1021/acs.chemrev.3c00054
Chem. Rev. 2023, 123, 9447−9496

Scheme 75. Zhu's Total Synthesis of Ecteinascidin 597 and Ecteinascidin 583

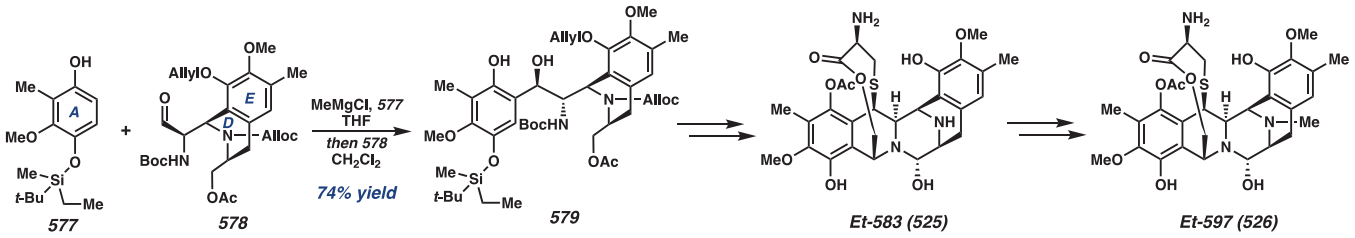

Scheme 76. Ma's Total Synthesis of Ecteinascidin 743 and Lurbinectedin

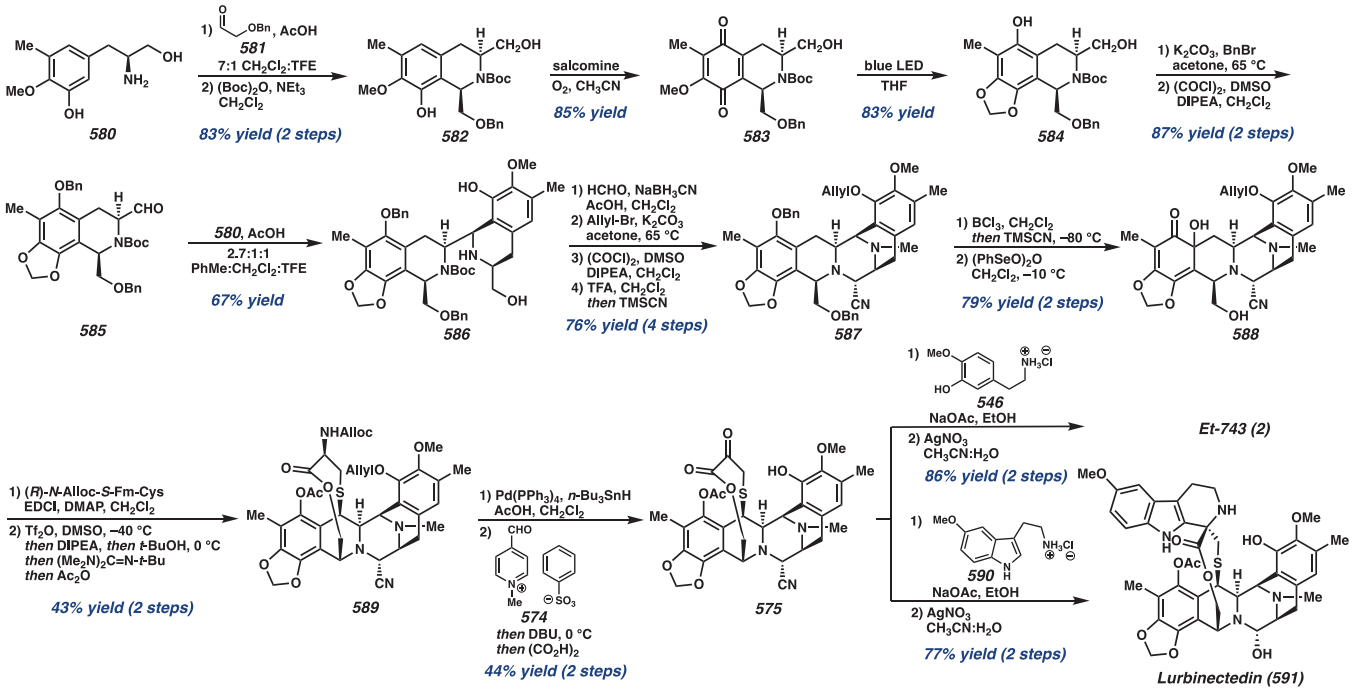

strategy for the total syntheses of Et-597 (**526**) and Et-583 (**525**), instead using phenol **577** to build the natural product scaffold through a sequence of aldol condensations followed by a Pictet–Spengler reaction (Scheme 75).[190]

More recently, Ma and co-workers described the total synthesis of Et-743 and lurbinectedin through a convergent Pictet–Spengler coupling event of an elaborated tetrahydroisoquinoline and tyrosine derivative **580** (Scheme 76).[191] Using the same intermediate **580** to construct both the western and eastern fragments of Et-743, a Pictet–Spengler reaction with benzyloxyacetaldehyde **581** and subsequent Boc-protection provided western THIQ **582** in 83% overall yield. After oxidation of phenol **582** to quinone **583**, a light-mediated C–H bond functionalization using blue LED light in THF allowed cyclization to deliver benzo[1,3]dioxole **584** in 83% yield. The formation of **584** could be scaled up to a multidecagram scale without compromising the yield.

After protection of the phenol and oxidation of **584** to aldehyde **585**, an intermolecular Pictet–Spengler reaction with amino alcohol **580** provided cyclization product **586** as the major isomer in 67% yield. This key coupling event allowed efficient construction of the natural product scaffold to install four of the six rings in a single step. Oxidation of the hydroxymethyl group then prepared for a subsequent Strecker reaction to construct amino nitrile **587**. With decagram quantities of the hexacyclic intermediate **587**, oxidation of the phenol with benzeneseleninic anhydride provided dihydroxy dienone **588**, which underwent elimination and macrocyclization according to Corey's one-pot procedure to obtain lactone **589**.[184] Finally, oxidation to the keto ester **575** and Pictet–Spengler reaction with phenethylamine **546** or tryptamine **590** followed by hydrolysis delivered either Et-743 (**2**) or lurbinectedin (**591**), respectively.

6. THIQ ALKALOIDS FROM THE NAPHTHYRIDINOMYCIN FAMILY

6.1. General Structure and Biosynthesis

Most alkaloids from the naphthyridinomycin family possess a hexacyclic skeleton, including four six-membered rings, a five-membered bridged ring, and an oxazolidine fragment (Figure 22). The A-ring can be in either the quinone or hydroquinone oxidation state. Members of this family are the naphthyridinomycin (**592**), cyanocyclines (**593**, **594**, **597**), bioxalomycins (**595**, **596**), aclidinomycins (**598**, **599**), and dnacins (**600**, **601**).

The biosynthesis of cyanocycline A was studied by Zmijewski and co-workers, where they discovered through feeding experiments that the core structure was assembled from tyrosine, methionine, glycine or serine, and ornithine.[192,193] Later in 2013, the Tang group analyzed the naphthyridinomycin gene cluster and proposed a pathway for the core formation via nonribosomal peptide synthetase

https://doi.org/10.1021/acs.chemrev.3c00054
Chem. Rev. 2023, 123, 9447–9496

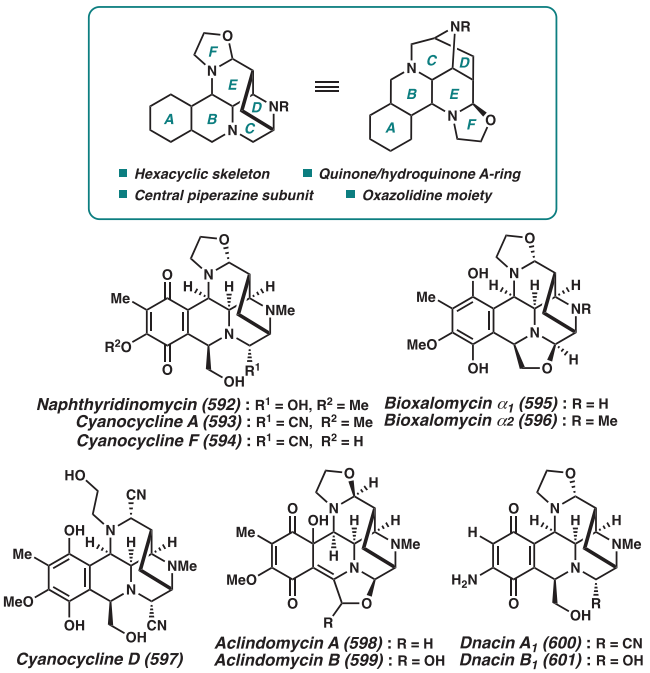

Figure 22. Core skeleton of THIQ alkaloids in the naphthyridinomycin family and representative examples.

(NRPS) NapL and NapJ modules.[194] The completed biosynthetic pathway, especially how the five-membered bridged ring is formed in the core structure, however, still has not been fully elucidated in this study.

6.2. Total Syntheses of Naphthyridinomycin Alkaloids

Although no recent total synthesis of the naphthyridinomycin alkaloids has been reported, several approaches for the formal synthesis of these natural products have been explored.[195] In 2007, Garner and co-workers disclosed an efficient synthetic approach toward the cyanocycline and bioxalomycin alkaloids harnessing their developed silver-catalyzed coupling reaction.[196,197] This key [C+NC+CC] coupling reaction provided rapid access to highly functionalized pyrrolidines, which could be converted to the target in one-third of the total number of steps compared to previously reported total syntheses.

The key coupling reaction was achieved by combining aldehyde **602** and Oppolzer's camphorsultam **603** in a methyl acrylate solvent with 10 mol % AgOAc (Scheme 77). The [3+2] cycloaddition was proposed to proceed through a pre-TS model such as **604**, in which the acrylate dipolarophile approaches the ylide from the least hindered *endosi* face approach. The *endo*-selective asymmetric coupling allowed the construction of pyrrolidine **605** as a single diastereomer.

To construct the rest of the natural product scaffold, **605** was subjected to hydrogenolysis to construct the lactam, and removal of the Boc group followed by a Pictet–pengler reaction with benzyloxyacetaldehyde produced THIQ **606**. After protection of the phenol, reduction with $LiAlH_4$ released the chiral auxiliary and converted the carbamate to the required *N*-methyl group. Oxidation of the primary alcohol **607** allowed construction of the diazobicyclo[3.2.1]octane core, followed by cyanide addition to deliver **608**. Finally, the oxazolidine ring was constructed from reduction of **608** to the imine that was reacted with hot ethylene oxide in MeOH to afford the late-stage intermediate **609**, a late-stage Fukuyama intermediate that was two steps away from the synthesis of cyanocycline A **593**.[198] Bioxalomycin β2 **610** was known to be convertible from **593**, demonstrating a formal synthesis of this natural product, as well. Overall, the successful application of the asymmetric Ag-catalyzed coupling reaction to install functionalized pyrrolidines allowed a rapid approach to this family of natural products.

7. THIQ ALKALOIDS FROM THE QUINOCARCIN FAMILY

7.1. General Structure and Biosynthesis

The quinocarcin family of THIQ alkaloids comprise quinocarcin **611**, quinocarcinol **612**, tetrazomine **613**, lemonomycin **614**, and aclidinomycins J and K (**615** and **616**).[199] These compounds are structurally similar, sharing a piperizinohydroisoquinoline motif as well as a 3,8-diazobicyclo[3.2.1]octane core (Figure 23). Quinocarcin and tetrazomine possess an additional oxazolidine ring, while lemonomycin contains a 2,6-dideoxy-4-amino sugar (lemonose) that is rarely found in nature. Compounds within the quinocarcin family display varying levels of antitumor and antibiotic properties. In particular, quinocarcin has exhibited potent antitumor activity against a variety of tumor cell lines and its citrate salt (KW2152) had been in clinical trials in Japan.[200]

In 2013, Oikawa and co-workers identified and analyzed the biosynthetic gene cluster (BGC) of quinocarcin and proposed its core assembly mechanism.[201] There are five modules (Qcn12, 13, 15, 17, and 19) for quinocarcin nonribosomal peptide synthetase (NRPS). Of these five modules, Qcn 17 and Qcn 19 are the two responsible for key C–C bond

Scheme 77. Garner's Formal Synthesis of Cyanocycline A and Bioxalomycin β2

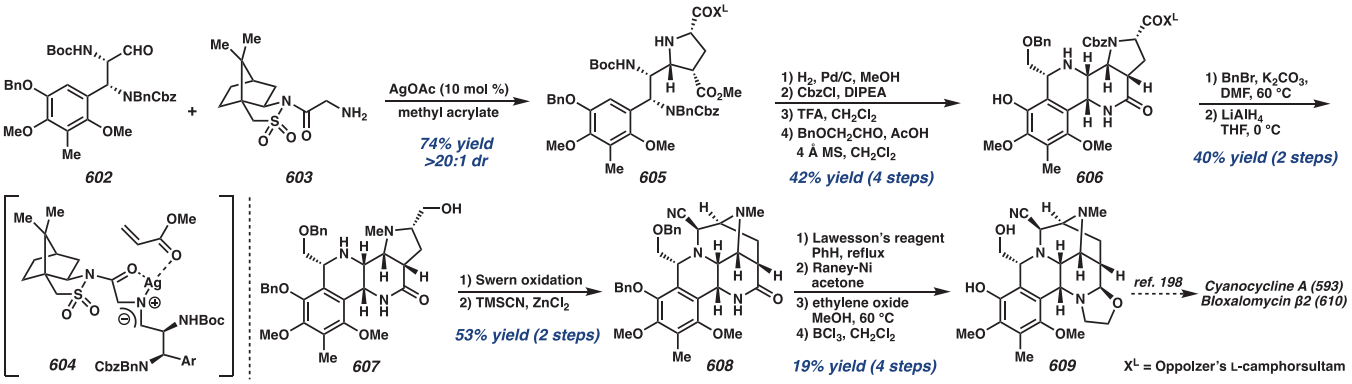

https://doi.org/10.1021/acs.chemrev.3c00054
Chem. Rev. 2023, 123, 9447–9496

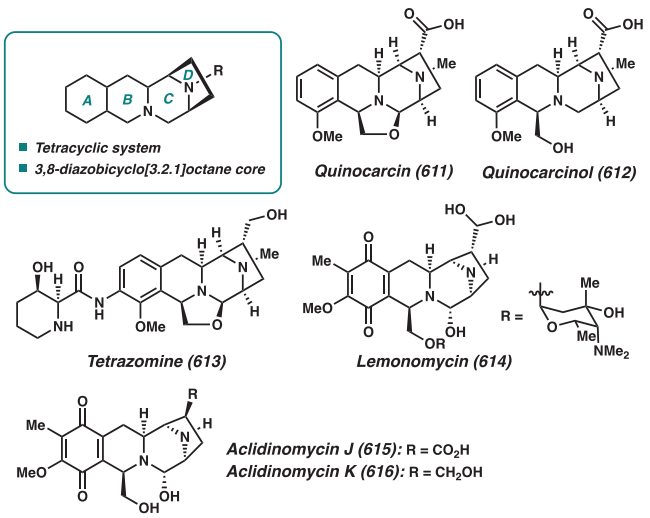

Figure 23. Skeleton of THIQ alkaloid members of the quinocarcin family.

formations. Particularly for Qcn17 which contains Pictet–Spengler (PS) and reduction (RE) domains, this module is SfmC-like and promotes successive Pictet–Spengler/Mannich cyclizations to generate pyrrolidine-substituted tetrahydroisoquinoline intermediate **621** (Scheme 78). The reductive

Scheme 78. Proposed Biosynthetic Mechanism for the Construction of Quinocarcin Core Scaffold

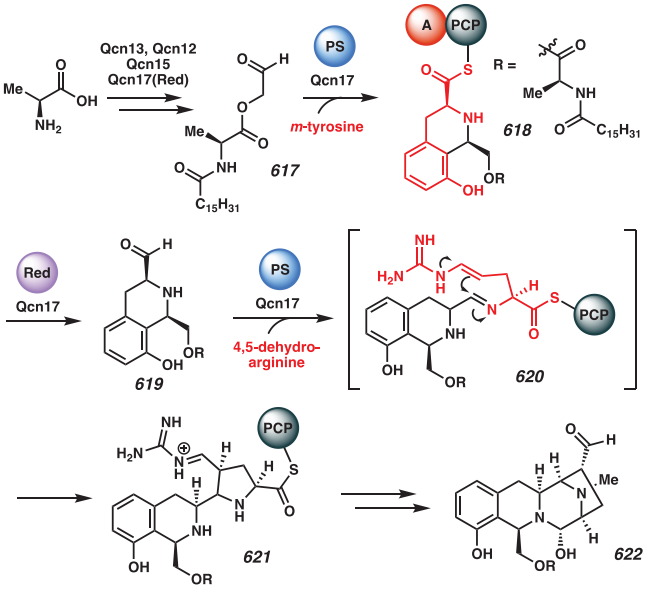

release of this species affords an aldehyde, which spontaneously undergoes an intramolecular cyclization to furnish the C-ring of the quinocarcin scaffold (**622**). In addition to the quinocarcin biosynthetic core assembly mechanism, this study also investigated the biosynthetic pathway for SF-1739, which is a member of the naphthyridinomycin family of THIQ alkaloids. The authors concluded that the mechanisms for the core assembly of these THIQ-pyrrolidine alkaloids are essentially the same but start from amino acids with different substitution patterns on the aromatic portion.

7.2. Total Syntheses of Quinocarcin

Toward the synthesis of (−)-quinocarcin (**611**), Myers and coworkers designed an extended approach of a previous strategy used by their lab to prepare (−)-saframycin A, involving a directed condensation of *C*- and *N*-protected α-amino aldehydes (Scheme 79).[202] *N*-protected α-amino aldehyde

Scheme 79. Myers' Total Synthesis of (−)-Quinocarcin

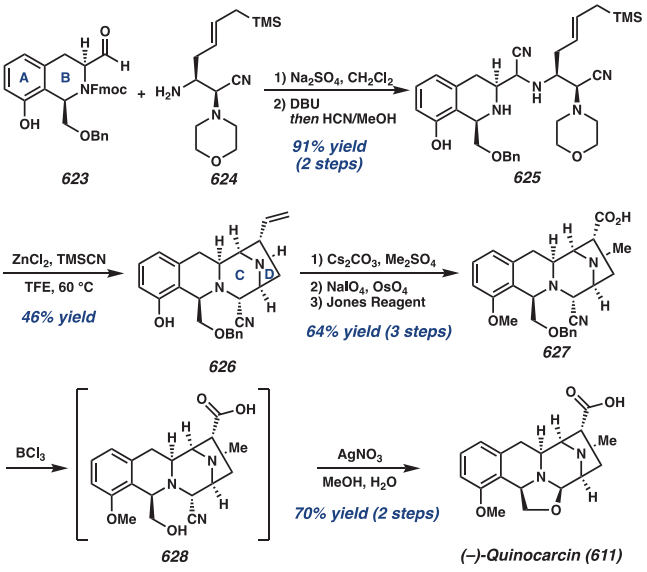

623, comprising the A- and B-rings of the target, and *C*-protected α-amino aldehyde **624** were subjected to condensation. Without isolation, the product was treated with DBU to cleave the Fmoc group, and then the addition of methanolic HCN provided Strecker addition product **625**. Treatment of **625** with trimethylsilyl cyanide and $ZnCl_2$ in TFE resulted in the cyclization of the C-ring via intramolecular amino nitrile exchange and subsequent closure of the D-ring through an allyl silane-imine addition reaction, forming tetracyclic core **626**. Bismethylation, followed by oxidative cleavage of the olefinic side chain and Jones oxidation, furnished acid **627**. Debenzylation in BCl_3 produced quinocarcin and its uncyclized precursor (DX-52-1) **628**, and treatment with silver nitrate in aqueous methanol converted the mixture entirely to yield (−)-quinocarcin (**611**).

In 2008, Zhu and co-workers reported the synthesis of (−)-quinocarcin through sequential ring cyclizations, and construction of the bridged bicycle by an intramolecular Mannich reaction using $AgBF_4$ (Scheme 80).[203] Selected as the A-ring scaffold, 3-hydroxybenzaldehyde **629** was converted to benzyl bromide **630**. In the presence of Corey–Lygo's phase-transfer catalyst (*O*-(9)-ally-*N*-(9′-anthracenylmethyl) cinchonidium bromide **C6**, **630** was used to alkylate *N*-(diphenylmethylene) glycine *tert*-butyl ester to produce **631** with >95% ee. A Pictet–Spengler reaction of ester **631** with benzoxyacetaldehyde **632** provided tetrahydroisoquinoline **633**, comprising the A- and B-rings. Amine **634** was subsequently acylated with **635** to form THIQ **636**. The ester moiety was selectively reduced before Swern oxidation to afford tricyclic hemiaminal **637** as a mixture of diastereomers. **637** was then converted to amino thioether **638** in the presence of EtSH and $Hf(OTf)_4$. The undesired diastereomer was recycled in the presence of PhSH and $Hf(OTf)_4$, before subjecting the resulting compound to the previous thioether-forming

https://doi.org/10.1021/acs.chemrev.3c00054
Chem. Rev. 2023, 123, 9447−9496

Scheme 80. Zhu's Total Synthesis of (−)-Quinocarcin

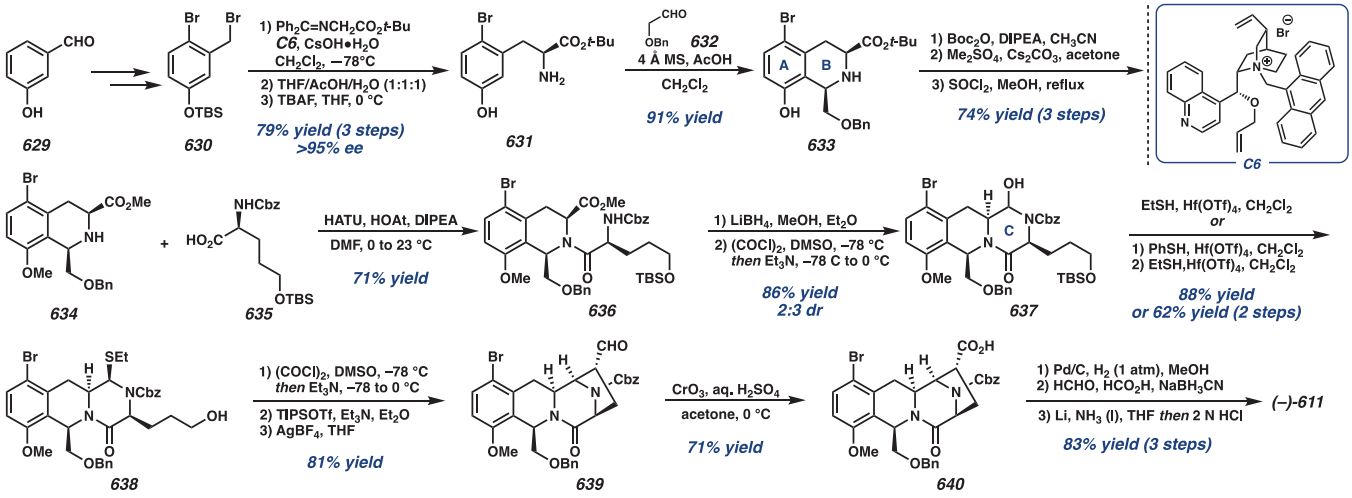

Scheme 81. Stoltz's Total Synthesis of (−)-Quinocarcin

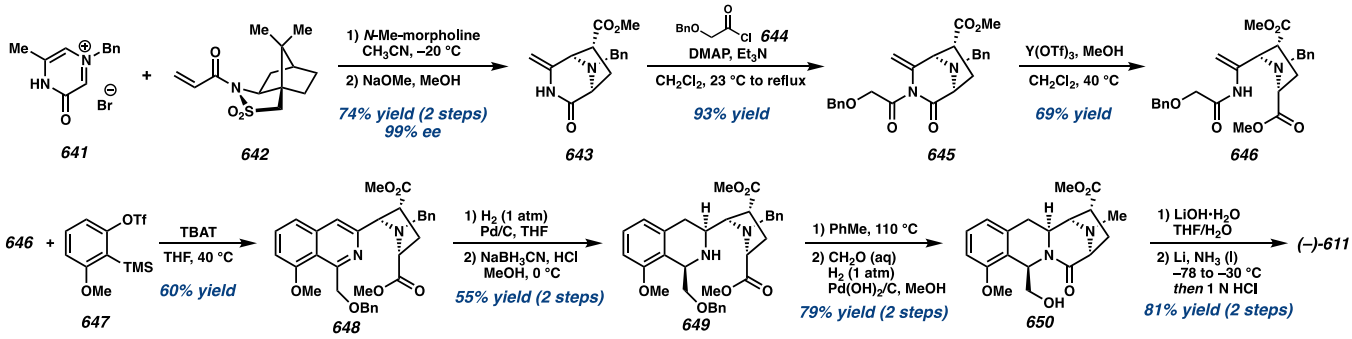

Scheme 82. Ohno's Total Synthesis of (−)-Quinocarcin

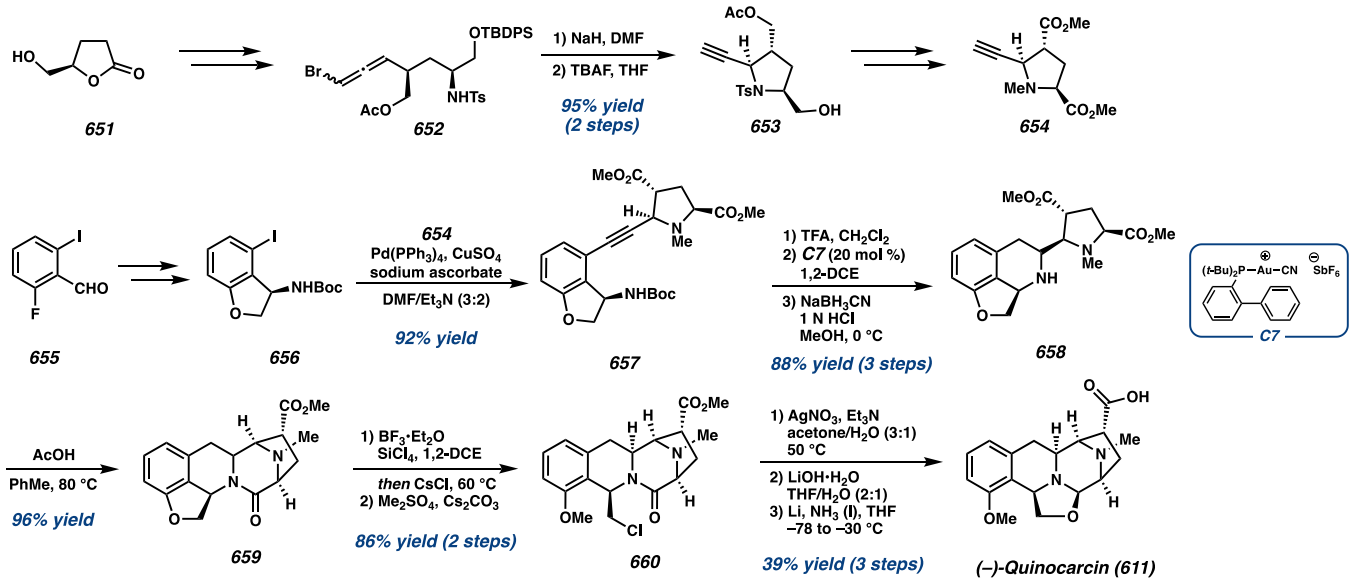

conditions again. A chemoselective Swern oxidation, silyl enol ether formation, and intramolecular Mannich reaction in the presence of silver tetrafluoroborate, an activator of the electrophile and nucleophile, led to a 5-*endo*-trig cyclization to furnish the tetracyclic compound **639** with an *exo*-oriented aldehyde moiety. Jones oxidation of **639** followed by global deprotection, *N*-methylation, partial lactam reduction, and ring closure under acidic conditions produced (−)-quinocarcin (**611**).

Harnessing a different approach toward the synthesis of (−)-quinocarcin, Stoltz and co-workers demonstrate the use of an aryne annulation reaction to assemble an isoquinoline precursor toward the THIQ moiety (Scheme 81).[204] Drawing from the synthetic strategy used by their group to synthesize

https://doi.org/10.1021/acs.chemrev.3c00054
Chem. Rev. 2023, 123, 9447−9496

Scheme 83. William's Total Synthesis of (−)-Tetrazomine

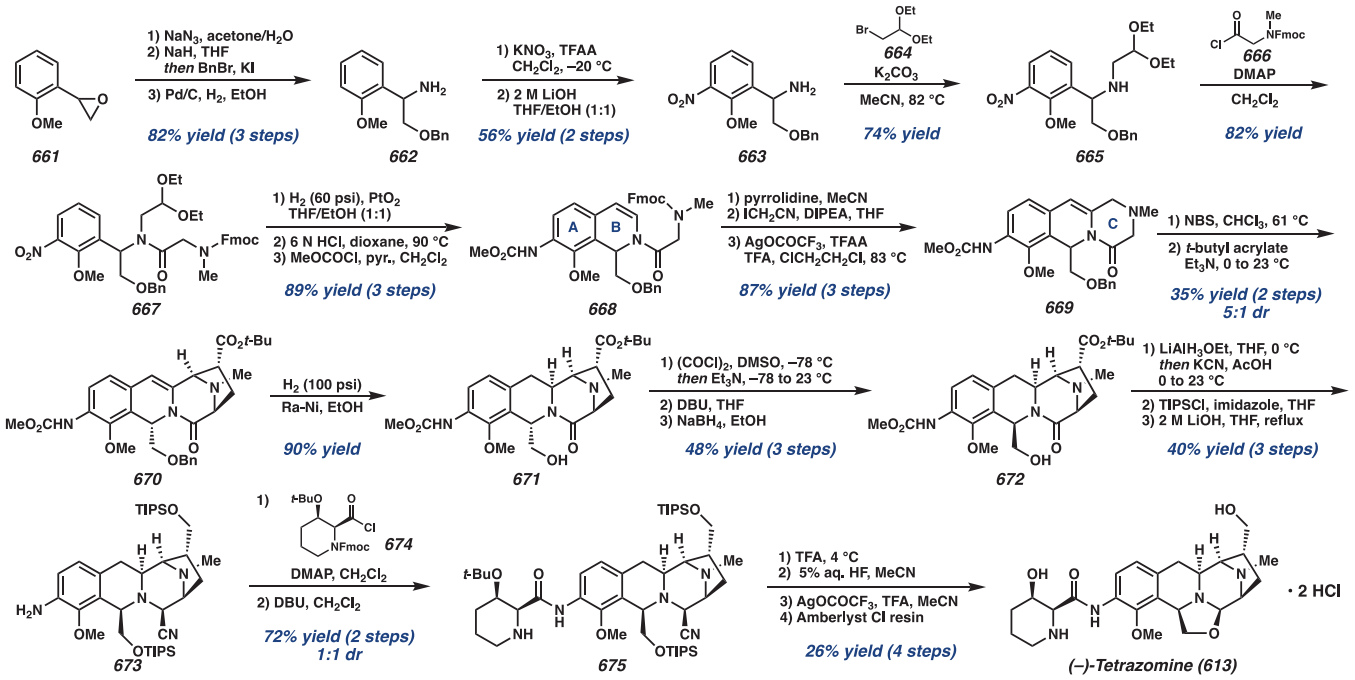

(−)-lemonomycin (vide infra), Stoltz and co-workers began with the cyclization of a deprotonated oxidopyrazinium bromide **641** with the acrylamide of Oppolzer's sultam **642** to deliver **643** with 99% ee. Basic methanolysis on the desired diastereomeric product followed by acylation with benzyloxyacetyl chloride **644** produced imide **645**. Regioselective methanolysis at the lactam carbonyl was conducted with yttrium(III) triflate to produce enamine **646**. The enamine and aryne precursors **647** were combined in the presence of tetra-*n*-butylammonium difluorotriphenylsilicate (TBAT) to generate isoquinoline **648**. Two consecutive reductions produced separable THIQs, with the desired diastereomer **649** as the major product obtained in 55% yield over two steps. After condensation to form the lactam, Pearlman's catalyst was used to remove the two benzyl groups and methylation of the unmasked amine afforded **650**. Saponification of methyl ester **650**, followed by partial reduction of the lactam and treatment of the resulting hemiaminal with a protic source, resulted in ring closure to form the oxazolidine ring and afford (−)-quinocarcin (**611**).

In a convergent approach toward the quinocarcin core, Ohno and co-workers employed a Sonogashira coupling and Au(I)-catalyzed intramolecular alkyne hydroamination to construct the scaffold of the THIQ core (Scheme 82).[205,206] Bromoallene **652** was constructed from γ-butyrolactone **651** and treated with NaH to provide 2,5-*cis*-pyrrolidine **653**. Further transformation produced pyrrolidine **654**. Enantioenriched dihydrobenzofuran **656** was prepared from aryl iodide **655**. A Sonogashira reaction was then utilized to couple building blocks **654** and **656** to produce the coupled product **657**. The Boc group was removed prior to Au(I)-catalyzed 6-*endo*-dig hydroamination using gold catalyst **C7** to form the B-ring of the THIQ. Due to the instability of the enamine generated, the product was directly reduced with $NaBH_3CN$ without isolation to form secondary amine **658**. Upon heating amine **658** in AcOH, condensation of the amine with one of the esters formed the diazobicyclo[3.2.1]octane core of intermediate **659**. Treatment of **659** with CsCl enabled ring-opening of the dihydrobenzofuran moiety and subsequent methylation of the phenol generated compound **660**. The alkyl halide was finally converted to the alcohol before cyclization to achieve (−)-**611**.

7.3. Total Syntheses of Tetrazomine

In 2002, Williams and co-workers utilized a [1,3]-dipolar cycloaddition in the synthesis of antitumor antibiotic (−)-tetrazomine **613** and its analogues (Scheme 83).[207] Starting with the ring-opening of aryl epoxide **661** using sodium azide, the resulting alcohol was protected, and the azide was hydrogenated to afford amine **662**. A nitro group was then installed *ortho* to the pre-existing methoxy group, and subsequent hydrolysis of the trifluoroacetamide furnished primary amine **663**. Alkylation of the amine with bromoacetaldehyde diethylacetal **664** provided secondary amine **665**, which was acylated with **666** to produce amide **667**. The nitro group was hydrogenated using PtO_2, and the resulting aniline underwent acid-promoted cyclization to yield dihydroisoquinoline **668**.

Cyclization of amine **668** then proceeded by treatment with Ag(I)trifluoroacetate in the presence of TFA and TFAA to deliver allylic amine **669** through a speculated *6-exo-tet* process. The amine **669** was then refluxed in chloroform with NBS to yield an iminium species that was treated with triethylamine and *tert*-butyl acrylate, producing ester **670** with a 5:1 dr. Hydrogenation afforded **671**, while the undesired diastereomer was epimerized at the C3 position and hydrogenated to produce the same product. Swern oxidation and treatment with DBU produced epimerized compound **672**. Subsequent reduction followed by trapping of the resulting carbinolamine afforded the aminonitrile moiety. TIPS protection of the two primary alcohols followed by hydrolysis of the methyl carbamate afforded aniline **673**.

Acid chloride **674** was prepared in three steps and coupled with aniline **673** in the presence of DMAP. Subsequent cleavage of the Fmoc group with DBU afforded **675** with a 1:1

https://doi.org/10.1021/acs.chemrev.3c00054
Chem. Rev. 2023, 123, 9447−9496

Scheme 84. Synthesis of Tetrazomine Analogues

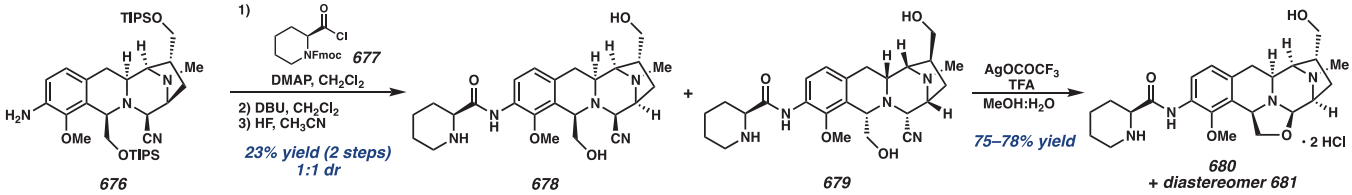

Scheme 85. Stoltz's Total Synthesis of (−)-Lemonomycin

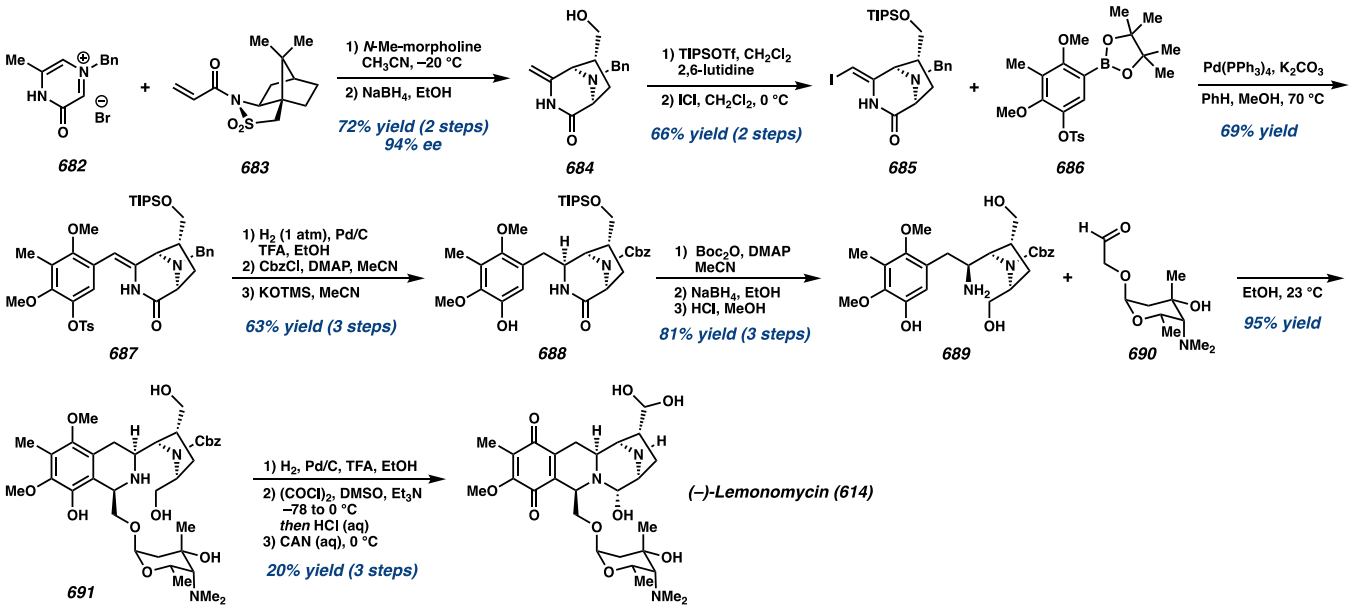

Scheme 86. Kan's Total Synthesis of (−)-Lemonomycin

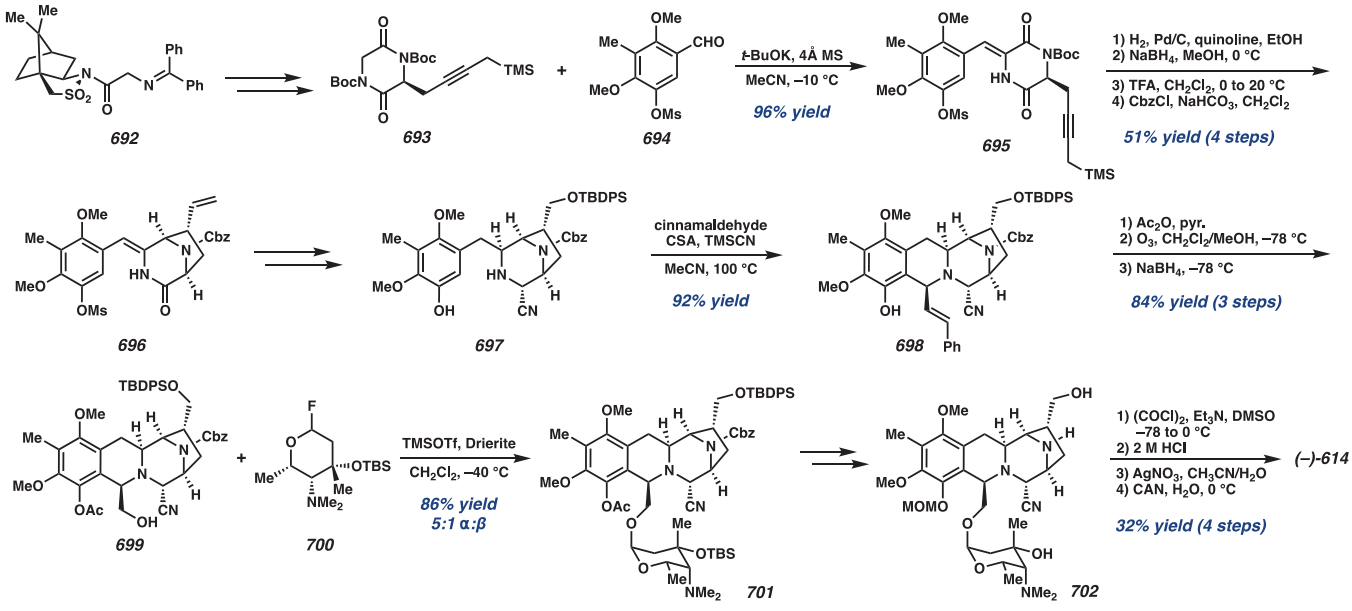

dr, which was isolable and carried on separately. Treatment of aminonitrile **675** with silver trifluoroacetate induced cyclization to form the oxazolidine ring, and addition of Amberlyst ion-exchange resin (Cl^- form), followed by filtration and lyophilization, afforded tetrazomine **613**. The other diastereomer of **675** was treated with the same steps to afford *ent, epi*-tetrazomine **613**.

In attempts to probe the biological activity of tetrazomine and its analogues, several novel analogues were prepared, as shown in Scheme 84.[207] Late-stage intermediate **676** was coupled to *N*-Fmoc-L-pipecolic acid chloride **677** followed by cleavage of the Fmoc and TIPS groups to afford both diastereomers **678** and **679** with a 1:1 dr. Treatment of both

https://doi.org/10.1021/acs.chemrev.3c00054
Chem. Rev. 2023, 123, 9447−9496

isomers with $AgOCOCF_3$ and TFA afforded two deoxytetrazomine analogs, **680** and **681**.

To examine the interaction of tetrazomine **613** and analogues **680** and **681** with DNA cleavage, these compounds were incubated with a synthetic ^{32}P-5′-end-labeled 45 bp duplex at pH 7 in phosphate buffer. While some analogues did not exhibit any DNA damage, tetrazomine **613** did display DNA cleavage in a nonsequence-specific manner. Additionally, all four oxazolidine and aminonitrile analogues were assayed against Gram-(+) bacteria (*Staphylococcus aureus*) and Gram-(−) bacteria (*Klebsiella pneumoniae*) via the disk diffusion method. Interestingly, deoxy compounds **680** and **681** displayed slightly better activity than either tetrazomine **613** or *ent*, *epi*-tetrazomine.

7.4. Total Syntheses of Lemonomycin

While there have been reports toward the formal synthesis of lemonomycin,[208] Stoltz and co-workers demonstrated a total synthesis of (−)-lemonomycin employing a stereoselective dipolar cycloaddition and diastereoselective Pictet−Spengler cyclization to form the tetracyclic compound (Scheme 85).[209] Cyclization of deprotonated bromide salt **682** with Oppolzer's sultam-derived acrylamide **683** provided bicycle **684** with a high ee. Enamide **684** was then converted to silyl ether and treated with ICI to produce *Z*-iodoenamide **685**. Suzuki coupling with aryl boronic ester **686** provided aryl enamide **687** and subsequent hydrogenation and protection of the amine and phenol deprotection produced amide **688**. Aminotriol **689** was accessed in three steps with an 81% overall yield from simultaneous activation of the amide and protection of the phenol with Boc_2O, reduction with $NaBH_4$, and cleavage of the Boc and TIPS moieties using methanolic HCl. Aldehyde **690** was separately prepared in eight steps (not shown) for the Pictet−Spengler reaction with aminotriol **689** to deliver THIQ **691**. Hydrogenolytic cleavage of the Cbz group, Swern oxidation, and treatment with CAN ultimately provided (−)-lemonomycin **614**.

Toward the synthesis of (−)-lemonomycin, Fukuyama and Kan and co-workers chose to couple the lemonose unit with the tetracyclic aglycon alkaloid subunit through a glycosidation reaction (Scheme 86).[210] Oppolzer's chiral auxiliary **692** was transformed to diketopiperazine **693** in four steps. Diketopiperazine **693** was subjected to a Perkin condensation reaction with **694** to give *Z*-enamide **695**, which was reduced and treated with TFA to produce the cyclized product **696**. Following several functional group transformations, the B-ring was constructed through a Pictet−Spengler reaction of **697** with cinnamaldehyde in the presence of CSA and TMSCN at 100 °C to deliver THIQ **698**. A one-pot conversion of **698** to aglycon alkaloid **699** was achieved through acetylation of the phenol group, ozonolysis, and subsequent reduction. Key intermediate **699** was coupled with functionalized lemonose **700** by treatment with TMSOTf and Drierite at −40 °C to deliver **701**. After several functional group manipulations, exposure of primary alcohol **702** to Swern oxidation produced the geminal diol and hemiaminal installation, followed by CAN-mediated oxidation of the A-ring to produce (−)-lemonomycin **614**.

8. CONCLUSION

The THIQ natural products are one of the most prominent families of alkaloids that exhibit a diverse range of biological activity as well as structural complexity. It is noteworthy that from simple benzyl THIQ alkaloids to complex ecteinascidin THIQ natural products, all possess interesting biological properties and reactivity that are of great interest to synthetic, biological, and medicinal chemists. From 2002 to 2020, research in the total synthesis of THIQ alkaloids has advanced greatly, especially in the development of novel methodologies such as photochemical and electrochemical pathways to facilitate creative disconnections. Not only do these modern chemical methods allow efficient chemical syntheses but they also provide access to a library of natural product analogues to uncover more of their biological activity.

Their challenging molecular architecture and their important therapeutic effects will surely continue to drive research to develop novel reactions toward their chemical syntheses and uncover new biosynthetic pathways. As of yet, there are still several families of natural products of which their biosynthesis is not fully understood, and the chemical syntheses of some THIQ alkaloids (e.g., safracin alkaloids) have not yet been explored. In addition, we foresee that the development of complementary strategies to access the THIQ natural product motif, which differs from biomimetic approaches, could open up exciting research avenues through the preparation of a wider range of analogues that deviate substantially from previous ones. The exploration of a more diverse chemical space, the identification of structural components required for the observed biological activity, and the structural simplification of efficacious analogues should have a profound impact on new drug development. Overall, we hope that this review will serve as a guide for future development in THIQ alkaloid chemistry and further medicinal and biological advancement.

AUTHOR INFORMATION

Corresponding Author

Brian M. Stoltz − *The Warren and Katharine Schlinger Laboratory for Chemistry and Chemical Engineering, Division of Chemistry and Chemical Engineering, California Institute of Technology, Pasadena, California 91125, United States;* orcid.org/0000-0001-9837-1528; Email: stoltz@caltech.edu

Authors

Alexia N. Kim − *The Warren and Katharine Schlinger Laboratory for Chemistry and Chemical Engineering, Division of Chemistry and Chemical Engineering, California Institute of Technology, Pasadena, California 91125, United States;* orcid.org/0000-0002-4060-8892

Aurapat Ngamnithiporn − *Laboratory of Medicinal Chemistry, Chulabhorn Research Institute, Bangkok 10210, Thailand*

Emily Du − *The Warren and Katharine Schlinger Laboratory for Chemistry and Chemical Engineering, Division of Chemistry and Chemical Engineering, California Institute of Technology, Pasadena, California 91125, United States*

Complete contact information is available at: https://pubs.acs.org/10.1021/acs.chemrev.3c00054

Author Contributions

The paper was written through contributions of all authors. All authors have given approval to the final version of the paper.

Notes

The authors declare no competing financial interest.

https://doi.org/10.1021/acs.chemrev.3c00054
Chem. Rev. 2023, 123, 9447−9496

Biographies

Dr. Alexia Kim was born in Arlington, VA, USA. She received her Bachelor's degree in Chemistry from Princeton University in 2017 under the supervision of Professor Robert Knowles. She then worked as a research assistant at Georgetown University from 2017 to 2018 under the guidance of Professor Tim Warren before pursuing her graduate studies at the California Institute of Technology. Currently, she is pursuing her Ph.D. under the tutelage of Professor Brian M. Stoltz exploring alkaloid synthesis.

Dr. Aurapat (Fa) Ngamnithiporn was born in Bangkok, Thailand before she moved to the U.S. and received her Bachelor's degree in Chemistry from Carleton College in 2015. She then obtained her Ph.D. degree in Organic Chemistry under the supervision of Professor Brian M. Stoltz at the California Institute of Technology in 2021. Currently, she is working as a research scientist at Chulabhorn Research Institute in Thailand. Her current research interests primarily focus on the development of transition-metal-catalyzed reactions for the syntheses of heterocycles.

Emily Du was born and raised in California. In 2022, they earned a B.Sc. in Chemistry and history from the California Institute of Technology, where they conducted research in the laboratory of Professor Brian M. Stoltz. They are currently pursuing their Ph.D. at Princeton University, where they are working on the development of new photocatalytic methods under the supervision of Professor Robert Knowles.

Professor Brian M. Stoltz was born in Philadelphia, PA, USA. After spending a year abroad at the Ludwig Maximilians Universität in München, Germany, he obtained his B.S. degree in Chemistry and B.A. degree in German from the Indiana University of Pennsylvania in Indiana, PA. Following graduate studies at Yale University in the labs of John L. Wood and an NIH postdoctoral fellowship at Harvard with E. J. Corey, he took a position at the California Institute of Technology in 2000. At Caltech, he is currently the Victor and Elizabeth Atkins Professor of Chemistry and an Investigator of the Heritage Medical Research Institute. His research interests lie in all areas of synthetic organic chemistry. He is the recipient of numerous award and accolades for his research and teaching including most recently the Feynman Teaching Prize from Caltech and the American Chemical Society Award for Creative Work in Synthetic Organic Chemistry. He is a fellow of the American Association for the Advancement of Science and the American Chemical Society.

ACKNOWLEDGMENTS

We thank NIH-NIGMS (R35GM145239) and the Heritage Medical Research Investigator Program for financial support of our research program.

REFERENCES

(1) Phillipson, J. D.; Roberts, M. F.; Zenk, M. H. Plants as a Source of Isoquinoline Alkaloids. In *The Chemistry and Biology of Isoquinoline Alkaloids*; Phillipson, J. D., Roberts, M. F., Zenk, M. H., Eds.; Springer, 1985; pp 1−23.
(2) Chrzanowska, M.; Grajewska, A.; Rozwadowska, M. D. Asymmetric Synthesis of Isoquinoline Alkaloids: 2004−2015. *Chem. Rev.* **2016**, *116*, 12369−12465.
(3) Scott, J. D.; Williams, R. M. Chemistry and Biology of the Tetrahydroisoquinoline Antitumor Antibiotics. *Chem. Rev.* **2002**, *102*, 1669−1730.
(4) Cassels, B. K. Alkaloids of the Cactaceae - The Classics. *Nat. Prod. Commun.* **2019**, *14*, 85−90.
(5) Fahmy, N. M.; Al-Sayed, E.; El-Shazly, M.; Singab, A. N. Alkaloids of Genus *Erythrina*: An Updated Review. *Nat. Prod. Res.* **2020**, *34*, 1891−1912.
(6) Barton, D. H. R.; James, R.; Kirby, G. W.; Widdowson, D. A. The Biosynthesis of the *Erythrina* Alkaloids. *Chem. Commun.* **1967**, 266−268.
(7) Maier, U. H.; Rödl, W.; Deus-Neumann, B.; Zenk, M. H. Biosynthesis of *Erythrina* Alkaloids in *Erythrina crista-galli*. *Phytochemistry* **1999**, *52*, 373−382.
(8) Zhang, F.; Simpkins, N. S.; Blake, A. J. New Approaches for the Synthesis of Erythrinan Alkaloids. *Org. Biomol. Chem.* **2009**, *7*, 1963−1979.
(9) Tietze, L. F.; Tölle, N.; Kratzert, D.; Stalke, D. Efficient Formal Total Synthesis of the Erythrina Alkaloid (+)-Erysotramidine, Using a Domino Process. *Org. Lett.* **2009**, *11*, 5230−5233.
(10) Mostowicz, D.; Dygas, M.; Kałuza, Z. Heck Cyclization Strategy for Preparation of Erythrinan Alkaloids: Asymmetric Synthesis of Unnatural (−)-Erysotramidine from L-Tartaric Acid. *J. Org. Chem.* **2015**, *80*, 1957−1963.
(11) Blackham, E. E.; Booker-Milburn, K. I. A Short Synthesis of (±)-3-Demethoxyerythratidinone by Ligand-Controlled Selective Heck Cyclization of Equilibrating Enamines. *Angew. Chem., Int. Ed.* **2017**, *56*, 6613−6616.
(12) Luu, H.-T.; Streuff, J. Development of an Efficient Synthesis of *rac*-3-Demethoxyerythratidinone via a Titanium(III) Catalyzed Imine-Nitrile Coupling. *Eur. J. Org. Chem.* **2019**, *2019*, 139−149.
(13) Yasui, Y.; Koga, Y.; Suzuki, K.; Matsumoto, T. A Novel Approach to Erythrinan Alkaloids by Utilizing Substituted Biphenyl as Building Block. *Synlett.* **2004**, *4*, 615−618.
(14) Yasui, Y.; Suzuki, K.; Matsumoto, T. Transmission of Axial Chirality to Spiro Center Chirality, Enabling Enantiospecific Access to Erythrinan Alkaloids. *Synlett.* **2004**, *4*, 619−622.
(15) Umihara, H.; Yoshino, T.; Shimokawa, J.; Kitamura, M.; Fukuyama, T. Development of a Divergent Synthetic Route to the Erythrina Alkaloids: Asymmetric Syntheses of 8-Oxo-erythrinine, Crystamidine, 8-Oxo-erythraline, and Erythraline. *Angew. Chem., Int. Ed.* **2016**, *55*, 6915−6918.
(16) Padwa, A.; Wang, Q. Synthesis of the Tetracyclic Framework of the Erythrina Alkaloids Using a [4 + 2]-Cycloaddition/Rh(I)-Catalyzed Cascade of 2-Imidofurans. *J. Org. Chem.* **2006**, *71*, 7391−7402.
(17) Allin, S. M.; Streetley, G. B.; Slater, M.; James, S. L.; Martin, W. P. A Formal Asymmetric Synthesis of Both Enantiomers of the *Erythrina* Alkaloid 3-demethoxyerythratidinone. *Tetrahedron Lett.* **2004**, *45*, 5493−5496.
(18) Moon, J. T.; Jung, J. A.; Ha, S. H.; Song, S. H.; Park, S. J.; Kim, J.; Choo, D. J.; Lee, Y. S.; Lee, J. Y. Synthetic Studies on *Erythrina* Alkaloids: Formal Total Synthesis of (+)-3-Demethoxyerythratidinone. *Synth. Commun.* **2011**, *41*, 1282−1292.
(19) Zhang, F.; Simpkins, N. S.; Wilson, C. An Enantiospecific Synthesis of (+)-Demethoxyerythratidinone from (*S*)-Malic Acid: Key Observations Concerning the Diastereocontrol in Malic Acid-Derived *N*-Acyliminium Ion Cyclisations. *Tetrahedron Lett.* **2007**, *48*, 5942−5947.
(20) Chuang, K. V.; Navarro, R.; Reisman, S. E. Benzoquinone-Derived Sulfinyl Imines as Versatile Intermediates for Alkaloid Synthesis: Total Synthesis of (−)-3-demethoxyerythratidinone. *Chem. Sci.* **2011**, *2*, 1086−1089.
(21) Paladino, M.; Zaifman, J.; Ciufolini, M. A. Total Synthesis of (+)-3-Demethoxyerythratidinone and (+)-Erysotramidine via the Oxidative Amidation of a Phenol. *Org. Lett.* **2015**, *17*, 3422−3425.
(22) Mostowicz, D.; Dygas, M.; Kaluza, Z. Heck Cyclization Strategy for Preparation of Erythrinan Alkaloids: Asymmetric Synthesis of Unnatural (−)-Erysotramidine from L-Tartaric Acid. *J. Org. Chem.* **2015**, *80*, 1957−1963.
(23) O'Connor, S. E. Alkaloid Biosynthesis. *Wiley Encycl. Chem. Biol.* **2008**, 1−16.
(24) Shamma, M.; Slusarchyk, W. A. The Aporphine Alkaloids. *Chem. Rev.* **1964**, *64*, 59−79.

https://doi.org/10.1021/acs.chemrev.3c00054
Chem. Rev. 2023, 123, 9447−9496

(25) Wang, F.-X.; Zhu, N.; Zhou, F.; Lin, D.-X. Natural Aporphine Alkaloids with Potential to Impact Metabolic Syndrome. *Molecules* **2021**, *26*, 6117−6139.
(26) Morris, J. S.; Facchini, P. J. Isolation and Characterization of Reticuline *N*-Methyltransferase Involved in Biosynthesis of the Aporphine Alkaloid Magnoflorine in Opium Poppy. *J. Biol. Chem.* **2016**, *291*, 23416−23427.
(27) Cuny, G. D. Synthesis of (±)-aporphine utilizing Pictet-Spengler and Intramolecular Phenol *ortho*-Arylation Reactions. *Tetrahedron Lett.* **2004**, *45*, 5167−5170.
(28) Lafrance, M.; Blaquière, N.; Fagnou, K. Direct Intramolecular Arylation of Unactivated Arenes: Application to the Synthesis of Aporphine Alkaloids. *Chem. Commun.* **2004**, 2874−2875.
(29) Nimgirawath, S.; Udomputtimekakul, P.; Pongphuttichai, S.; Wanbanjob, A.; Taechowisan, T. Total Synthesis and Antimicrobial Activity of (±)-Laurelliptinhexadecan-1-one and (±)-Laurelliptinoctadecan-1-one. *Molecules.* **2008**, *13*, 2935−2947.
(30) Zhong, M.; Jiang, Y.; Chen, Y.; Yan, Q.; Liu, J.; Di, D. Asymmetric Total Synthesis of (*S*)-isocorydine. *Tetrahedron: Asymmetry.* **2015**, *26*, 1145−1149.
(31) Pieper, P.; McHugh, E.; Amaral, M.; Tempone, A. G.; Anderson, E. A. Enantioselective Synthesis and Anti-parasitic Properties of Aporphine Natural Products. *Tetrahedron.* **2020**, *76*, 130814−130821.
(32) Anakabe, E.; Carrillo, L.; Badía, D.; Vicario, J. L.; Villegas, M. Stereoselective Synthesis of Aporphine Alkaloids Using a Hypervalent Iodine(III) Reagent-Promoted Oxidative Nonphenolic Biaryl Coupling Reaction. Total Synthesis of (*S*)-(±)-Glaucine. *Synthesis* **2004**, *7*, 1093−1101.
(33) Fürstner, A.; Mamane, V. Concise Total Synthesis of the Aporphine Alkaloid 7,7′-bisdehydro-*O*-methylisopiline by an $InCl_3$ Mediated Cycloisomerization Reaction. *Chem. Commun.* **2003**, 2112−2113.
(34) Perecim, G. P.; Rodrigues, A.; Raminelli, C. A Convenient Formation of Aporphine Core via Benzyne Chemistry: Conformational Analysis and Synthesis of (*R*)-Aporphine. *Tetrahedron Lett.* **2015**, *56*, 6848−6851.
(35) Rossini, A. F. C.; Muraca, A. C. A.; Casagrande, G. A.; Raminelli, C. Total Syntheses of Aporphine Alkaloids via Benzyne Chemistry: An Approach to the Formation of Aporphine Cores. *J. Org. Chem.* **2015**, *80*, 10033−10040.
(36) Perecim, G. P.; Deflon, V. M.; Martins, G. R.; Pinto, L. M. C.; Casagrande, G. A.; Oliveira-Silva, D.; Raminelli, C. Stereoselective Total Syntheses of (*S*)- and (*R*)-Nuciferine using Benzyne Chemistry. *Tetrahedron* **2020**, *76*, 131461−131468.
(37) Nimgirawath, S.; Udomputtimekakul, P. Total Syntheses of Telisatin A, Telisatin B and Lettowianthine. *Molecules* **2009**, *14*, 917−924.
(38) Ku, A. F.; Cuny, G. D. Synthetic Studies of 7-Oxygenated Aporphine Alkaloids: Preparation of (−)-Oliveroline, (−)-Nornuciferidine, and Derivatives. *Org. Lett.* **2015**, *17*, 1134−1137.
(39) Ku, A. F.; Cuny, G. D. Access to 6a-Alkyl Aporphines: Synthesis of (±)-*N*-Methylguattescidine. *J. Org. Chem.* **2016**, *81*, 10062−10070.
(40) Honda, T.; Shigehisa, H. Novel and Efficient Synthetic Path to Proaporphine Alkaloids: Total Synthesis of (±)-Stepharine and (±)-Pronuciferine. *Org. Lett.* **2006**, *8*, 657−659.
(41) Magnus, P.; Marks, K. D.; Meis, A. New Strategy for the Synthesis of Proaporphine and Homoproaporphine-type Alkaloids from a Common Intermediate. *Tetrahedron* **2015**, *71*, 3872−3877.
(42) Yoshida, K.; Fujino, Y.; Takamatsu, Y.; Matsui, K.; Ogura, A.; Fukami, Y.; Kitagaki, S.; Takao, K. Enantioselective Total Synthesis of (−)-Misramine. *Org. Lett.* **2018**, *20*, 5044−5047.
(43) Yoshida, K.; Itatsu, Y.; Fujino, Y.; Inoue, H.; Takao, K. Enantioselective Organocatalytic Construction of Spiroindane Derivatives by Intramolecular Friedel-Crafts-Type 1,4-Addition. *Angew. Chem., Int. Ed.* **2016**, *55*, 6734−6738.
(44) Lafrance, M.; Blaquiere, N.; Fagnou, K. Aporphine Alkaloid Synthesis and Diversification via Direct Arylation. *Eur. J. Org. Chem.* **2007**, *2007*, 811−825.
(45) Payne, J. T.; Valentic, T. R.; Smolke, C. D. Complete Biosynthesis of the Bisbenzylisoquinoline Alkaloids Guattegaumerine and Berbamunine in Yeast. *Proc. Natl. Acad. Sci. U.S.A.* **2021**, *118*, 1−12.
(46) Watanabe, H.; Uramoto, H.; Maeda-Hagiwara, M.; Kikuchi, T. Antidopaminergic Effects of Bisbenzyl and Benzyl Tetrahydroisoquinoline Alkaloids. *Arch. Int. Pharmacodyn. Ther.* **1985**, *278*, 53−60.
(47) Blank, N.; Opatz, T. Enantioselective Synthesis of Tetrahydroprotoberberines and Bisbenzylisoquinoline Alkaloids from a Deprotonated α-Aminonitrile. *J. Org. Chem.* **2011**, *76*, 9777−9784.
(48) Otto, N.; Ferenc, D.; Opatz, T. A Modular Access to (±)-Tubocurine and (±)-Curine - Formal Total Synthesis of Tubocurarine. *J. Org. Chem.* **2017**, *82*, 1205−1217.
(49) Schütz, R.; Meixner, M.; Antes, I.; Bracher, F. A Modular Approach to the Bisbenzylisoquinoline Alkaloids Tetradine and Isotetradine. *Org. Biomol. Chem.* **2020**, *18*, 3047−3068.
(50) Wang, Y.-C.; Georghiou, P. E. First Enantioselective Total Synthesis of (−)-Tejedine. *Org. Lett.* **2002**, *4*, 2675−2678.
(51) Kawabata, Y.; Naito, Y.; Saitoh, T.; Kawa, K.; Fuchigami, T.; Nishiyama, S. Synthesis of (+)-*O*-Methylthalibrine by Employing a Stereocontrolled Bischler-Napieralski Reaction and an Electrochemically Generated Diaryl Ether. *Eur. J. Org. Chem.* **2014**, *2014*, 99−104.
(52) Naito, Y.; Tanabe, T.; Kawabata, Y.; Ishikawa, Y.; Nishiyama, S. Electrochemical Construction of the Diaryl Ethers: A Synthetic Approach to *O*-methylthalibrine. *Tetrahedron Lett.* **2010**, *51*, 4776−4778.
(53) Huang, Z.; Ji, X.; Lumb, J.-P. Total Synthesis of (*S*, *S*)-Tetramethylmagnolamine via Aerobic Desymmetrization. *Org. Lett.* **2019**, *21*, 9194−9197.
(54) Vasconcelos Leitao Da-Cunha, E.; Fechine, I. M.; Guedes, D. N.; Barbosa-Filho, J. M.; Sobral da Silva, M. Protoberberine Alkaloids. In *Alkaloids: Chemistry and Biology*; Knölker, H.-J., Ed.; Elsevier Inc., 2005; Vol. *62*, pp 1−75.
(55) Kutchan, T. M.; Dittrich, H. Characterization and Mechanism of the Berberine Bridge Enzyme, a Covalently Flavinylated Oxidase of Benzophenanthridine Alkaloid Biosynthesis in Plants. *J. Biol. Chem.* **1995**, *270*, 24475−24481.
(56) Dewick, P. M. Modified Benzyltetrahydroisoquinoline Alkaloids. In *Medicinal Natural Products: A Biosynthetic Approach*, 2nd ed.; John Wiley & Sons, 2002; pp 336−359.
(57) Davis, F. A.; Mohanty, P. K. Asymmetric Synthesis of the Protoberberine Alkaloid (*S*)-(−)-Xylopinine Using Enantiopure Sulfinimines. *J. Org. Chem.* **2002**, *67*, 1290−1296.
(58) Davis, F. A.; Melamed, J. Y.; Sharik, S. S. Total Synthesis of (−)-Normalindine via Addition of Metalated 4-Methyl-3-cyanopyridine to an Enantiopure Sulfinimine. *J. Org. Chem.* **2006**, *71*, 8761−8766.
(59) Mastranzo, V. M.; Yuste, F.; Ortiz, B.; Sánchez-Obregón, R.; Toscano, R. A.; García Ruano, J. L. Asymmetric Synthesis of (*S*)-(−)-Xylopinine. Use of the Sulfinyl Group as an *Ipso* Director in Aromatic S_E. *J. Org. Chem.* **2011**, *76*, 5036−5041.
(60) Cheng, J.; Fu, L.; Ling, C.; Yang, Y. Total Synthesis of (*S*)-(−)-Stepholidine using (*S*)-*tert*-Butanesulfinylimine. *Heterocycles.* **2010**, *81*, 2581−2592.
(61) Grajewska, A.; Rozwadowska, M. D. Diastereoselective Pomeranz-Fritsch-Bobbitt Synthesis of (*S*)-(−)-*O*-Methylbharatamine using (*S*)-*N*-*tert*-Butanesulfinimine as a Substrate. *Tetrahedron: Asymmetry* **2007**, *18*, 2910−2914.
(62) Nguyen Le, T.; Cho, W.-J. Novel Synthesis of the Natural Protoberberine Alkaloids: Oxypalmatine and Oxypseudopalmatine. *Bull. Korean Chem. Soc.* **2007**, *28*, 763−766.
(63) Fukuda, T.; Iwao, M. Synthesis of Both Enantiomers of Protoberberines via Laterally Lithiated (*S*)-4-Isopropyl-2-(*o*-tolyl)-oxazolines. *Heterocycles* **2007**, *74*, 701−720.

https://doi.org/10.1021/acs.chemrev.3c00054
Chem. Rev. 2023, 123, 9447−9496

(64) Chrzanowska, M.; Dreas, A.; Rozwadowska, M. D. Asymmetric Synthesis of (*R*)-(+)- and (*S*)-(−)-2,3-methylenedioxy-8-oxoberbine (gusanlung D). *Tetrahedron: Asymmetry* **2004**, *15*, 1113−1120.
(65) Meissner, Z.; Chrzanowska, M. Enantiospecific Synthesis of (*S*)-(−)-8-oxoxylopinine. *Tetrahedron: Asymmetry* **2015**, *26*, 225−229.
(66) Boudou, M.; Enders, D. Asymmetric Synthesis of Tetrahydropalmatine via Tandem 1,2-Addition/Cyclization. *J. Org. Chem.* **2005**, *70*, 9486−9494.
(67) Gao, S.; Cheng, J.-J.; Ling, C.-Y.; Chu, W.-J.; Yang, Y.-S. A Practical Enantioselective Total Synthesis of (−)-(*S*)-Stepholidine. *Tetrahedron Lett.* **2014**, *55*, 4856−4859.
(68) Gadhiya, S.; Ponnala, S.; Harding, W. W. A Divergent Route to 9,10-Oxygenated Tetrahydroprotoberberine and 8-Oxoprotoberberine Alkaloids: Synthesis of (±)-Isocorypalmine and Oxypalmatine. *Tetrahedron* **2015**, *71*, 1227−1231.
(69) Zein, A. L.; Dawe, L. N.; Georghiou, P. E. Enantioselective Total Synthesis and X-ray Structures of the Tetrahydroprotoberberine Alkaloids (−)-(*S*)-Tetrahydropalmatrubine and (−)-(*S*)-Corytenchine. *J. Nat. Prod.* **2010**, *73*, 1427−1430.
(70) Kayhan, J.; Wanner, M. J.; Ingemann, S.; van Maarseveen, J. H.; Hiemstra, H. Consecutive Pictet-Spengler Condensations toward Bioactive 8-Benzylprotoberberines: Highly Selective Total Syntheses of (+)-Javaberine A(+)-Javaberine B, and (−)-Latifolian A. *Eur. J. Org. Chem.* **2016**, *2016*, 3705−3708.
(71) Horst, B.; Wanner, M. J.; Jørgensen, S. I.; Hiemstra, H.; van Maarseveen, J. H. Total Synthesis of the Ortho-Hydroxylated Protoberberines (*S*)-Govaniadine, (*S*)-Caseamine, and (*S*)-Clarkeanidine via a Solvent-Directed Pictet-Spengler Reaction. *J. Org. Chem.* **2018**, *83*, 15110−15117.
(72) Orejarena Pacheco, J. C.; Lahm, G.; Opatz, T. Synthesis of Alkaloids by Stevens Rearrangement of Nitrile-Stabilized Ammonium Ylides: (±)-Laudanosine, (±)-Laudanidine, (±)-Armepavine, (±)-7-Methoxycryptopleurine, and (±)-Xylopinine. *J. Org. Chem.* **2013**, *78*, 4985−4992.
(73) Stubba, D.; Lahm, G.; Geffe, M.; Runyon, J. W.; Arduengo III, A. J.; Opatz, T. Xylochemistry - Making Natural Products Entirely from Wood. *Angew. Chem., Int. Ed.* **2015**, *54*, 14187−14189.
(74) Lahm, G.; Deichmann, J.-G.; Rauen, A. L.; Opatz, T. A One-Pot Cascade to Protoberberine Alkaloids via Stevens Rearrangement of Nitrile-Stabilized Ammonium Ylides. *J. Org. Chem.* **2015**, *80*, 2010−2016.
(75) Gatland, A. E.; Pilgrim, B. S.; Procopiou, P. A.; Donohoe, T. J. Short and Efficient Syntheses of Protoberberine Alkaloids using Palladium-Catalyzed Enolate Arylation. *Angew. Chem., Int. Ed.* **2014**, *53*, 14555−14558.
(76) Garad, D. N.; Mhaske, S. B. Pd(II)-Catalyzed Intramolecular Tandem Olefin Amidation/C-H Activation Protocol for the Syntheses of the Protoberberine Class of Natural Products. *Org. Lett.* **2016**, *18*, 3862−3865.
(77) Jayakumar, J.; Cheng, C.-H. Direct Synthesis of Protoberberine Alkaloids by Rh-catalyzed C-H Bond Activation as the Key Step. *Chem. Eur. J.* **2016**, *22*, 1800−1804.
(78) Lerchen, A.; Knecht, T.; Koy, M.; Daniliuc, C. G.; Glorius, F. A General Cp*Co^{III}-Catalyzed Intramolecular C-H Activation Approach for the Efficient Total Syntheses of Aromathecin, Protoberberine, and Tylophora Alkaloids. *Chem. Eur. J.* **2017**, *23*, 12149−12152.
(79) Zhou, S.; Tong, R. A General, Concise Strategy that Enables Collective Total Syntheses of Over 50 Protoberberine and Five Aporhoeadane Alkaloids within Four to Eight Steps. *Chem. Eur. J.* **2016**, *22*, 7084−7089.
(80) Yu, J.; Zhang, Z.; Zhou, S.; Zhang, W.; Tong, R. Evolution of Two Routes for Asymmetric Total Synthesis of Tetrahydroprotoberberine Alkaloids. *Org. Chem. Front.* **2018**, *5*, 242−246.
(81) Lichman, B. R.; Lamming, E. D.; Pesnot, T.; Smith, J. M.; Hailes, H. C.; Ward, J. M. One-Pot Triangular Chemoenzymatic Cascades for the Syntheses of Chiral Alkaloids from Dopamine. *Green Chem.* **2015**, *17*, 852−855.
(82) Novak, B. H.; Hudlicky, T.; Reed, J. W.; Mulzer, J.; Trauner, D. Morphine Synthesis and Biosynthesis - An Update. *Curr. Org. Chem.* **2000**, *4*, 343−362.
(83) Blakemore, P. R.; White, J. D. Morphine, the Proteus of Organic Molecules. *Chem. Commun.* **2002**, 1159−1168.
(84) Hagel, J. M.; Facchini, P. J. Dioxygenases Catalyze the *O*-Demethylation Steps of Morphine Biosynthesis in Opium Poppy. *Nat. Chem. Biol.* **2010**, *6*, 273−275.
(85) Gates, M.; Tschudi, G. The Synthesis of Morphine. *J. Am. Chem. Soc.* **1952**, *74*, 1109−1110.
(86) Rinner, U.; Hudlicky, T. Synthesis of Morphine Alkaloids and Derivatives. In *Alkaloid Synthesis. Topics in Current Chemistry*; Knölker, H.-J., Ed.; Springer, 2011; Vol. *309*, pp 33−66.
(87) Zezula, J.; Hudlicky, T. Recent Progress in the Synthesis of Morphine Alkaloids. *Synlett* **2005**, 388−405.
(88) Taber, D. F.; Neubert, T. D.; Schlecht, M. F. Chapter 11 The enantioselective synthesis of morphine. In *Strategies and Tactics in Organic Synthesis*; Harnata, M., Ed.; Elsevier: London, 2004; Vol. *5*, pp 353−389.
(89) Novak, B. H.; Hudlicky, T.; Reed, J. W.; Mulzer, J.; Trauner, D. Morphine Synthesis and Biosynthesis - An Update. *Curr. Org. Chem.* **2000**, *4*, 343−362.
(90) Uchida, K.; Yokoshima, S.; Kan, T.; Fukuyama, T. Total Synthesis of (±)-Morphine. *Org. Lett.* **2006**, *8*, 5311−5313.
(91) Uchida, K.; Yokoshima, S.; Kan, T.; Fukuyama, T. Total Synthesis of (±)-Morphine. *Heterocycles* **2009**, *77*, 1219−1234.
(92) Koizumi, H.; Yokoshima, S.; Fukuyama, T. Total Synthesis of (−)-Morphine. *Chem. Asian. J.* **2010**, *5*, 2192−2198.
(93) Umihara, H.; Yokoshima, S.; Inoue, M.; Fukuyama, T. Total Synthesis of (−)-Morphine. *Chem. Eur. J.* **2017**, *23*, 6993−6995.
(94) Ichiki, M.; Tanimoto, H.; Miwa, S.; Saito, R.; Sato, T.; Chida, N. Synthesis of (−)-Morphine: Application of Sequential Claisen/Claisen Rearrangement of an Allylic Vicinal Diol. *Chem. Eur. J.* **2013**, *19*, 264−269.
(95) Varin, M.; Barré, E.; Iorga, B.; Guillou, C. Diastereoselective Synthesis of (±)-Codeine. *Chem. Eur. J.* **2008**, *14*, 6606−6608.
(96) Chu, S.; Münster, N.; Balan, T.; Smith, M. D. A Cascade Strategy Enables a Total Synthesis of (±)-Morphine. *Angew. Chem., Int. Ed.* **2016**, *55*, 14306−14309.
(97) Zhang, Q.; Zhang, F.-M.; Zhang, C.-S.; Liu, S.-Z.; Tian, J.-M.; Wang, S.-H.; Zhang, X.-M.; Tu, Y.-Q. Enantioselective Synthesis of *cis*-Hydrobenzofurans Bearing All-Carbon Quaternary Stereocenters and Application to Total Synthesis of (−)-Morphine. *Nat. Commun.* **2019**, *10*, 2507−2513.
(98) Kimishima, A.; Umihara, H.; Mizoguchi, A.; Yokoshima, S.; Fukuyama, T. Synthesis of (−)-Oxycodone. *Org. Lett.* **2014**, *16*, 6244−6247.
(99) Park, K.-H.; Chen, D. Y.-K. A Desymmetrization-based Approach to Morphinans: Application in the Total Synthesis of Oxycodone. *Chem. Commun.* **2018**, *54*, 13018−13021.
(100) Park, K.-H.; Chen, R.; Chen, D. Y.-K. Programmed Serial Stereochemical Relay and its Application in the Synthesis of Morphinans. *Chem. Sci.* **2017**, *8*, 7031−7037.
(101) Geffe, M.; Opatz, T. Enantioselective Synthesis of (−)-Dihydrocodeine and Formal Synthesis of (−)-Thebaine, (−)-Codeine, and (−)-Morphine from a Deprotonated α-Aminonitrile. *Org. Lett.* **2014**, *16*, 5282−5285.
(102) Lipp, A.; Ferenc, D.; Gütz, C.; Geffe, M.; Vierengel, N.; Schollmeyer, D.; Schäfer, H. J.; Waldvogel, S. R.; Opatz, T. A Regio- and Diastereoselective Anodic Aryl-Aryl Coupling in the Biomimetic Total Synthesis of (−)-Thebaine. *Angew. Chem., Int. Ed.* **2018**, *57*, 11055−11059.
(103) Lipp, A.; Selt, M.; Ferenc, D.; Schollmeyer, D.; Waldvogel, S. R.; Opatz, T. Total Synthesis of (−)-Oxycodone via Anodic Aryl-Aryl Coupling. *Org. Lett.* **2019**, *21*, 1828−1831.
(104) Makarova, M.; Endoma-Arias, M. A. A.; Dela Paz, H. E.; Simionescu, R.; Hudlicky, T. Chemoenzymatic Total Synthesis of *ent*-Oxycodone: Second-, Third-, and Fourth-Generation Strategies. *J. Am. Chem. Soc.* **2019**, *141*, 10883−10904.

https://doi.org/10.1021/acs.chemrev.3c00054
Chem. Rev. 2023, 123, 9447−9496

(105) Li, Q.; Zhang, H. Total Synthesis of Codeine. *Chem. Eur. J.* **2015**, *21*, 16379−16382.
(106) Dongbang, S.; Pedersen, B.; Ellman, J. A. Asymmetric Synthesis of (−)-Naltrexone. *Chem. Sci.* **2019**, *10*, 535−541.
(107) Wang, Y.; Hennig, A.; Küttler, T.; Hahn, C.; Jäger, A.; Metz, P. Total Synthesis of (±)-Thebainone A by Intramolecular Nitrone Cycloaddition. *Org. Lett.* **2020**, *22*, 3145−3148.
(108) Gözler, B.; Lantz, M. S.; Shamma, M. The Pavine and Isopavine Alkaloids. *J. Nat. Prod.* **1983**, *46*, 293−309.
(109) Gee, K. R.; Barmettler, P.; Rhodes, M. R.; McBurney, R. N.; Reddy, N. L.; Hu, L.-Y. R.; Cotter, E.; Hamilton, P. N.; Weber, E.; Keana, J. F. W. 10,5-(Iminomethano)-10,11-dihydro-5H-dibenzo-[a,d]cycloheptene and Derivatives. Potent PCP Receptor Ligands. *J. Med. Chem.* **1993**, *36*, 1938−1946.
(110) Brown, D. W.; Dyke, S. F.; Hardy, G.; Sainsbury, M. Isopavine Alkaloids: Synthesis and Biosynthetic Speculations. *Tetrahedron Lett.* **1969**, *10*, 1515−1517.
(111) Dyke, S. F.; Ellis, A. C. The Synthesis of Isopavine Alkaloids - 1. *Tetrahedron* **1971**, *27*, 3803−3809.
(112) Torres, M. A.; Hoffarth, E.; Eugenio, L.; Savtchouk, J.; Chen, X.; Morris, J. S.; Facchini, P. J.; Ng, K. K.-S. Structural and Functional Studies of Pavine *N*-Methyltransferase from *Thalictrum flavum* Reveal Novel Insights into Substrate Recognition and Catalytic Mechanism. *J. Biol. Chem.* **2016**, *291*, 23403−23415.
(113) Youte, J.-J.; Barbier, D.; Al-Mourabit, A.; Gnecco, D.; Marazano, C. An Enantioselective Access to 1-Alkyl-1,2,3,4-tetrahydroisoquinolines. Application to a New Synthesis of (−)-Argemonine. *J. Org. Chem.* **2004**, *69*, 2737−2740.
(114) Nishigaichi, Y.; Ohmuro, Y.; Hori, Y.; Ohtani, T. Extremely Facile Formation of the Pavine Alkaloid Skeleton by the Photoreaction between Isoquinoline and Benzyltrifluoroborate. *Chem. Lett.* **2020**, *49*, 118−120.
(115) Sun, L.; Li, D.; Zhou, X.; Zhang, D.; Wang, J.; He, Z.; Jiang, R.; Chen, W. General and Catalytic Enantioselective Approach to Isopavine Alkaloids. *J. Org. Chem.* **2017**, *82*, 12899−12907.
(116) Tambar, U. K.; Ebner, D. C.; Stoltz, B. M. A Convergent and Enantioselective Synthesis of (+)-Amurensinine via Selective C-H and C-C Bond Insertion Reactions. *J. Am. Chem. Soc.* **2006**, *128*, 11752−11753.
(117) Krishnan, S.; Bagdanoff, J. T.; Ebner, D. C.; Ramtohul, Y. K.; Tambar, U. K.; Stoltz, B. M. Pd-Catalyzed Enantioselective Aerobic Oxidation of Secondary Alcohols: Applications to the Total Synthesis of Alkaloids. *J. Am. Chem. Soc.* **2008**, *130*, 13745−13754.
(118) Sunderhaus, J. D.; Dockendorff, C.; Martin, S. F. Applications of Multicomponent Reactions for the Synthesis of Diverse Heterocyclic Scaffolds. *Org. Lett.* **2007**, *9*, 4223−4226.
(119) Miura, Y.; Saito, Y.; Goto, M.; Nakagawa-Goto, K. First Total Synthesis of the Pavine Alkaloid (±)-Neocaryachine and its Optical Resolution. *Chem. Pharm. Bull.* **2020**, *68*, 899−902.
(120) TAKAHASHI, K.; KUBO, A. A New Antibiotics, Saframycins A, B, C, D, and E. *J. Antibiot.* **1977**, *30*, 1015−1018.
(121) Mikami, Y.; Takahashi, K.; Yazawa, K.; Hour-Young, C.; Arai, T.; Saito, N.; Kubo, A. Structural Studies on Minor Components of Saframycin Group Antibiotics Saframycins F, G, and H. *J. Antibiot.* **1988**, *41*, 734−740.
(122) Lown, J. W.; Hanstock, C. C.; Joshua, A. V.; Arai, T.; Takahashi, K. Structure and Conformation of Saframycin R Determined by High Field 1H and 13C NMR and Its Interactions with DNA in Solution. *J. Antibiot.* **1983**, *36*, 1184−1194.
(123) Irschik, H.; Trowitzsch-Kienast, W.; Gerth, K.; Hofle, G.; Reichenbach, H. Saframycin Mx1, A New Natural Saframycin Isolated from a Myxobacterium. *J. Antibiot.* **1988**, *41*, 993−998.
(124) Yazawa, K.; Takahashi, K.; Mikami, Y.; Arai, T.; Saito, N.; Kubo, A. Isolation and Structural Elucidation of New Saframycins Y3, Yd-1, Yd-2, Ad-1, Y2b, and Y2b-d. *J. Antibiot.* **1986**, *39*, 1639−1650.
(125) Lown, J. W.; Joshua, A. V.; Lee, J. S. Molecular Mechanisms of Binding and Single-Strand Scission of DNA by the Antitumor Antibiotics Saframycins A and C. *Biochemistry* **1982**, *21*, 419−428.
(126) Mikami, Y.; Takahashi, K.; Yazawa, K.; Arai, T.; Namikoshi, M.; Iwasaki, S.; Okuda, S. Biosynthetic Studies on Saframycin A, A Quinone Antitumor Antibiotic Produced by Streptomyces Lavendulae. *J. Biol. Chem.* **1985**, *260*, 344−348.
(127) Li, L.; Deng, W.; Song, J.; Ding, W.; Zhao, Q.-F; Peng, C.; Song, W.-W; Tang, G.-L; Liu, W. Characterization of the Saframycin A Gene Cluster from Streptomyces lavendulae NRRL 11002 Revealing a Nonribosomal Peptide Synthetase System for Assembling the Unusual Tetrapeptidyl Skeleton in an Iterative Manner. *J. Bacteriol.* **2008**, *190*, 251−263.
(128) Koketsu, K.; Watanabe, K.; Suda, H.; Oguri, H.; Oikawa, H. Reconstruction of the Saframycin Core Scaffold Defines Dual Pictet-Spengler Mechanisms. *Nat. Chem. Biol.* **2010**, *6*, 408−410.
(129) Koketsu, K.; Minami, A.; Watanabe, K.; Oguri, H.; Oikawa, H. Pictet-Spenglerase Involved in Tetrahydroisoquinoline Antibiotic Biosynthesis. *Curr. Opin. Chem. Biol.* **2012**, *16*, 142−149.
(130) Song, L.-Q.; Zhang, Y.-Y.; Pu, J.-Y.; Tang, M.-C.; Peng, C.; Tang, G.-L. Catalysis of Extracellular Deamination by a FAD-Linked Oxidoreductase after Prodrug Maturation in the Biosynthesis of Saframycin A. *Angew. Chem., Int. Ed.* **2017**, *56*, 9116−9120.
(131) Dong, W.; Liu, W.; Liao, X.; Guan, B.; Chen, S.; Liu, Z. Asymmetric Total Synthesis of (−)-Saframycin A from l-Tyrosine. *J. Org. Chem.* **2011**, *76*, 5363−5368.
(132) Vincent, G.; Lane, J. W.; Williams, R. M. Regioselectivity of Pictet-Spengler Cyclization Reactions to Construct the Pentacyclic Frameworks of the Ecteinascidin-Saframycin Class of Tetrahydroisoquinoline Antitumor Antibiotics. *Tetrahedron Lett.* **2007**, *48*, 3719−3722.
(133) Martinez, E. J.; Corey, E. J. A New, More Efficient, and Effective Process for the Synthesis of a Key Pentacyclic Intermediate for Production of Ecteinascidin and Phthalascidin Antitumor Agents. *Org. Lett.* **2000**, *2*, 993−996.
(134) Kimura, S.; Saito, N. A Stereocontrolled Total Synthesis of (±)-Saframycin A. *Tetrahedron* **2018**, *74*, 4504−4514.
(135) Saito, N.; Kimura, S.; Kawai, S.; Azuma, M.; Koizumi, Y.; Yokoya, M.; Umehara, Y. Synthetic Studies on Saframycin Anibiotics: An Improved Synthesis of Tricyclic Lactam Intermediate and Construction of the Core Ring System of Saframycin A. *Heterocycles* **2015**, *90*, 327−343.
(136) Matsuo, K.; Okumura, M.; Tanaka, K. Total Synthesis of Mimocin, an Isoquinolinequinone Antibiotic. *Chem. Pharm. Bull.* **1982**, *30*, 4170−4174.
(137) Tanifuji, R.; Koketsu, K.; Takakura, M.; Asano, R.; Minami, A.; Oikawa, H.; Oguri, H. Chemo-Enzymatic Total Syntheses of Jorunnamycin A. Saframycin A, and N-Fmoc Saframycin Y3. *J. Am. Chem. Soc.* **2018**, *140*, 10705−10709.
(138) Ikeda, Y.; Idemoto, H.; Hirayama, F.; Yamamoto, K.; Iwao, K.; Asao, T.; Munakata, T. Safracins, New Antitumor Antibiotics I. Producing Organism, Fermentation and Isolation. *J. Antibiot.* **1983**, *36*, 1279−1283.
(139) Cuevas, C.; Pérez, M.; Martín, M. J.; Chicharro, J. L.; Fernández-Rivas, C.; Flores, M.; Francesch, A.; Gallego, P.; Zarzuelo, M.; de la Calle, F.; et al. Synthesis of Ecteinascidin ET-743 and Phthalascidin Pt-650 from Cyanosafracin B. *Org. Lett.* **2000**, *2*, 2545−2548.
(140) Velasco, A.; Acebo, P.; Gomez, A.; Schleissner, C.; Rodríguez, P.; Aparicio, T.; Conde, S.; Muñoz, R.; de La Calle, F.; Garcia, J. L.; et al. Molecular Characterization of the Safracin Biosynthetic Pathway from Pseudomonas Fluorescens A2−2: Designing New Cytotoxic Compounds. *Mol. Microbiol.* **2005**, *56*, 144−154.
(141) Zhang, Y.-Y.; Shao, N.; Wen, W.-H.; Tang, G.-L. A Cryptic Palmitoyl Chain Involved in Safracin Biosynthesis Facilitates Post-NRPS Modifications. *Org. Lett.* **2022**, *24*, 127−131.
(142) Saito, N.; Harada, S.; Yamashita, M.; Saito, T.; Yamaguchi, K.; Kubo, A. Synthesis of Saframycins. XI. Synthetic Studies toward a Total Synthesis of Safracin A. *Tetrahedron* **1995**, *51*, 8213−8230.
(143) Saito, N. Chemical Research on Antitumor Isoquinoline Marine Natural Products and Related Compounds. *Chem. Pharm. Bull.* **2021**, *69*, 155−177.

https://doi.org/10.1021/acs.chemrev.3c00054
Chem. Rev. 2023, 123, 9447−9496

(144) Suwanborirux, K.; Amnuoypol, S.; Plubrukarn, A.; Pummangura, S.; Kubo, A.; Tanaka, C.; Saito, N. Chemistry of Renieramycins. Part 3. Isolation and Structure of Stabilized Renieramycin Type Derivatives Possessing Antitumor Activity from Thai Sponge Xestospongia Species, Pretreated with Potassium Cyanide. *J. Nat. Prod.* **2003**, *66*, 1441−1446.
(145) Amnuoypol, S.; Suwanborirux, K.; Pummangura, S.; Kubo, A.; Tanaka, C.; Saito, N. Chemistry of Renieramycins. Part 5. Structure Elucidation of Renieramycin-Type Derivatives O, Q, R, and S from Thai Marine Sponge Xestospongia Species Pretreated with Potassium Cyanide. *J. Nat. Prod.* **2004**, *67*, 1023−1028.
(146) Oku, N.; Matsunaga, S.; van Soest, R. W. M.; Fusetani, N. Renieramycin J, a Highly Cytotoxic Tetrahydroisoquinoline Alkaloid, from a Marine Sponge Neopetrosia Sp. *J. Nat. Prod.* **2003**, *66*, 1136−1139.
(147) Daikuhara, N.; Tada, Y.; Yamaki, S.; Charupant, K.; Amnuoypol, S.; Suwanborirux, K.; Saito, N. Chemistry of Renieramycins. Part 7: Renieramycins T and U, Novel Renieramycin-Ecteinascidin Hybrid Marine Natural Products from Thai Sponge Xestospongia Sp. *Tetrahedron Lett.* **2009**, *50*, 4276−4278.
(148) Saito, N.; Yoshino, M.; Charupant, K.; Suwanborirux, K. Chemistry of Renieramycins. Part 10: Structure of Renieramycin V, a Novel Renieramycin Marine Natural Product Having a Sterol Ether at C-14 Position. *Heterocycles* **2012**, *84*, 309−314.
(149) Charupant, K.; Suwanborirux, K.; Amnuoypol, S.; Saito, E.; Kubo, A.; Saito, N. Jorunnamycins A—C, New Stabilized Renieramycin-Type Bistetrahydroisoquinolines Isolated from the Thai Nudibranch *Jorunna Funebris*. *Chem. Pharm. Bull.* **2007**, *55*, 81−86.
(150) Tatsukawa, M.; Punzalan, L. L. C.; Magpantay, H. D. S.; Villaseñor, I. M.; Concepcion, G. P.; Suwanborirux, K.; Yokoya, M.; Saito, N. Chemistry of Renieramycins. Part 13: Isolation and Structure of Stabilized Renieramycin Type Derivatives, Renieramycins W-Y, from Philippine Blue Sponge Xestospongia Sp., Pretreated with Potassium Cyanide. *Tetrahedron* **2012**, *68*, 7422−7428.
(151) He, W.-F.; Li, Y.; Feng, M.-T.; Gavagnin, M.; Mollo, E.; Mao, S.-C.; Guo, Y.-W. New Isoquinolinequinone Alkaloids from the South China Sea Nudibranch Jorunna Funebris and Its Possible Sponge-Prey Xestospongia Sp. *Fitoterapia* **2014**, *96*, 109−114.
(152) Huang, R.-Y.; Chen, W.-T.; Kurtán, T.; Mándi, A.; Ding, J.; Li, J.; Li, X.-W.; Guo, Y.-W. Bioactive Isoquinolinequinone Alkaloids from the South China Sea Nudibranch Jorunna Funebris and Its Sponge-Prey Xestospongia Sp. *Future Med. Chem.* **2016**, *8*, 17−27.
(153) Tianero, M. D.; Balaich, J. N.; Donia, M. S. Localized Production of Defence Chemicals by Intracellular Symbionts of Haliclona Sponges. *Nat. Microbiol.* **2019**, *4*, 1149−1159.
(154) Chan, C.; Heid, R.; Zheng, S.; Guo, J.; Zhou, B.; Furuuchi, T.; Danishefsky, S. J. Total Synthesis of Cribrostatin IV: Fine-Tuning the Character of an Amide Bond by Remote Control. *J. Am. Chem. Soc.* **2005**, *127*, 4596−4598.
(155) Vincent, G.; Williams, R. M. Asymmetric Total Synthesis of (−)-Cribrostatin 4 (Renieramycin H). *Angew. Chem., Int. Ed.* **2007**, *46*, 1517−1520.
(156) Jin, W.; Metobo, S.; Williams, R. M. Synthetic Studies on Ecteinascidin-743: Constructing a Versatile Pentacyclic Intermediate for the Synthesis of Ecteinascidins and Saframycins. *Org. Lett.* **2003**, *5*, 2095−2098.
(157) Chen, X.; Zhu, J. Total Synthesis of the Marine Natural Product (−)-Cribrostatin 4 (Renieramycin H). *Angew. Chem., Int. Ed.* **2007**, *46*, 3962−3965.
(158) Yokoya, M.; Ito, H.; Saito, N. Chemistry of Renieramycins. Part 11: Total Synthesis of (±)-Cribrostatin 4. *Tetrahedron* **2011**, *67*, 9185−9192.
(159) Yokoya, M.; Kobayashi, K.; Sato, M.; Saito, N. Chemistry of Renieramycins. Part 14: Total Synthesis of Renieramycin I and Practical Synthesis of Cribrostatin 4 (Renieramycin H). *Marine Drugs* **2015**, *13*, 4915−4933.
(160) Lane, J. W.; Chen, Y.; Williams, R. M. Asymmetric Total Syntheses of (−)-Jorumycin, (−)-Renieramycin G, 3-Epi-Jorumycin, and 3-Epi-Renieramycin G. *J. Am. Chem. Soc.* **2005**, *127*, 12684−12690.
(161) Magnus, P.; Matthews, K. S. Synthesis of the Tetrahydroisoquinoline Alkaloid (±)-Renieramycin G and a (±)-Lemonomycinone Analogue from a Common Intermediate. *J. Am. Chem. Soc.* **2005**, *127*, 12476−12477.
(162) Magnus, P.; Matthews, K. S. A Divergent Strategy for Synthesis of the Tetrahydroisoquinoline Alkaloids Renieramycin G and a Lemonomycin Analog. *Tetrahedron* **2012**, *68*, 6343−6360.
(163) Wu, Y.-C.; Zhu, J. Asymmetric Total Syntheses of (−)-Renieramycin M and G and (−)-Jorumycin Using Aziridine as a Lynchpin. *Org. Lett.* **2009**, *11*, 5558−5561.
(164) Liao, X. W.; Liu, W.; Dong, W. F.; Guan, B. H.; Chen, S. Z.; Liu, Z. Z. Total Synthesis of (−)-Renieramycin G from l-Tyrosine. *Tetrahedron* **2009**, *65*, 5709−5715.
(165) Liu, W.; Dong, W.; Liao, X.; Yan, Z.; Guan, B.; Wang, N.; Liu, Z. Synthesis and Cytotoxicity of (−)-Renieramycin G Analogs. *Bioorg. Med. Chem. Lett.* **2011**, *21*, 1419−1421.
(166) Liu, W.; Liao, X.; Dong, W.; Yan, Z.; Wang, N.; Liu, Z. Total Synthesis and Cytotoxicity of (−)-Jorumycin and Its Analogues. *Tetrahedron* **2012**, *68*, 2759−2764.
(167) Du, E.; Dong, W.; Guan, B.; Pan, X.; Yan, Z.; Li, L.; Wang, N.; Liu, Z. Asymmetric Total Synthesis of Three Stereoisomers of (−)-Renieramycin G and Their Cytotoxic Activities. *Tetrahedron* **2015**, *71*, 4296−4303.
(168) Yokoya, M.; Shinada-Fujino, K.; Saito, N. Chemistry of Renieramycins. Part 9: Stereocontrolled Total Synthesis of (±)-Renieramycin G. *Tetrahedron Lett.* **2011**, *52*, 2446−2449.
(169) Yokoya, M.; Shinada-Fujino, K.; Yoshida, S.; Mimura, M.; Takada, H.; Saito, N. Chemistry of Renieramycins. Part 12: An Improved Total Synthesis of (±)-Renieramycin G. *Tetrahedron* **2012**, *68*, 4166−4181.
(170) Kubo, A.; Saito, N.; Yamato, H.; Masubuchi, K.; Nakamura, M. Stereoselective Total Synthesis of (±)-Saframycin B. *J. Org. Chem.* **1988**, *53*, 4295−4310.
(171) Zheng, Y.; Li, X.-D.; Sheng, P.-Z.; Yang, H.-D.; Wei, K.; Yang, Y.-R. Asymmetric Total Syntheses of (−)-Fennebricin A, (−)-Renieramycin J, (−)-Renieramycin G, (−)-Renieramycin M, and (−)-Jorunnamycin A via C-H Activation. *Org. Lett.* **2020**, *22*, 4489−4493.
(172) He, J.; Li, S.; Deng, Y.; Fu, H.; Laforteza, B. N.; Spangler, J. E.; Homs, A.; Yu, J.-Q. Ligand-Controlled C(sp^3)-H Arylation and Olefination in Synthesis of Unnatural Chiral α-Amino Acids. *Science* **2014**, *343*, 1216−1220.
(173) Yokoya, M.; Toyoshima, R.; Suzuki, T.; Le, V. H.; Williams, R. M.; Saito, N. Stereoselective Total Synthesis of (−)-Renieramycin T. *J. Org. Chem.* **2016**, *81*, 4039−4047.
(174) Fishlock, D.; Williams, R. M. Synthetic Studies on Et-743. Asymmetric, Stereocontrolled Construction of the Tetrahydroisoquinoline Core via Radical Cyclization on a Glyoxalimine. *Org. Lett.* **2006**, *8*, 3299−3301.
(175) Fishlock, D.; Williams, R. M. Synthetic Studies on Et-743. Assembly of the Pentacyclic Core and a Formal Total Synthesis. *J. Org. Chem.* **2008**, *73*, 9594−9600.
(176) Kimura, S.; Saito, N. Construction of the Pentacyclic Core and Formal Total Synthesis of (Rac)-Renieramycin T. *ChemistryOpen* **2018**, *7*, 764−771.
(177) Jia, J.; Chen, R.; Liu, H.; Li, X.; Jia, Y.; Chen, X. Asymmetric Synthesis of (−)-Renieramycin T. *Org. Biomol. Chem.* **2016**, *14*, 7334−7344.
(178) Rath, C. M.; Janto, B.; Earl, J.; Ahmed, A.; Hu, F. Z.; Hiller, L.; Dahlgren, M.; Kreft, R.; Yu, F.; Wolff, J. J.; et al. Meta-omic Characterization of the Marine Invertebrate Microbial Consortium That Produces the Chemotherapeutic Natural Product ET-743. *ACS Chem. Biol.* **2011**, *6*, 1244−1256.
(179) Chen, R.; Liu, H.; Chen, X. Asymmetric Total Synthesis of (−)-Jorunnamycins A and C and (−)-Jorumycin from l-Tyrosine. *J. Nat. Prod.* **2013**, *76*, 1789−1795.
(180) Welin, E. R.; Ngamnithiporn, A.; Klatte, M.; Lapointe, G.; Pototschnig, G. M.; McDermott, M. S. J.; Conklin, D.; Gilmore, C.

https://doi.org/10.1021/acs.chemrev.3c00054
Chem. Rev. 2023, 123, 9447−9496

D.; Tadross, P. M.; Haley, C. K.; et al. Concise Total Syntheses of (−)-Jorunnamycin A and (−)-Jorumycin Enabled by Asymmetric Catalysis. *Science* **2019**, *363*, 270−275.
(181) Cuevas, C.; Francesch, A. Development of Yondelis® (Trabectedin, Et-743). A Semisynthetic Process Solves the Supply Problem. *Nat. Prod. Rep.* **2009**, *26*, 322−337.
(182) Kerr, R. G.; Miranda, N. F. Biosynthetic Studies of Ecteinascidins in the Marine Tunicate Ecteinascidia Turbinata. *J. Nat. Prod.* **1995**, *58*, 1618−1621.
(183) Rath, C. M.; Janto, B.; Earl, J.; Ahmed, A.; Hu, F. Z.; Hiller, L.; Dahlgren, M.; Kreft, R.; Yu, F.; Wolff, J. J.; et al. Meta-Omic Characterization of the Marine Invertebrate Microbial Consortium That Produces the Chemotherapeutic Natural Product ET-743. *ACS Chem. Biol.* **2011**, *6*, 1244−1256.
(184) Corey, E. J.; Gin, D. Y.; Kania, R. S. Enantioselective Total Synthesis of Ecteinascidin 743. *J. Am. Chem. Soc.* **1996**, *118*, 9202−9203.
(185) Cuevas, C.; Pérez, M.; Martín, M. J.; Chicharro, J. L.; Fernández-Rivas, C.; Flores, M.; Francesch, A.; Gallego, P.; Zarzuelo, M.; de la Calle, F.; et al. Synthesis of Ecteinascidin ET-743 and Phthalascidin Pt-650 from Cyanosafracin B. *Org. Lett.* **2000**, *2*, 2545−2548.
(186) Endo, A.; Yanagisawa, A.; Abe, M.; Tohma, S.; Kan, T.; Fukuyama, T. Total Synthesis of Ecteinascidin 743. *J. Am. Chem. Soc.* **2002**, *124*, 6552−6554.
(187) Kawagishi, F.; Toma, T.; Inui, T.; Yokoshima, S.; Fukuyama, T. Total Synthesis of Ecteinascidin 743. *J. Am. Chem. Soc.* **2013**, *135*, 13684−13687.
(188) Zheng, S.; Chan, C.; Furuuchi, T.; Wright, B. J. D.; Zhou, B.; Guo, J.; Danishefsky, S. J. Stereospecific Formal Total Synthesis of Ecteinascidin 743. *Angew. Chem., Int. Ed.* **2006**, *45*, 1754−1759.
(189) Chen, J.; Chen, X.; Bois-Choussy, M.; Zhu, J. Total Synthesis of Ecteinascidin 743. *J. Am. Chem. Soc.* **2006**, *128*, 87−89.
(190) Chen, J.; Chen, X.; Willot, M.; Zhu, J. Asymmetric Total Syntheses of Ecteinascidin 597 and Ecteinascidin 583. *Angew. Chem., Int. Ed.* **2006**, *45*, 8028−8032.
(191) He, W.; Zhang, Z.; Ma, D. A Scalable Total Synthesis of the Antitumor Agents Et-743 and Lurbinectedin. *Angew. Chem., Int. Ed.* **2019**, *58*, 3972−3975.
(192) Zmijewski, M. J. Jr.; Mikolajczak, M.; Viswanatha, V.; Hruby, V. J. Biosynthesis of the Antitumor Antibiotic Naphthyridinomycin. *J. Am. Chem. Soc.* **1982**, *104*, 4969−4971.
(193) Zmijewski, M. J.; Palaniswamy, V. A.; Gould, S. J. Naphthyridinomycin Biosynthesis. The Involvement of Ornithine and the Origin of the Oxazolidine Nitrogen. *J. Chem. Soc., Chem. Commun.* **1985**, *18*, 1261−1262.
(194) Pu, J.-Y.; Peng, C.; Tang, M.-C.; Zhang, Y.; Guo, J.-P.; Song, L.-Q.; Hua, Q.; Tang, G.-L. Naphthyridinomycin Biosynthesis Revealing the Use of Leader Peptide to Guide Nonribosomal Peptide Assembly. *Org. Lett.* **2013**, *15*, 3674−3677.
(195) Woo, G. H. C.; Kim, S.-H.; Wipf, P. π-Allyl Palladium Approach Toward the Diazobicyclo[3.2.1]octane Core of the Naphthyridinomycin Alkaloids. *Tetrahedron* **2006**, *62*, 10507−10517.
(196) Ümit Kaniskan, H.; Garner, P. An Efficient Synthetic Approach to Cyanocycline A and Bioxalomycin β2 via [C+NC +CC] Coupling. *J. Am. Chem. Soc.* **2007**, *129*, 15460−15461.
(197) Garner, P.; Ümit Kaniskan, H.; Keyari, C. M.; Weerasinghe, L. Asymmetric [C+NC+CC] Coupling Entry to the Naphthyridinomycin Natural Product Family: Formal Total Synthesis of Cyanocycline A and Bioxalomycin β2. *J. Org. Chem.* **2011**, *76*, 5283−5294.
(198) Fukuyama, T.; Li, L.; Laird, A. A.; Frank, R. K. Stereocontrolled Total Synthesis of (±)-Cyanocycline A. *J. Am. Chem. Soc.* **1987**, *109*, 1587−1589.
(199) Aclidinomycins J, K were recently isolated; see: Yang, J.; Song, Y.; Tang, M.-C.; Li, M.; Deng, J.; Wong, N.-K.; Ju, J. Genome-Directed Discovery of Tetrahydroisoquinolines from Deep-Sea Derived Streptomyces Niveus SCSIO 3406. *J. Org. Chem.* **2021**, *86*, 11107−11116.
(200) Kanamaru, R.; Konishi, Y.; Ishioka, C.; Kakuta, H.; Sato, T.; Ishikawa, A.; Asamura, M.; Wakui, A. The Mechanism of Action of Quinocarmycin Citrate (KW 2152) on Mouse L1210 Cells in vitro. *Cancer Chemother. Pharmacol.* **1988**, *22*, 197−200.
(201) Hiratsuka, T.; Koketsu, K.; Minami, A.; Kaneko, S.; Yamazaki, C.; Watanabe, K.; Oguri, H.; Oikawa, H. Core Assembly Mechanism of Quinocarcin/SF-1739: Bimodular Complex Nonribosomal Peptide Synthetases for Sequential Mannich-Type Reactions. *Chemistry & Biology* **2013**, *20*, 1523−1535.
(202) Kwon, S.; Myers, A. G. Synthesis of (−)-Quinocarcin by Directed Condensation of α-Amino Aldehydes. *J. Am. Chem. Soc.* **2005**, *127*, 16796−16797.
(203) Wu, Y.-C.; Liron, M.; Zhu, J. Asymmetric Total Synthesis of (−)-Quinocarcin. *J. Am. Chem. Soc.* **2008**, *130*, 7148−7152.
(204) Allan, K. M.; Stoltz, B. M. A Concise Total Synthesis of (−)-Quinocarcin via Aryne Annulation. *J. Am. Chem. Soc.* **2008**, *130*, 17270−17271.
(205) Chiba, H.; Oishi, S.; Fujii, N.; Ohno, H. Total Synthesis of (−)-Quinocarcin by Gold(I)-Catalyzed Regioselective Hydroamination. *Angew. Chem., Int. Ed.* **2012**, *51*, 9169−9172.
(206) Chiba, H.; Sakai, Y.; Ohara, A.; Oishi, S.; Fujii, N.; Ohno, H. Convergent Synthesis of (−)-Quinocarcin Based on the Combination of Sonogashira Coupling and Gold(I)-Catalyzed 6-*endo*-*dig* Hydroamination. *Chem. Eur. J.* **2013**, *19*, 8875−8883.
(207) Scott, J. D.; Williams, R. M. Total Synthesis of (−)-Tetrazomine. Determination of the Stereochemistry of Tetrazomine and the Synthesis and Biological Activity of Tetrazomine Analogues. *J. Am. Chem. Soc.* **2002**, *124*, 2951−2956.
(208) For formal synthesis of (−)-lemonomycin, see: Siengalewicz, P.; Brecker, L.; Mulzer, J. Stereocontrolled Synthesis of the Tetracyclic Core Framework of (−)-Lemonomycin. *Synlett.* **2008**, *2008*, 2443−2446.
(209) Ashley, E. R.; Cruz, E. G.; Stoltz, B. M. The Total Synthesis of (−)-Lemonomycin. *J. Am. Chem. Soc.* **2003**, *125*, 15000−15001.
(210) Yoshida, A.; Akaiwa, M.; Asakawa, T.; Hamashima, Y.; Yokoshima, S.; Fukuyama, T.; Kan, T. Total Synthesis of (−)-Lemonomycin. *Chem. Eur. J.* **2012**, *18*, 11192−11195.

https://doi.org/10.1021/acs.chemrev.3c00054
Chem. Rev. 2023, 123, 9447−9496